Trinity College Dublin

The University of Dublin

Exploring the Role of Death Receptors in ER Stress-Associated Cell Death and Inflammation

MSc. Genetics

Hazel O'Connor B.A.

Principal Supervisor:

Seamus J. Martin

Declaration

I declare that this thesis has not been submitted as an exercise for a degree at this or any other university and it is entirely my own work.
I agree to deposit this thesis in the University's open access institutional repository or allow the Library to do so on my behalf, subject to Irish Copyright Legislation and Trinity College Library conditions of use and acknowledgement.

Signed:

_____

Hazel O'Connor B.A.
May 2018

Contents

Acknowledgements

First and foremost, I would like to offer my deepest gratitude to my supervisor, Professor Seamus J. Martin, for your extensive guidance, knowledge, encouragement and support throughout the course of my time in your laboratory.

To Dr. Graeme Sullivan, I would like to convey my sincerest thanks for your invaluable discussions and support. It was a pleasure to work alongside you on this project. To Dr. Conor Henry and Dr. Danielle Clancy for your continued mentorship, assistance and editorial support, I offer my thanks. To everyone in the Martin laboratory, it was fantastic to work with you all and I wish you the best in the future.

I would also like to thank Dr. Cristina Muñoz Pinedo for your collaboration, time and expertise in the glucose deprivation studies of my project.

Finally, a special thanks to my family and friends, particularly Leila Smith for your never-ending encouragement, support and advice throughout the course of this project.

Abstract

Cell death induced in response to ER stress, particularly in response to classical ER stress-inducing agents thapsigargin, brefeldin A and tunicamycin, has been shown to be dependent on the ER stress-dependent upregulation of the death receptor TRAIL-R2 (DR5) (Lu et al., 2014). ER stress responses have additionally been associated with cytokine production and tumour-associated inflammatory responses. Here we show that ER stress-induced DR5 upregulation contributes to death receptor-dependent inflammatory gene activation and ultimately cytokine production. CRISPR-mediated ablation of the ER stress-associated transcription factor CHOP, death receptors TRAIL-R1 (DR4) and DR5 and death receptor-associated molecule FADD afforded protection from ER stress-associated cytokine production. Overall, these data suggest that TRAIL-R signalling may play a previously unappreciated role in solid tumour-associated, ER stress driven tumour inflammation, immune cell recruitment, angiogenesis and metastasis.

Microtubule disruptors paclitaxel (Taxol) and docetaxel (Taxotere) are widely used chemotherapeutic agents that kill rapidly replicating tumour cells. However, these agents also trigger NFκB activation and have been associated with metastasis and tumour progression. How these taxanes promote NFκB activation and concurrent cytokine production is unknown. Here we implicate an ER stress-associated, TRAIL death receptor-dependent signalling pathway in the induction of inflammatory signalling in response to these agents. More precisely, we show that paclitaxel and docetaxel induce and ER stress response, which ultimately promotes a CHOP-dependent upregulation of the death receptor DR5. Taxane-induced cytokines are dependent on TRAIL death receptors and downstream death receptor-associated signalling molecules FADD and caspase-8. CRISPR-mediated ablation of the aforementioned molecules (CHOP, DR4, DR5, FADD and caspase-8) in HeLa cells afforded protection from taxane-induced cytokine production. Collectively, these data suggest that death receptor-induced inflammatory signatures may contribute to previously observed taxane-associated tumour metastasis and tumour progression.

Abbreviations

TNF	*Tumour necrosis factor*
ATF6α	Activating transcription factor 4 α
BIR	Baculovirus IAP repeat
BSA	Bovine serum albumin
CARD	Caspase recruitment domain
Cas	CRISPR-associated
CHOP	C/EBP homologous protein
CRISPR	Clustered regularly interspaced short palindromic repeats
crRNA	CRISPR RNA
CTLA4	Cytotoxic T lymphocyte antigen-4
DcR	Decoy receptor
DD	Death domain
DED	Death effector domain
DISC	Death-inducing signalling complex
DR4	Death receptor 4
DR5	Death receptor 5
ELISA	Enzyme-linked immunosorbent assay
EMT	Epithelial-to-mesenchymal transition
ER	Endoplasmic reticulum
ERAD	ER associated degradation
ERO1α	ER oxidase 1 α
EtBr	Ethidium bromide
FADD	Fas-associated death domain
FBS	Foetal bovine serum
HDR	Homology directed repair
HRP	Horseradish peroxidase
IAP	Inhibitor of apoptosis
IBM	IAP binding motifs

iNOS	Inducible nitric oxide synthase
ISR	Integrated stress response
LB	Lysogeny broth
LUBAC	Linear ubiquitin chain assembly complex
MAPK	Mitogen activated protein kinase
MDSC	Myeloid-derived suppressor cell
MLKL	Mixed-lineage kinase domain-like protein
MOMP	Mitochondrial outer membrane permeabilisation
NaI	Sodium Iodide
NHEJ	Non-homologous end-joining
NSCLC	Non-small cell lung cancer
OPG	Osteoprotegrin
PAM	Protospacer adjacent motif
PARP	Poly ADP ribose polymerase
PBS	Phosphate buffered saline
PD-1	Programmed death-1
PDAC	Pancreatic ductal adenocarcinoma
PERK	PKR-like ER kinase
RIDD	Regulated IRE1-dependent RNA decay
RING	Really interesting new gene
ROS	Reactive oxygen species
SDS	Sodium dodecyl sulphate
SOB	Super optimal broth
TAM	Tumour-associated macrophage
TBS	Tris-buffered saline
TNFR	Tumour necrosis factor receptor
tracrRNA	Trans-activating RNA
TRAIL	TNF-related apoptosis-inducing ligand
UPR	Unfolded protein response
xBP1	x-box binding protein 1

Introduction

1.1 TRAIL Signalling

1.1.1 A History

The tumour necrosis factor receptor (TNFR) family of cell surface receptors have been shown over the past two decades to induce inflammation, cellular proliferation, survival, differentiation or apoptosis - playing diverse roles in regulating functions such as inflammation, haematopoiesis, morphogenesis, immune signalling, tumorigenesis and viral replication (Aggarwal, 2003). In 1975, TNF, the first of a subset of TNF family members termed “death ligands”, was shown to have the ability to kill some endotoxin-induced cancers selectively (Carswell et al., 1975). However, it was quickly realised that the main function of TNF signalling is to promote inflammation – a property which was found to be responsible for the severe toxicity of this cytokine when introduced systemically (Roberts et al., 2011, Tracey et al., 1988, Tracey et al., 1987, Kettelhut et al., 1987). Interest then quickly turned to an additional death-inducing pathway: that of Fas/APO-1 which was found in a study aimed at characterising cell surface molecules involved in the control of the growth of malignant lymphocytes (Trauth et al., 1989). Monoclonal antibodies were raised against a human B lymphoblast cell line and subsequently tested against several malignant cell lines, including some patient derived leukaemic cells. Anti-Fas was found to induce apoptosis, or programmed cell death, in cell lines and xenotransplanted mice. A seminal study in the same year further characterised Fas as a target, with the introduction of a second anti-Fas antibody (Yonehara et al., 1989). However, anti-Fas antibodies were soon realised to cause apoptosis of primary human hepatocytes and to be lethal in mice due to an observed hepatotoxicity, as well as causing damage to the thymus and spleen (Ni et al., 1994, Ogasawara et al., 1993, Nishimura et al., 1997).

Finally in 1995, two decades after the first description of TNF, TNF-related apoptosis inducing ligand (TRAIL) was identified due to its 65% sequence homology to Fas ligand (Wiley et al., 1995). Wiley et al. showed that TRAIL, in contrast to other death ligands, is widely expressed in a range of tissues. Subsequent functional studies demonstrated the ligands ability to selectively kill an assortment of cancer cells, with most untransformed lines being resistant (Walczak et al., 1999, Jo et al., 2000, El-Deiry, 2001). Additionally, and importantly, TRAIL exhibited potent anticancer activity without the significant toxicity in normal tissues previously associated with CD95 and TNF therapies (Ashkenazi et al., 1999).

1.1.2 Apoptotic Signalling Pathways

Apoptosis is a form of death which allows for cells to be effectively removed when damaged or sufficiently aged, while minimising damage to surrounding cells. Apoptotic cells are morphologically very distinct, displaying cell shrinkage, rapid condensation and fragmentation of chromatin and budding of apoptotic bodies which contain cellular material from the cell surface. Ultimately, these cells are recognised and ingested by phagocytes (Arends and Wyllie, 1991, Kerr et al., 1994).

Three alternative signalling pathways signal apoptosis in mammalian cells – the cell extrinsic, cell intrinsic and granzyme B pathways (Bratton et al., 2000, Taylor et al., 2008). The intrinsic pathway is triggered in response to DNA damage, UV radiation and other types of cell stress which initiate mitochondrial outer membrane permeabilisation (MOMP) (Norbury and Hickson, 2001). Channel formation promoted by pro-apoptotic members of the Bcl-2 family (Bax and Bak) allows for release of cytochrome *c* (along with other factors) from the space between the inner and outer membranes of the mitochondria. Conversely, antiapoptotic Bcl-2 family members such as Bcl-2, Bcl-xL and Mcl-1 prevent channel formation (Cande et al., 2002, Cory and Adams, 2002). Upon its release cytochrome c binds to Apaf-1, ATP and procaspase-9 in the cytoplasm, forming the 'apoptosome', leading to proteolytic activation of procaspase-9 (Cain et al., 1999, Zou et al., 1999). Caspase-9 cleaves and activates 'effector caspases', initiating a cascade of caspase cleavages - caspase-3, -6 and -7 being important effectors (Taylor et al., 2008, Slee et al., 1999). SMAC/DIABLO, another factor released during MOMP, promotes apoptosis by binding to and inactivating inhibitor of apoptosis (IAP) proteins, thereby preventing them from attenuating caspase activation (Du et al., 2000, Verhagen et al., 2000). Activated caspase-3 has been shown to proteolytically cleave over 1000 intracellular substrates, ultimately leading to the phenotypical characteristics of programmed cell death. Poly (ADP) ribose polymerase (PARP), cytokeratins and laminins are examples, though there is a range of both structural and regulatory proteins on the list (Nicholson, 1999, Taylor et al., 2008). **(Figure 1.1)**.

The extrinsic pathway involves death receptor engagement and subsequent propagation of proapoptotic signals intracellularly. TRAIL is a type II transmembrane protein which signals via distinct receptors (Pitti et al., 1996, Wiley et al., 1995). It can be cleaved from the cell surface via its extracellular domain, then forming homotrimers that can recruit and bind to similarly complexed receptors on cellular membranes, (Hymowitz et al., 1999, Mongkolsapaya et al., 1999, Monleon et al., 2001). Currently, five concurrent receptors have been identified for TRAIL. Death receptor 4 (DR4)/TRAIL-R1 and death receptor 5 (DR5)/TRAIL-R2 are two homologous death receptors which contain intracellular death domains (DD) and signal apoptosis (Pan et al., 1997,

Sheridan et al., 1997, Walczak et al., 1997). Two decoy receptors (DcR) – DcR1 and DcR2, have been shown to bind TRAIL extracellularly but are unable to transduce signalling intracellularly. DcR1 lacks a cytosolic region and is anchored to the plasma membrane through a glycophospholipid moiety, while DcR2 contains a truncated and non-functional DD (Sheridan et al., 1997, Degli-Esposti et al., 1997, Marsters et al., 1997). Osteoprotegrin (OPG) is an additional receptor which has been shown to bind TRAIL, though the function of this interaction is not fully understood (Emery et al., 1998).

1.1.3 Death Receptor-Induced Cell Death

Trimerised receptor complexes have been shown to induce programmed cell death most aggressively (Hymowitz et al., 1999), inducing apoptotic signalling by facilitating a conformational change and the oligomerisation of intracellular DDs (Hymowitz et al., 1999). Trimerised receptor DDs recruit the adaptor molecular Fas associated death domain (FADD) via homotypic interactions with a similar DD in FADD (Jeong et al., 1999). FADD binds to caspases-8 (and to some extent caspase-10) via it's death effector domain (DED), allowing for clustering and trans-cleavage and autoactivation of these 'initiator caspases' by induced proximity (Cohen, 1997, Thornberry and Lazebnik, 1998, Carrington et al., 2006). This complex has been named the death-inducing signalling complex (DISC). Signalling mechanisms downstream of caspase-8 differ in mammalian cells depending on the cellular abundance of this caspase. In type II cells, where abundance of caspase-8 is relatively low and that of the caspase-3 inhibitor XIAP is high, it appears that there is not sufficient proteolytic presence to adequately cleave and activate downstream effector caspases (Cory and Adams, 2002). Instead, caspase-8 has been shown to cleave and activate BID, a Bcl-2 family member with a BH3 only domain which can translocate to mitochondria and allow for permeabilisation of the mitochondrial outer membrane and cytochrome c release (Cory and Adams, 2002). However, in type I cells, where caspase-8 is more abundant and XIAP less abundant, caspase-8 can directly cleave and activate 'effector' proapoptotic caspases (Muzio et al., 1998). **(Figure 1.1)**

1.1.4 IAPs As Regulators of Apoptotic Signalling Pathways

An important modulator of these signalling pathways are IAPs. Their function as caspase inhibitors has been well elucidated, though it is clear that they have important other functions in inflammation, NFκB activation and cancer. (Gyrd-Hansen and Meier, 2010). The three-main mammalian IAPs – XIAP, cIAP1 and cIAP2 – are homologous, containing baculovirus IAP repeat (BIR) domains (Birnbaum et al., 1994), a ubiquitin-associated domain, a really interesting new gene (RING) domain and a caspase

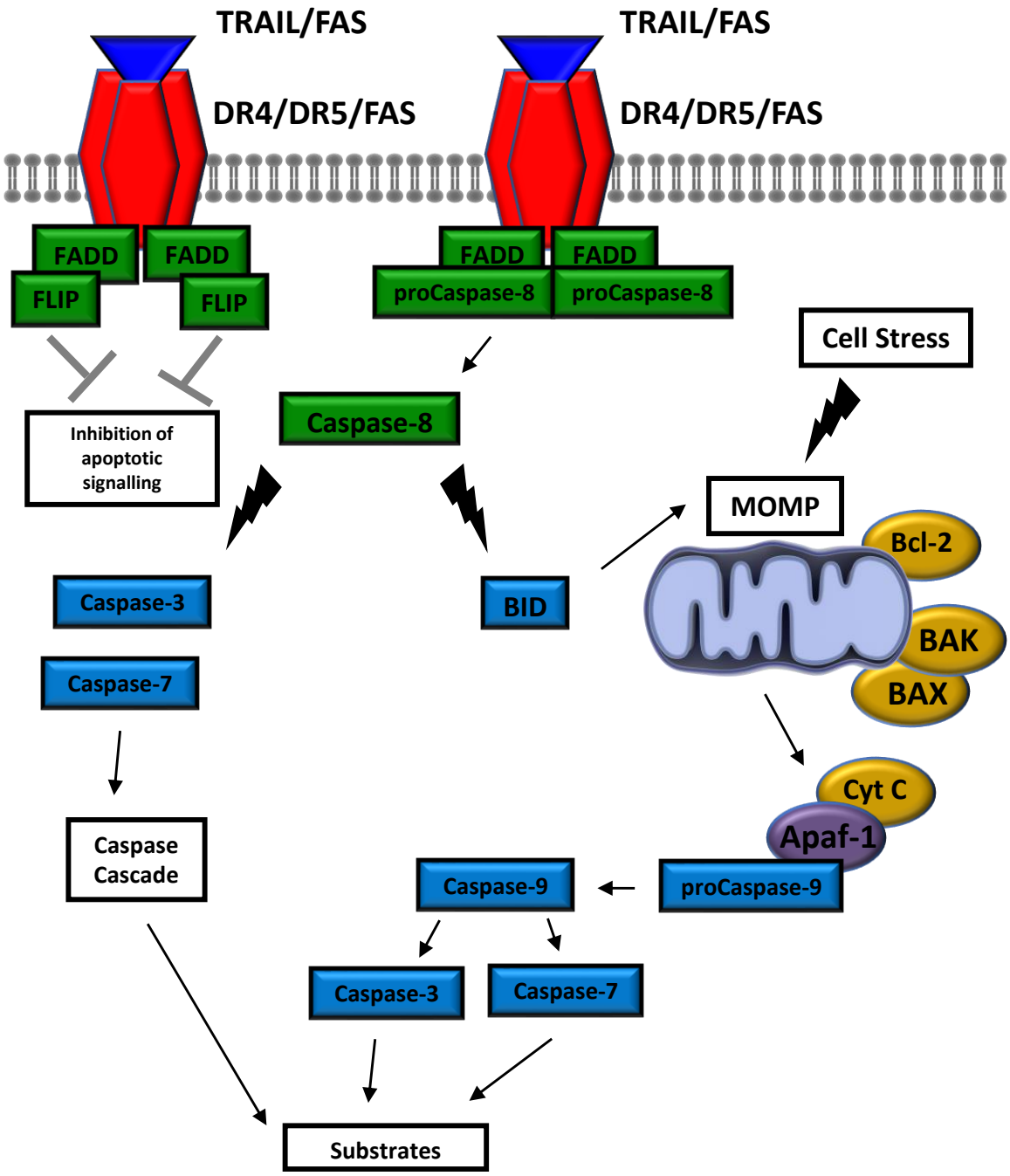

Figure 1.1 Apoptosis signalling pathways

Apoptosis can be initiated via the (a) intrinsic or (b) extrinsic pathway.

(a) Stimulation of death receptors (DR4, DR5 or CD95) by their cognate ligands (TRAIL or Fas Ligand) engages the extrinsic pathway of apoptosis. Ligation leads to receptor aggregation and recruitment of the adaptor molecules FADD and caspase-8. In type I cells caspase-8 becomes autolytically activated and directly cleaves effector caspases, initiating a cascade of downstream caspase cleavages which ultimately mediate apoptosis. In type II cells, caspase-8 cleaves BH3 only protein Bid, which subsequently translocates to the mitochondrial outer membrane, causing permeabilisation and ultimately apoptosis. The extrinsic pathway is regulated by levels of FLIP, an enzymatically dead homologue of caspase-8.

(b) The intrinsic pathways of apoptosis is initiated by cellular stress signals. Proapoptotic Bcl-2 family members such as BAX and BAK form channels in the mitochondrial outer membrane, allowing for release of apoptosome components cytochrome c, apaf-9 and procaspase-9 from the intermembrane space. Apoptosome formation allows for cleavage and release of mature caspase-9, which directly cleaves caspas-3 and induces apoptosis.

recruitment domain (CARD) (Dueber et al., 2011, Lopez et al.). The ring domain acts as an E3-ubiquitin ligase, while the ubiquitin-associated domain allows for binding of poly-ubiquitin chains. Activation of the CARD domain has been shown to inhibit the E3-ligase activity of IAPs (Lopez et al.). Meanwhile, the zinc-binding BIR domains allow for protein-protein interactions (Birnbaum et al., 1994). Type I BIR domains mediate interactions with a range of effectors such as TAB1, TAK1 and TRAF2, in some cases facilitating ubiquitination of these molecules. cIAP1 mediated binding and ubiquitination of TRAF2 has been shown to mediate TRAF2 driven NFκB activation. Similarly, cIAP2 and MALT1 interaction has been shown to stimulate formation of ubiquitin-dependent complexes that drive NFκB activation. (Samuel et al., 2006, Varfolomeev et al., 2006). Generation of K63- and M1-linked ubiquitin chains are particularly important for the formation of signalling complexes that promote MAPK and NFκB activation. Especially important targets are the ubiquitin binding proteins NEMO and TAB2 which are the regulatory subunits of IKK and TAK1 kinase complexes respectively (Chen, 2012, Schmukle and Walczak, 2012). In the context of TNF signalling cIAPs which are recruited to the receptor-associated signalling complex allow for ubiquitination of RIPK1, which subsequently conscripts three complexes which function to drive inflammatory signalling – the kinase complex (TAK1-TAB2-TAB3), the IKK complex (NEMO-IKKα-IKKβ) and finally, the linear ubiquitin chain assembly complex (LUBAC) (Silke, 2011). Type II BIR domains containing cleft abundant in hydrophobic residues which allows for complimentary binding to IAP binding motifs (IBMs) found in caspases and SMAC/DIABLO (Verhagen et al., 2006, Wu et al., 2000). XIAP specifically inhibits caspase-3 and -7 by binding directly to the active site of these enzymes, thereby preventing substrate entry and inactivating them (Deveraux et al., 1997). Similarly, XIAP binds to the dimerization domain of caspase-9, thereby preventing dimerization-induced activation of this caspase (Feltham et al., 2011).

IAPs are frequently seen to be upregulated in malignant tissues and this is often associated detrimentally with apoptosis resistance and the proliferation and survival of cancers – thus making them a very attractive target for drug development. The most widely developed therapeutic strategy to combat this effect are IAP antagonists (Fulda and Vucic, 2012). Specifically, mimetics of SMAC (an endogenous IAP antagonist) have been shown to directly trigger apoptosis of cancer cells, but also to sensitise cancer cells to cell death induced by cytotoxic agents such as conventional chemotherapies (LaCasse et al., 0000, Fulda, 2015, Zobel et al., 2006, Li et al., 2004). These antagonists bind to the BIR domains of IAPs, allowing for an activating conformational change and causing their autoubiquitination and proteosomal degradation (Sun et al., 2008).

The ripoptosome, a caspase-8/FADD/RIPK1 cytoplasmic death-inducing complex, assembles spontaneously in response to simultaneous deletion of cIAP1, cIAP2 and XIAP, (which occurs in response to genotoxic stress), as well as after treatment with SMAC mimetics. Ordinarily upon TNF stimulation, a TNFR1-associated complex I containing TRADD, RIPK1, TRAF2/5, LUBAC and IAPs forms, signalling canonical NFκB activation. Inhibition of RIPK1 ubiquitination (by deletion of IAPs) leads to the formation of a cytoplasmic complex II (the ripoptosome) where FADD and caspase-8 are recruited to free RIPK1. Ripoptosome formation is negatively regulated by IAPs, via targeting of ripoptosome components for proteosomal degradation. SMAC mimetic-induced ripoptosome formation can prime cells for cell death (assumedly by depleting IAPs). It has been shown that a genotoxic or cell stress-associated second stimulus then activates death (Tenev et al., 2011, Feoktistova et al., 2011).

1.1.5 Death Receptor-Induced Inflammation

Sporadic studies have found that TRAIL stimulation induces activation of NFκB and signals independently of apoptosis. This is interesting given that NFκB activation in this context was classically associated with having an anti-apoptotic effect (for example via the upregulation of IAPs, Bcl-xL or cFLIP) and inhibition of NFκB signalling (by overexpression of mutant IκBα) has been shown to increase sensitivity for induction of apoptosis (Jeremias et al., 1998, Keane et al., 2000). It is notable however that it has been shown in several instances that TRAIL receptor engagement can also result in the production of proinflammatory cytokines and chemokines, the importance of which has been largely overlooked (Berg et al., 2009). Indeed, TRAIL stimulation has additionally been shown to promote cell proliferation, motility and invasion and metastasis in K-Ras driven tumours models such as non-small cell lung cancer (NSCLS) and pancreatic ductal adenocarcinoma (PDAC) (Hoogwater et al., 2010, von Karstedt et al., Azijli et al., 2012).

TRAIL receptors are upregulated in many malignant tissues (Oikonomou et al., 2009). It seems paradoxical that death receptors are upregulated in cancers if indeed their main function is to confer sensitivity to death. A larger role for TRAIL in inflammatory signalling than has previously been appreciated may explain this. Indeed, TRAIL receptor expression has been, in some cases, associated with driving tumour growth (Baader et al., 2005, Siegmund et al., 2016). While it has been clear for some time that TRAIL receptor signalling can lead to diverse functions besides from apoptosis, the molecular determinants of these signalling pathways have been poorly understood until very recently.

A seminal paper in 2013 by Cullen et al. showed that engagement of the Fas death receptor-induced a plethora of chemokines which included IL-6, IL-8, CXCL1, MCP1 and GMCSF. It was elucidated that IL-8 and MCP-1 in particular were important for migration of phagocytic cells towards apoptotic cells, serving as what were dubbed "find-me" signals. They additionally showed that RIPK1 and IAPs are required for chemokine production (Cullen et al., 2013). Interestingly, release of receptor localised caspase-8 into cytoplasmic complexes has been shown to be necessary for effective apoptosis (Kang et al., 2008). It is interesting to note that levels of Fas stimulation that are insufficient to induce killing can still induce NFκB, potentially making this a more physiologically relevant function of death receptor signalling (O' Reilly et al., 2009).

Two very recent studies in Molecular Cell have highlighted the similar importance of TRAIL-induced inflammation. A study from our group highlighted the role of caspase-8 as a scaffold, independent of its enzymatic functions, in propagating signals downstream of death receptors and FADD (Henry and Martin, 2017). The study showed that while caspase-8 knockout or knockdown ablated TRAIL-induced death and cytokines, caspase inhibition blocked cell death, but not cytokine production seen in response to TRAIL. Indeed, in some cell types, this inhibition increased the production of some cytokines. This is likely due to caspase inhibition leading to stabilisation of the secondary cytoplasmic signalling complex, which has been previously described in the context of both Fas (Geserick et al., 2009) and TRAIL (Varfolomeev et al., 2005). Varfolomeev and colleagues observed an initial receptor associated DISC of FADD and caspase-8 (complex I) and a secondary cytoplasmic complex which retains FADD and caspase-8 but also recruits NFκB driving effector molecules such as RIPK1, TRAF2 and NEMO (Varfolomeev et al., 2005). Henry et al. additionally proposed the formation of a receptor-associated and potentially cytoplasmic "FADDosome" complex containing FADD, caspase-8, RIPK1, $FLIP_L$, caspase-10, TRAF2, NEMO and TAK1 (Henry and Martin, 2017), a pathway which shows striking similarities to that of TNF-induced cytokine and chemokine production (Walczak, 2011). **(Figure 1.2)**

Henry et al. additionally showed that TRAIL produces very physiologically relevant amounts of chemokines and cytokines that are capable of inducing chemotaxis of neutrophils and monocytes (Henry and Martin, 2017). Hartwig et al. similarly showed that TRAIL-induced CCL2/MCP-1 was capable of polarising macrophages towards the M2 phenotype (Hartwig et al., 2017) which has been shown to promote tumour growth.

Elucidation of the importance of TRAIL-induced cytokines proposed many questions for previous studies and clinical trials which may have underestimated the importance of these effects. Additionally, while it is clear that the molecular pathway of

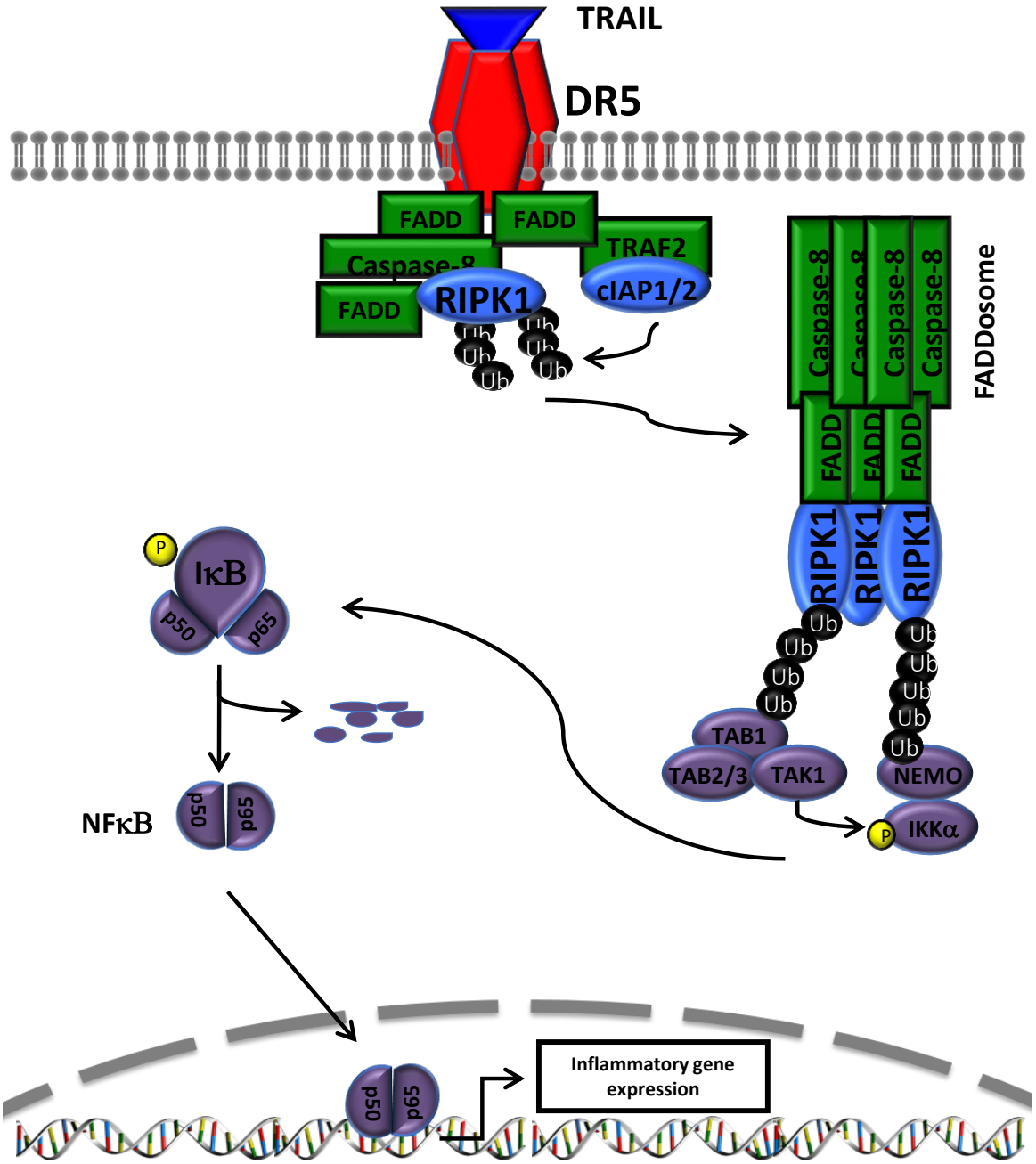

Figure 1.2 Death receptor ligation promotes the formation of inflammatory signalling complexes that drive NFkB activation and inflammatory cytokine and chemokine production

Ligation of death receptors DR4 or DR5 by their cognate TRAIL ligand leads to receptor trimerisation and formation of the DISC. FADD is recruited to the DISC via its DD, while caspase-8 is recruited downstream via its DEDs. RIPK1 associates with the receptor-associated complex via DD interactions with FADD. Oligomerisation of caspase-8 occurs via homotypic DED2-DED2 interactions, allowing for the formation of a soluble aggregate that act as a scaffold. Stabilised FADD associates with caspase-8 and facilitates the successive recruitment of RIPK1 to form what has been dubbed the "FADDosome" complex. TRAF2 binding to FADD allows for IAP association with the complex and subsequent addition of ubiquitin chains to RIPK1. Modified RIPK1 can recruit the TAB/TAK1 and IKK complexes, ultimately leading to the phosphorylation and degradation of IkB. The p50 and p65 NFkB subunits are then free to translocate to the nucleus, leading to downstream activation of inflammatory signalling.

TRAIL-induced inflammation has now been described in detail, it is currently unclear in what specific contexts TRAIL may promote inflammation and where it may be most important physiologically.

1.2 ER Stress

1.2.1 ER Stress Pathways

The endoplasmic reticulum (ER) is an essential organelle in eukaryotic cells that acts as the site of folding for transmembrane and secreted proteins, with many posttranslational modifications such as glycosylation and the formation of disulphide bonds being performed within (Araki and Nagata, 2011). The protein folding capacity of the ER is plastic and can increase rapidly and transiently in a number of different scenarios, including during plasma cell antibody secretion (Ma and Hendershot, 2003). Similarly, pathological, physiological and often environmental conditions can alter the homeostasis of protein folding in the ER, leading to an accumulation of misfolded proteins in the lumen (Walter and Ron, 2011). Quality control mechanisms ensure that misfolded proteins are removed from the ER and that fidelity is maintained (Walter and Ron, 2011). The ER-associated degradation (ERAD) pathway, which is dependent on E3 ubiquitin ligases and proteosomal degradation, ensures that misfolded proteins are removed (Smith et al., 2011).

The unfolded protein response (UPR) is a collective term used to describe a number of signalling pathways that have evolved to detect ER stress and maintain homeostasis within the ER. Three sensors, transmembrane proteins in the outer membrane of the ER, sense the accumulation of misfolded proteins in the lumen. Namely, PKR-like ER kinase (PERK), inositol-requiring enzyme 1α (IRE1α) and activating transcription factor α (ATF6 α), are maintained in an inactive, monomeric state by the binding immunoglobulin protein (BiP) (Bertolotti et al., 2000a, Shen et al., 2002). Increased levels of improperly folded substrates (beyond the capacity of foldases, chaperones, glycosylases etc.) leads to sequestration of BIP away from these ER sensors, allowing for their oligomerisation, autophosphorylation and activation (Bertolotti et al., 2000b, Shen et al., 2002). Activation of these ER stress pathways leads to a widespread attenuation of protein synthesis and the upregulation of many genes, including those encoding foldases, glycosylases and chaperones - effects which collectively attempt to restore the homeostasis of the ER **(Figure 1.3)**.

PERK homodimerizes and autophosphorylates after BiP dissociation, becoming activated (Volmer et al., 2013). PERK attenuates translation directly by phosphorylating the eukaryotic translation initiation factor eIF2α, thus inactivating the guanine nucleotide

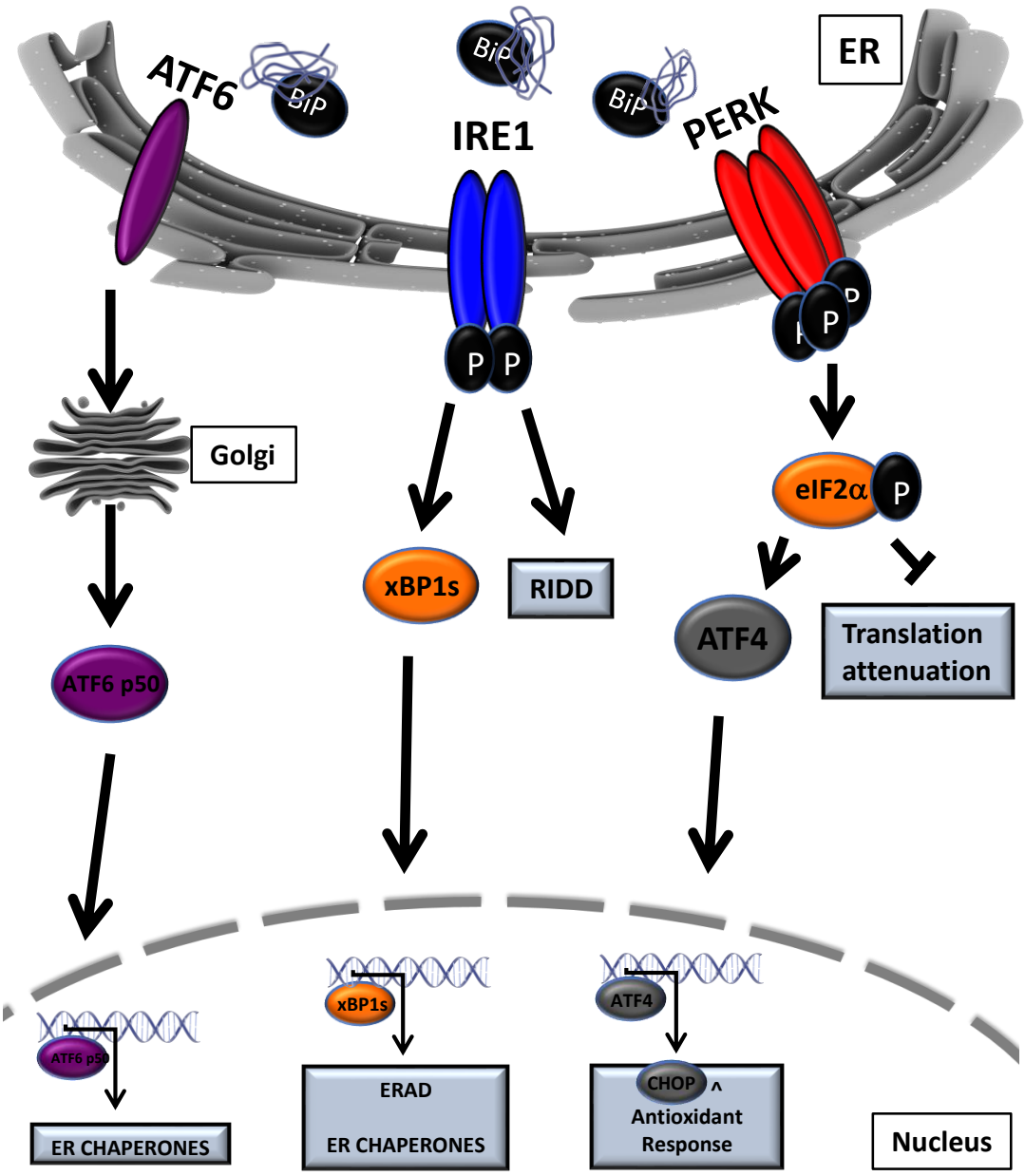

Figure 1.3 The unfolded protein response

Increased levels of improperly folded proteins in the ER lumen leads to sequestration of BiP away from ER membrane associated receptors ATF6, IRE1 and PERK. Free PERK and IRE1 oligomerise and are activated by autophosphorylation. Activated PERK phosphorylates eIF2a, leading to widespread translation attenuation and selective upregulation of the transcription factor ATF4. ATF4 transcriptionally upregulates the transcription factor CHOP. Activated IRE1 processes xBP1 to its active form, xBP1s. IRE1s endonuclease domain carries out RIDD of selected mRNA. Released ATF6 is translocated to the golgi in COPII coated vesicles. It then undergoes regulated intramembrane proteolysis by site 1 and site 2 proteases (S1P and S2P), releasing an active bZIP transcription factor from its amino terminal which can then translocate into the nucleus.

Overall, the UPR leads to upregulation of genes encoding chaperones, foldases, glycosylases, oxidoreductases, the antioxidant response and ERAD machinery in an attempt to restore ER homeostasis.

exchange factor that recycles it to its active GTP bound form (Harding et al., 1999). General translation attenuation selectively promotes the translation of some transcripts that contain short upstream open reading frames in the 5' untranslated regions. The bZIP, ER stress-associated activating transcription factor 4 (ATF4) is an example of this (Harding et al., 1999). ATF4 promotes the upregulation of an additional transcription factor named C/EBP homologous protein (CHOP), though it is notable that xBP1s and ATF6 may also upregulate CHOP (B'Chir et al., 2013, Ron and Walter, 2007). These transcription factors collectively upregulate genes that are associated with increased amino acid biosynthesis and transport, as well an increase in autophagy, of which amino acids are a by-product (B'Chir et al., 2013, Han et al., 2013). CHOP induction of the ER oxidase 1α (ERO1α) promotes oxidative protein folding in an attempt to restore protein folding homeostasis (Marciniak et al., 2004). Increased reactive oxygen species (ROS) production due to increased disulphide bond formation and increased amino acid biosynthesis is combatted by PERK phosphorylation and stabilisation of the transcription factor Nrf2 (which mediates an antioxidant response) (Cullinan et al., 2003) and an enhanced glutathione synthesis (Rouschop et al., 2013). ATF4 additionally plays a cytoprotective role by upregulating genes involved in amino acid biosynthesis and transport (Harding et al., 2003). This collective ATF4/CHOP-dependent response has been termed the integrated stress response (ISR).

The ERs second transmembrane sensor, IRE1, contains two functional domains – an endoribonuclease domain and a kinase domain. Upon BiP sequestration away from the receptor, IRE1 undergoes dimerization and autophosphorylation, which leads to a conformational change which in turn allows for allosteric activation of its endoribonuclease domain. The main downstream function of IRE1s endoribonuclease domain is direct cleavage of a 26-nucleotide fragment from the mRNA of x-box binding protein 1 (xBP1) (which is later re-ligated), allowing for the formation of the active transcription factor xBP1s (Lu et al., 2014b, Yoshida et al., 2001). xBP1s is a highly functioning transcription factor that upregulates genes such as those encoding foldases, oxidoreductases, glycosylases and ERAD machinery (Shoulders et al., 2013).

ATF6 is a type II transmembrane protein with a carboxyl terminal that faces the ER lumen, while a bZIP transcription factor is at its amino terminal. In response to ER stress, following release from BiP, reduced monomeric ATF6 is transported to the Golgi apparatus in COPII coated vesicles (Haze et al., 1999, Yoshida et al., 1998). ATF6 then undergoes regulated intramembrane proteolysis by site 1 and site 2 proteases (S1P and S2P) (Ye et al., 2000), releasing an active bZIP transcription factor from its amino terminal which can then translocate into the nucleus. Active ATF6α upregulates genes

encoding foldases and ERAD machinery (Adachi et al., 2008), as well as xBP1 (Yoshida et al., 2001).

1.2.2 ER Stress-Induced DR5 Upregulation and Cell Death

Subsequent to ATF4 upregulation of CHOP, expression of GADD34 (a phosphatase subunit) is also induced. GADD34 dephosphorylates eIF2α, allowing for the resumption of protein synthesis after unfolded proteins have been removed from the ER lumen (Marciniak et al., 2004). However, reestablishment of ER homeostasis is not always achievable. Chronic activation of ER stress leads to programmed cell death if the corrective measures of the UPR are insufficient (Wang and Kaufman, 2014). The molecular determinants of this have very recently been elucidated. **(Figure 1.4)**

ER stress in some cases correlates with or activates the intrinsic or mitochondrial apoptotic pathway. Downregulation of antiapoptotic molecules has been observed in several instances of ER stress. For example, Mcl-1 has been shown to be downregulated due to the inhibitory effect PERK has on protein synthesis in response to 2-deoxy-glucose, while Bcl-2 has been shown to be downregulated at the transcriptional level by CHOP (McCullough et al., 2001, Ramirez-Peinado et al., 2011). Additionally, IRE1-dependent JNK activation has been linked to phosphorylation and inactivation of Bcl-2 and Bcl-xL (Fan et al., 2000). BH3-only proteins such as Puma and Noxa also appear to be important in some contexts of ER stress-induced cell death, as knock-out of the latter desensitises cells to thapsigargin and tunicamycin (Kim et al., 2009, Reimertz et al., 2003). Noxa has additionally been shown to be upregulated in response to glucose deprivation and ROS dependent ER stress (Ramirez-Peinado et al., 2011, Verfaillie et al., 2013). Caspase-9 and caspase-3, but not caspase-8, deficient MEF cells are resistant to thapsigargin, tunicamycin and brefeldin A (Masud et al., 2007). CHOP has been shown to sensitise cells to ER stress by downregulating antiapoptotic Bcl-2 family members, causing sensitisation to tunicamycin and thapsigargin (McCullough et al., 2001).

There are also several mitochondrial-independent forms of cell death that occur in response to ER stress. While general activation of the ER membrane sensor IRE1 appears to mediate prosurvival signalling, prolonged engagement can be proapoptotic. RIDD of ER associated mRNA and microRNAs is mediated in a sequence specific manner via IRE1s cytoplasmic nuclease domain and has been shown to be ultimately proapoptotic (Hollien et al., 2009, Lerner et al., 2012, Moore and Hollien, 2015, Hollien and Weissman, 2006). IRE1 has been shown to recruit apoptosis signalling kinase 1 (ASK1), which in turn engages TRAF2 and its downstream target x-Jun N-terminal kinase (JNK) which has been shown to induce apoptotic pathways (Urano et al., 2000).

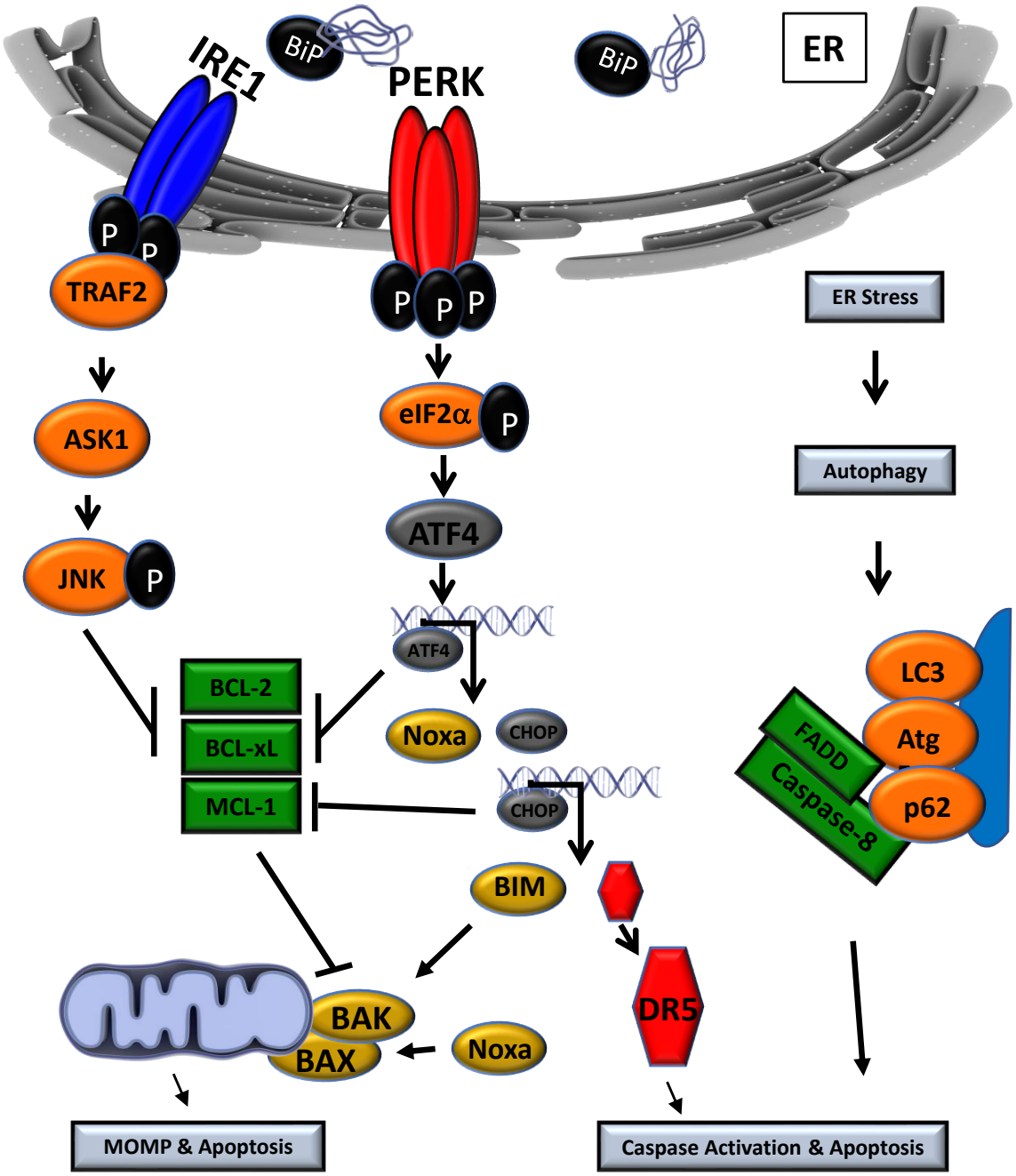

Figure 1.4 The unfolded protein response and cell death

Under conditions of ER stress, PERK-dependent activation of ATF4 and Noxa. CHOP, which can be induced downstream of PERK, or ATF6, induces expression of Bim. BIM and Noxa activate the mitochondrial pathway of apoptosis. CHOP and ATF4 also inhibit antiapoptotic BcL-2 family members such as Bcl-2, Bcl-xL and Mcl-1. IRE1 can recruit TRAF2, which activates ASK1 and its downstream target JNK. JNK can then induce apoptosis by inhibiting anti-apoptotic proteins such as Bcl-2 and Bcl-xL.

Persistent ER stress can result in cell death through CHOP-induced expression of DR5, thus promoting caspase-8 activation and cell death.

Autophagy can be induced upon ER stress condition and a death platform on autophagosomal membranes can be formed upon ubiquitination of caspase-8 and its recruitment by p62 on this platform. A complex of LC3, Atg5, FADD, p62 and caspase-8 has been described under ER stress on autophagosomal membranes, resulting in oligomerization and activation of caspase-8.

IRE1 has also been shown to promote mRNA mediated decay of antiapoptotic proteins (Chen and Brandizzi, 2013).

Extended periods of cellular ER stress has for years been associated with death receptor upregulation, with classical ER stress inducing agents such as Tunicamycin being shown to increase surface expression of both DR4 and DR5 (Jin et al., 2004). While persistent ER stress in response to agents such as thapsigargin, tunicamycin or brefeldin A is associated with accumulation of DR5 via PERK-dependent upregulation by the transcription factor CHOP and apoptosis induction, regulated IRE1-dependent RNA decay (RIDD) has been shown to transiently reduce DR5 mRNA levels (Lu et al., 2014a). DR5 has additionally been proposed to be upregulated in a PERK-dependent but CHOP-independent manner in response to these agents (Martin-Perez et al., 2012). DR5 was thus proposed as a molecule of convergence for several ER stress-associated signals, acting to control cell fate decisions depending of the context of ER homeostasis. In summary, unrelenting ER stress was shown to lead to a ligand-independent activation of DR5 signalling, leading to caspase-8-dependent apoptosis (Lu et al., 2014a).

ER stress has also been linked with a ligand-independent, TNF-R1 mediated, induction of necroptosis, a regulated RIPK1/RIPK3 and mixed lineage kinase domain-like protein (MLKL)-dependent form of necrosis (Saveljeva et al., 2015). Repression of TNF-R1, RIPK1 or MLKL led to a switch to apoptosis mediated cell death, while concurrent caspase inhibition mediated a switch back to RIPK1 dependent necroptosis (Saveljeva et al., 2015). More recently, it has been shown that persistent ER stress can lead to death ligand-independent cell death via caspase-8 under conditions of autophagy and apoptosis (Tomar et al., 2013). Autophagy is activated in response to ER stress and can degrade misfolded proteins, though it also plays an important role in apoptosis. Caspase-9, FADD and Atg5 were recruited to the membrane of autophagosomes, resulting in a caspase-8 dependent cell death. This phenomenon has been illustrated in response to tunicamycin and thapsigargin (Tomar et al., 2013). Additionally, RIPK1 has been proposed as an upstream interactor of caspase-8 in a death receptor-independent complex which induces apoptosis under unresolved ER stress conditions (Estornes et al., 2014). The authors proposed that RIPK1 regulates caspase-8 activity through its interaction with IRE1.

1.2.3 ER Stress Inducing Agents

Classically, three chemical activators have been used in studies of ER stress in vitro: Thapsigargin, Tunicamycin and Brefeldin A.

Thapsigargin, a sesquiterpene lactone isolated from the *Thapsia garancia* plant, was widely used in traditional medicine (Gerard, 1974). Early studies attributed the

effects of Thapsia to the organic compounds called sesquiterpenoids, claiming that they cause histamine release (Christensen et al., 1997, Rasmussen et al., 1978). Later studies elucidated that Thapsigargin is a specific inhibitor of the ER Ca^{2+} ATPases, acting to arrest the pump and causing discharge of Ca^{2+} from the ER into the cytosol of cells (Thastrup et al., 1990). It does so irreversibly and very effectively, even at subnanomolar concentrations (Sagara and Inesi, 1991). Inhibition in this way ultimately causes apoptosis, a characteristic that was quickly exploited for cancer therapy (Christensen et al., 1999). Given the lack of cell type specific targeting associated with thapsigargin and its analogues, a prostate cell specific, membrane antigen activated, prodrug was developed which took advantage of the expression of prostate specific antigen and carboxypeptidase prostate-specific membrane antigen specifically on prostate cancer endothelial cells (Denmeade et al., 2012). Mipsagargin (G-202) is currently in phase II clinical trials.

Brefeldin A is a *Candida albicans* metabolite which was initially isolated for its apparent antibiotic properties (Tamura et al., 1968). There appears to be multiple targets for this molecule, though the main one seems to be ADP ribosylation factor, a factor responsible for the association of coat protein to vesicles trafficking at the golgi apparatus (Helms and Rothman, 1992). Brefeldin A reversibly impedes anterograde transport from the ER to the golgi, leading to an accumulation of proteins in the ER and a blockage in protein secretion (Klausner et al., 1992, Pelham, 1991). Prolonged exposure to Brefeldin A induces programmed cell death (Shao et al., 1996).

Tunicamycin, isolated from *Streptomyces lysosuperifcus* in 1970, was initially observed for its antibiotic properties (Takatsuki and Tamura, 1971). It also selectively inhibits glycoprotein component formation in microorganisms, as well as protein glycosylation in mammalian cells (Takatsuki et al., 1975, Tkacz and Lampen, 1975, Olden et al., 1979)

1.2.4 ER Stress And Inflammation

It is now well known that ER stress can induce inflammation in a number of contexts, including in response to metabolic stress, glucose deprivation and ROS (Kim et al., 2015, Zhang and Kaufman, 2008). Malignancy-associated inflammation has additionally been associated with being ER stress derived in some cases (Verfaillie et al., 2013). Additionally, the ER stress-inducing agent thapsigargin has sporadically been associated with having proinflammatory effects, including stimulation of histamine release from immune cells, NFκB activation and cytokine production (Keestra-Gounder et al., 2016, Kim et al., 2012). Also in line with this, treatment of tumour-bearing mice with thapsigargin induced ER stress-dependent infiltration of tumour suppressive

myeloid derived suppressor cells into the tumour microenvironment (Lee et al., 2014). Thus, we wondered whether DR5 upregulation in response to ER stress may be causative for cytokine and chemokine production that has sporadically been reported.

1.3 Apoptosis Pathways in Cancer and Chemotherapy

1.3.1 Apoptosis Pathways, Tumour Resistance and Chemotherapy

Monoclonal agonistic antibodies against both DR4 and DR5 have showed potent tumour killing activity in preclinical *in vitro* and mouse studies (Chuntharapai et al., 2001, Ichikawa et al., 2001). These antibodies were subsequently put through numerous clinical trials and while agonistic TRAIL antibodies were well tolerated and widely anticipated, they showed disappointing results in clinical trials – both alone and in combination with chemotherapeutic drugs (Takeda et al., 0000). While TRAIL is a very attractive therapeutic target, a problem remains: many tumours eventually develop resistance. Disruption of death receptor signalling pathways has been associated with the development of resistance to TRAIL in tumorigenic cells, primarily due to a decrease in the expression of or malfunctioning proapoptotic molecules or an increase in the expression on anti-apoptotic molecules.

High expression of TRAIL decoy receptors has been associated with conferring resistance, presumably by competing with DR4 and DR5 for TRAIL. DcR1 has been shown to be overexpressed in tumours of the gastrointestinal tract in response to genotoxic stress, conferring resistance from TRAIL induced-apoptosis (Sheikh et al., 1999). Both DcR1 and DcR2 are differentially expressed in pancreatic cancer cells in comparison to normal pancreatic cells, while DcR1 has been found to be highly expressed in leukemic blasts and associated with poor outcome and resistance (Liao et al., 2001, Chamuleau et al., 2011).

c-FLIP is a homologue of procaspase-8 which harbours a non-functional catalytic domain, but contains DEDs and is capable of binding to FADD in a similar manner to caspase-8 (Irmler et al., 1997). These interactions can prevent proapoptotic signalling from propagating downstream of death receptors. It has been proposed that high levels of c-FLIPs may contribute to TRAIL resistance by competing with caspase-8 and this appears to be the case in several instances (Leverkus et al., 2000, Harper et al., 2001, MacFarlane et al., 2002). It is possible that FLIP recruitment determines whether the outcome of death receptor engagement is apoptosis or survival. Interestingly, cFLIP has also been proposed to inhibit cell death in response to some chemotherapeutics (Longley et al., 2006).

Death receptors are seen to be downregulated or not present in a range of resistant types of tumour. Impaired trafficking of DR4 and DR5 from intracellular

compartments to the cell membrane has been associated with TRAIL resistance in colon cancer cells (Jin et al., 2004). Both DR4 and DR5 are located on chromosome region 8q, where loss of heterozygosity is frequently seen in cancers and is often associated with aggressive forms of disease (Adams et al., 2005, Yaremko et al., 1996). For example, this phenomenon has been attributed to loss of DR4 or DR5 function in studies in nasopharygeal, head and neck cancers and non-Hodgkins lymphoma (Ozoren et al., 2000, Pai et al., 1998, Lee et al., 2001).

A persistent mechanism that appears to account for the synergistic effect of TRAIL and widely used cytotoxic agents is the transcriptional upregulation of TRAIL receptors DR4 and/or DR5 (Gibson et al., 2000, Arts et al., 2004, Meng and El-Deiry, 2001b). Ionising or γ-irradiation was early on shown to sensitise breast cancer cells to TRAIL-induced apoptosis, with the effect being attributed to irradiation-induced upregulation of DR5 (Chinnaiyan et al., 2000). An additional study showed a correlation between effectiveness of combined therapy with TRAIL and irradiation and cell types expressing at least one agonistic TRAIL receptor, FADD and caspase-8 or caspase-10 (Marini et al., 2003). In human gliomas it has been shown that DNA damaging agents such as cisplatin and etoposide upregulate DR5 and that cooperative effects of combination therapy can be blocked with DR5-Fc neutralisation of TRAIL or with caspase inhibitors (Nagane et al., 2000). Similarly in resistant colonic carcinoma cells, CPT-11 treatment caused a p53-dependent activation of DR5 which reconstituted a TRAIL-associated type I apoptotic pathway (Wang and El-Deiry, 2003). It is clear however that p53 is not necessary in all cases as the glucocorticoid dexamethasone elevated DR5 in glioblastoma, ovarian cancer, and colon cancer cell lines with mutant p53. This induction was inhibited by the transcriptional inhibitor actinomycin D (Meng and El-Deiry, 2001a).

One particularly interesting synergy is that of TRAIL and taxanes. Cooperative effects have been shown in multiple cell types, including glioblastoma multiforme and prostate cancer, with the latter being attributed to an increased expression of DR4 and DR5 protein levels (Dorsey et al., 2009, Nimmanapalli et al., 2001). Initial TRAIL therapy formulations in combination with paclitaxel were disappointing, however. A phase II study combining Dulanermin (a soluble, recombinant TRAIL) and paclitaxel for treatment of NSCLC showed that the dual-therapy had no impact on overall survival or progression free survival of patients (Soria et al., 2011). The combination of paclitaxel and mapatumumab or tigatuzumab, agonistic antibodies against DR4 and DR5 respectively, made it as far as Phase II clinical trials in patients with advanced NSCLC (von Pawel et al., 2014, Reck et al., 2013). However, neither study elucidated any clinical benefit from additive therapies. Min and colleagues in 2015 developed a nanoparticle albumin-bound

paclitaxel formulation with TRAIL embedded, an effective method for delivering hydrophobic chemotherapeutics (Min et al., 2015). The formulation showed promising results in *in vitro* and *in vivo* pancreatic cancer models, even in comparison to a nanoparticle albumin-bound paclitaxel alone. Following clinical trials, paclitaxel albumin-stabilised nanoparticle formulation called Abraxane was approved for metastatic pancreatic cancer, NSCLC and breast cancer as of September 2013 (Gradishar et al., 2005). This leaves much hope for the combined formulation.

It is interesting to note that some chemotherapeutic agents have classically been associated with secondary inflammation and NFκB activation, ultimately leading to tumour metastasis and tumour recurrence (Toste et al., 2016). Cisplatin, paclitaxel, doxorubicin and 5'flourouracil are examples of chemotherapeutic agents which have been associated with inflammation and ultimate tumour metastasis in a range of different cancers (Ohta et al., 2006, Mabuchi et al., 2004, Vyas et al., 2014). Overall low response to Paclitaxel, especially in breast cancer patients, limits its clinical use, primarily because of recurrence after cessation of therapy (Gradishar et al., 2005). Initial data generated by our group (Henry C.M. & Sullivan G. personal communication) elucidated a role for DR5 in taxane-induced cytokine production. Here we aimed to elucidate this pathway further.

1.3.2 Taxanes

Taxanes, a class of microtubule disruptor including Paclitaxel, Docetaxel and Carbazitaxel have been widely used as a cancer chemotherapeutic since 1993 when Paclitaxel was first approved for use in ovarian cancer. They have since been used to treat lung, breast, prostate, head and neck and a range of other cancers. In 1971 the structure of an extract from the pacific yew tree, *Taxus brevifolia* (which was then named Taxol) was first elucidated following a natural products screening programme carried out by the US National Cancer Institute (Wani et al., 1971). The use of plant cell fermentation by Bristol-Myers Squib allowed for the more efficient production of Taxol (Paclitaxel) and the introduction of a new taxane – Docetaxel – which is produced from the European yew, *Taxus baccata*. Docetaxel went on to become a leading treatment for late stage breast cancer following a series of clinical trials (Jones et al., 2005, Nabholtz et al., 1999). However, it was noted that while Docetaxel showed greater efficacy, Paclitaxel showed greater tolerance. This provided a rationale for providing more regular doses with the result of a greater overall outcome (Marchetti et al., 2002). Both early taxanes have since been shown to also be efficacious in early stage breast cancer (De Laurentiis et al., 2008, Ellis et al., 2009). Today Docetaxel (Taxotere) is in many cases the first line

treatment for prostate cancer, while Paclitaxel (Taxol) is the first line treatment for ovarian cancer.

It was subsequently shown that Taxol prevented the replication of cancer cells by over-stabilising microtubules, thus arresting cells in the G2-M phase of the cell cycle due to inhibition of the normal processes of mitosis (Schiff and Horwitz, 1980). Preventing the formation of the mitotic spindle and disrupting sister chromosome orientation leads to chronic activation of the spindle assembly checkpoint and ultimately cell cycle arrest (Kelling et al., 2003, Musacchio and Salmon, 2007). Binding to tubulin, taxanes promote the assembly of microtubules by shifting the binding equilibrium of tubulin in favour of assembly, thereby reducing disassembly (Schiff et al., 1979, Diaz and Andreu, 1993, Diaz et al., 1993). The blockage of mitosis in this way has been shown to induce programmed cell death in cancer cells (Martin and Cotter, 1990, Wertz et al., 2011).

1.4 CRISPR-Mediated Gene Editing

Clustered regularly interspaced short palindromic repeats (CRISPR) are repetitive regions of prokaryotic genomes, that are found in approximately 40% of prokaryotes and almost all archaea. These genomes contain CRISPR arrays - non-repetitive elements, which have been termed spacers, interspaced by direct repeats (Jansen et al., 2002, Kunin et al., 2007). In 2005, three separate groups identified the spacers between CRISPR repeats as derived from phage DNA or extrachromosomal DNA such as plasmids (Pourcel et al., 2005, Mojica et al., 2005, Bolotin et al., 2005). Bolotin et al. hypothesised that the spacer elements are traces of past invasions by extrachromosomal elements. These elements serve as a heritable sort of adaptive immune system against specific elements in prokaryotes (Morange, 2015). In 2007 this idea was illustrated when it was shown that after viral challenge, bacteria integrated new spacers derived from phage genomic sequences. Removal or addition of particular spacers modified the phage-resistance phenotype (Barrangou et al., 2007a).

CRISPR-associated (Cas) proteins, which are encoded for by Cas genes which flank CRISPR arrays in the genome, are important players in the execution of the three steps of CRISPR-derived immunity - acquisition, integration and interference. CRISPR-Cas systems are classified into “Types” based on the signature genes present. The most widely studied is that of Type II CRISPR systems, where Cas9 is the sole CRISPR associated nuclease required for interference (Makarova et al., 2011).

Firstly, integration of short sequences from invading microorganisms are incorporated into the genome as spacers. Selection of protospacer sequence from invading genomes is dependent on the presence of an adjacent protospacer adjacent

motif (PAM) (Mojica et al., 2009). This requirement acts to prevent self-targeting of the PAM-free CRISPR loci. In some systems, spacer integration has been show to occur at the leading end of CRISPR repeats, causing duplication of the first repeat to maintain the repeat-spacer framework (Barrangou et al., 2007b). Secondly, CRISPR loci are transcribed and processed to form small guide RNA molecules called CRISPR RNA (crRNA). In type II systems, precrRNA which is transcribed from CRISPR arrays, is base paired by a trans-activating crRNA (tracrRNA) which has a sequence complimentary to the CRISPR repeat sequence (Deltcheva et al., 2011). This complex is stabilised by Cas9, allowing RNase III to cleave the precrRNA at the repeat (Garrett et al., 2015). Lastly, crRNA serve as templates for interference of target DNA (van der Oost et al.). In *Steptococcus pyogenes*, a commonly studied type II system, trimming by an unknown nuclease then occurs to convert a 30 nucleotide sequence to the 20 nucleotide sequence that acts as a template for Cas9 (Deltcheva et al., 2011). **(Figure 1.5)**

The architecture of Cas9 is separated into two lobes – the nuclease lobe and the nucleic acid binding lobe. In its inactive state, Cas9 is restricted and incapable of DNA binding. However, it has been shown that upon association with a guide RNA, it undergoes a conformational change which allows for interaction with DNA (Jinek et al., 2014). The nuclease domain contains a C-terminal end which is essential for initial PAM binding. In *S. pyogenes*, the PAM sequence recognised by Cas9 is a 5'-NGG-3'. Upon recognition of the PAM, the nucleic acid binding lobe encourages unwinding of target DNA in the 3' direction, beginning at the seed region directly adjacent to the PAM (Anders et al., 2014, Sternberg et al., 2014). Two nuclease domains which are orientated to span and cleave opposite ends of double-stranded DNA. The RuvC domain is positioned to cleave the non-target strand, while the HNH domain is positioned to cleave the target strand (Nishimasu et al., 2014). Mismatches outside the seed region are more tolerated than those closer to the PAM (Cong et al., 2013).

Jinek and colleagues engineered a combined single-guide RNA by fusing the previously described tracrRNA and crRNA. By manipulating the spacer sequence, they could use their fusion in combination with Cas9 to direct targeted cleavage (Jinek et al., 2012). In 2011, Feng Zhang's group in the Broad Institute of MIT and Harvard were the first to describe the adaptation of CRISPR-Cas9 for genome engineering in mammals. They demonstrated targeted cleavage of human genomes using two prepared Cas9 molecules – from *S. pyogenes* and *S. thermophiles* respectively. They showed that Cas9 could be directed towards genomic loci (Cong et al., 2013). In the same issue of Science, George Churches group showed very similar findings (Mali et al., 2013).

Double-strand breaks such as those introduced by Cas9 are repaired primarily by two pathways in mammalian cells – non-homologous end-joining (NHEJ) or homology

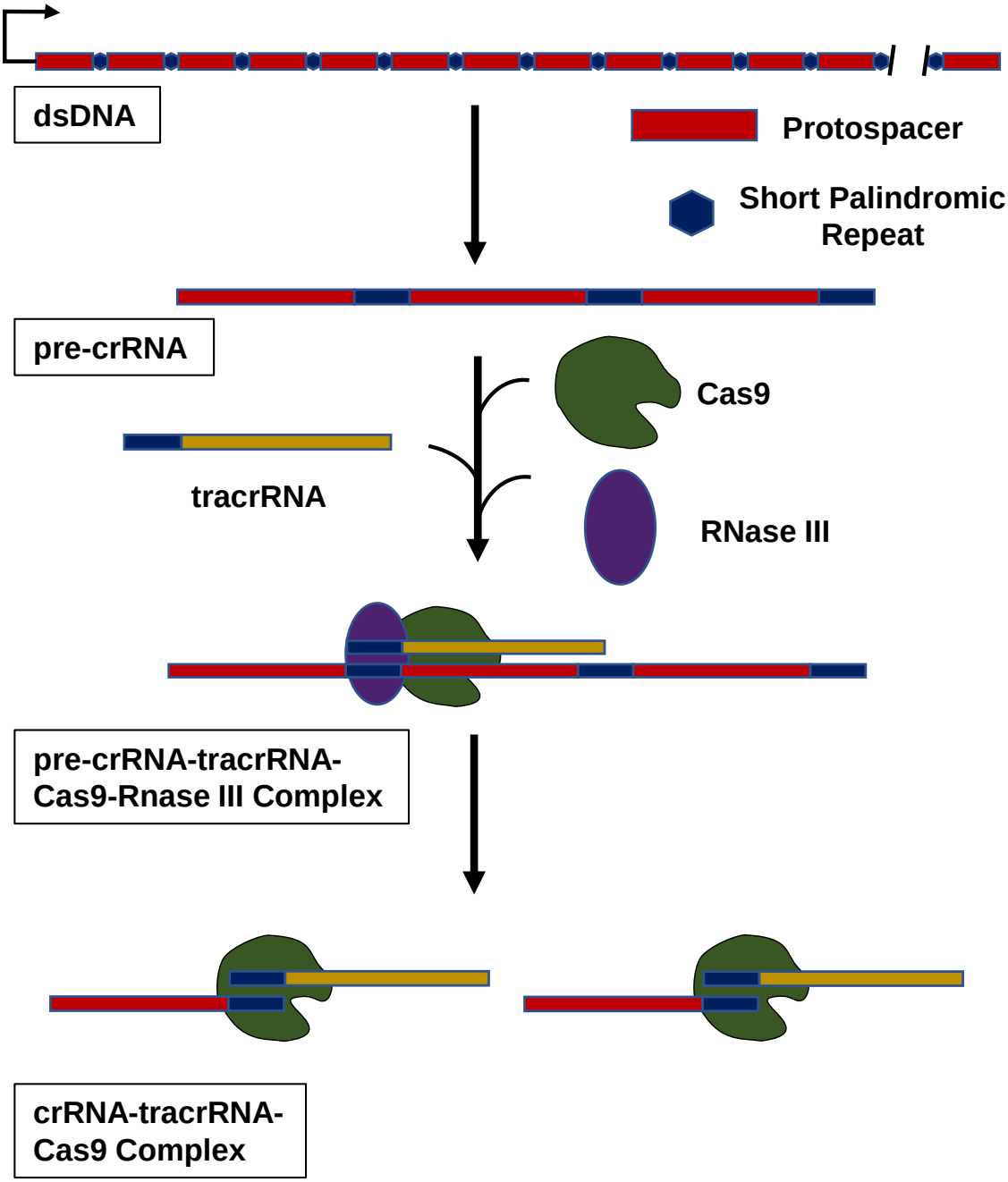

Figure 1.5 CRISPR interference
Prokaryotic genomes contain CRISPR arrays which are composed of non-repetitive elements, termed spacers, interspaced by direct repeats. Protospacers and short palindromic repeats are transcribed from CRISPR loci to form a pre-crRNA template. Cas9 and Rnase III form a complex with pre-crRNA and a complimentary tracrRNA, allowing for cleavage of pre-crRNA into protospacer-palliindromic repeat segments which are still in complex with Cas9. crRNA-tracrRNA-Cas9 complexes remain. Cas9 is then associated with a guide protospacer sequence with which it will scan the genome.

directed repair (HDR). NHEJ is the most common repair mechanism that occurs. It is a rapid and efficient process that is active throughout the cell cycle. It is however, prone to errors and frequently leads to the introduction of base insertions or deletions at the site of repair. This can often lead to loss of function mutations. HDR is less efficient and only occurs in the G2 phase of the cell cycle but it has the advantage of being higher fidelity and less error prone as repair occurs based on the sequence of a homologous template strand (Shrivastav et al., 2008). Inhibitors of components of NHEJ complexes have been used in order to increase the occurrence of HDR so that genomes can be edited. This involves the introduction of Cas9 and a targeted sgRNA, along with a template strand to direct repair. However, utilising CRISPR to generate gene knock-outs relies on the naturally error prone NHEJ. Introduction of Cas9 and an sgRNA into a cell population will promote a diverse array of mutations and ultimately gene knock-out.

1.5 Thesis Aims

Here, we set out to explore whether:

(A) ER stress-induced inflammation was dependent on the previously described upregulation of DR5 (TRAIL-R2) during this process.

(B) Taxol-induced inflammation (and inflammation induced by related compounds) was also dependent on upregulation of one or more receptors for TRAIL.

Materials & Methods

2.1 Materials

Material	Supplier & Product Code
Rockefeller Park Memorial Institute (RPMI) 1640	Thermo Fisher Scientific, 31870082
Dulbecco's Modified Eagle Medium (DMEM)	Sigma Aldrich, 51435C
L-glutamine	Thermo Fisher Scientific, 25030081
Foetal bovine serum (FBS)	Sigma Aldrich, F242
Trypsin-EDTA	Sigma Aldrich, T4049
10 cm plates	Corning, CLS430167
6 well plates	Starstedt, 83.3920.005
Paclitaxel	Sigma Aldrich, T7402
Docetaxel	Sigma Aldrich, 01885
Thapsigargin	Sigma Aldrich, T9033
Brefeldin A	Sigma Aldrich, B6542
Tunicamycin	Sigma Aldrich, T7765
SuperKiller TRAIL	Adipogen, AG-40T-0002-C020
CH11	Merck Millipore, 05-201
zVAD-fmk	Bachem, N-1560.005
BV6	Thermo Fisher Scientific, 14025092
TRAIL-R2-Fc	Adipogen, AG-40B-0071-C050
D-Glucose	Sigma Aldrich, G8270
Hanks Balanced Salts Solution	Thermo Fisher Scientific, 14025092
TRIZMA Base	Sigma Aldrich, T1503
Sodium dodecyl sulphate (SDS)	Sigma Aldrich, L3771
Glycerol	Sigma Aldrich, G5516
Bromophenol blue	Sigma Aldrich, B0126
□-mercaptoethanol	Sigma Aldrich, M6250
Human IL6 ELISA DuoSet	R&D Systems, DY206
Human IL8 ELISA DuoSet	R&D Systems, DY208
Human CXCL1 ELISA DuoSet	R&D Systems, DY275
Human RANTES ELISA DuoSet	R&D Systems, DY278
Murine IL6 ELISA DuoSet	R&D Systems, DY406
Murine MCP1 ELISA DuoSet	R&D Systems, DY479
Murine CXCL1 ELISA DuoSet	R&D Systems, DY453
Murine RANTES ELISA DuoSet	R&D Systems, DY578
Tween – 20	Sigma Aldrich, P1379
Bovine serum albumin (BSA)	Sigma Aldrich, 05470
Tetramethylbenzidine (TMB)	Sigma Aldrich, 860336

Tetrabutylammonium bromide (TBABH)	Sigma Aldrich, 426288
N,N-Dimethylacetamide (DMA)	Sigma Aldrich, 72336
Potassium citrate	Sigma Aldrich, 60153
Hydrogen peroxide (H_2O_s)	Sigma Aldrich, 289132
Sulphuric acid	Sigma Aldrich, 339741
Glycine	Sigma Aldrich, G8898
Sodium chloride	Sigma Aldrich, S7653
Methanol	Sigma Aldrich, 322415
Ammonium persulphate	Sigma Aldrich, A3678
Amersham Protran 0.2µm Nitrocellulose	GE Healthcare, 10600001
Anti-PERK	Cell Signalling, C33E1
Anti-IRE1	Cell Signalling, I4C10
Anti-xBP1	Cell Signalling, D2C1F
Anti-CHOP	Santa Cruz Biotechnology, sc7351
Anti-ATF4	Cell Signalling, D4B8
Anti-DR4	Cell Signalling, D9S1R
Anti-DR5	Cell Signalling, D4E9
Anti-TRAIL	Novus Biologicals, NB100-56518
Anti-CD95	Santa Cruz Biotechnology, sc715
Anti-TNFR1	Cell Signalling, C2SC1
Anti-FADD	BD Transduction Laboratories, 610400
Anti-Caspase-8	Adipogen, AG20T0138C100
Anti-Cas 9	Cell Signalling, 4C3
Anti-IκB	BD Transduction Laboratories, 610690
Anti-phospho IκB	BD Transduction Laboratories, 551818
Anti-p65	Santa Cruz Biotechnology, sc372
Anti-phosphop65	Cell Signalling, 3033P
Anti-mTRAILR2	eBiosciences, CD262
Anti-mFADD	Santa Cruz Biotechnology, H181
Anti-mFas	Cell Signalling 80235
Peroxidase Affini Pure goat anti-mouse IgG (H+L)	Jackson Immuno Research, 115-035-003
Peroxidase Affini Pure goat anti-rabbit IgG (H+L)	Jackson Immuno research, 111-035-003
SuperSignal chemiluminescent substrates	Thermo Fisher Scientific, 34080
Carestream Kodak Developer	Sigma Aldrich, P7042
Carestream Kodak Fixer	Sigma Aldrich, P7167
UltraCruz Autoradiography film	Santa Cruz Biotechnology, sc-201696
Bacto tryptone	Sigma Aldrich, T9410
Yeast Extract	Sigma Aldrich, Y1625

Bacto Agar	Becton, Dickson, 214010
Agarose UltraPure	Thermo Fisher Scientific, 16500500
Potassium chloride	Sigma Aldrich, P9333
Magnesium chloride	Sigma Aldrich, M8266
Magnesium sulphate	Sigma Aldrich, M7899
PIPES	Sigma Aldrich, P6757
Manganese chloride	Sigma Aldrich, M8054
Calcium chloride	Sigma Aldrich, C5670
Dimethyl sulfoxide (DMSO)	Sigma Aldrich, D2650
Stbl3 bacteria	Thermo Fisher Scientific, C737303
lentiCRISPRv2 plasmid	Addgene plasmid 52961
pLentiGuidePuro plasmid	Addgene plasmid 52963
Fast Digest BsmBI	New England Biolabs, B7024
Dithiolthreitol (DTT)	Sigma Aldrich, D0632
Fast alkaline phosphatase	Thermo Fisher Scientific, EF0654
Sodium iodide	Sigma Aldrich, 217301
Silica	Sigma Aldrich, S5505
Ethanol	Sigma Aldrich, 652261
Ethidium bromide	Sigma Aldrich, E7653
Ethylenediaminetetraacetic acid (EDTA)	Sigma Aldrich, E6758
T4 polynucleotide kinase	New England Biolabs, M0201
T4 ligation buffer	New England Biolabs, B0202S
Quick ligase	New England Biolabs, M2200
Ampicillin	Sigma Aldrich, A9393
QIAprep Spin Miniprep Columns	QIAGEN, 27106
RNase A	Roche, 10109134001
QIAGEN Midiprep Kit	QIAGEN, 12145
Isopropanol	Sigma Aldrich, W292907
GenJet Transfection Reagent	SignaGen, SL100488
HEPES	Sigma Aldrich, H3375
Blasticidin S hydrochloride	Sigma Aldrich, 15205
Puromycin dihydrochloride	Sigma Aldrich, P9620

2.2 Methods

2.2.1 Cell Culture and Stimulation

HeLa and HCT116 cells were cultured in RPMI supplemented with 5% foetal bovine serum (FBS) and 100μg/mL L-glutamine. A549, CT26 and SKOV3 cells were cultured in RPMI supplemented with 10% FBS and 100μg/mL L-glutamine, 3LL cells were cultured in DMEM supplemented with with 10% FBS and 100μg/mL L-glutamine. All cells were cultured in 10cm culture dishes at 37°C in 5% CO_2. Cells were passaged when they reached 80% confluency with 0.05% trypsin-EDTA.

For experimentation, cells were plated at a density of 2 x 10^5 cells/well in 6-well plates and cultured for a further 24h before treatment. Cells were stimulated with Paclitaxel, Docetaxel, Thapsigargin, Brefeldin A, Tunicamycin, TRAIL, CH11 or TNF at the indicated concentrations and for the indicated timepoints. For neutralisation experiments, neutralising antibodies were added alongside the above stimuli. For inhibitor experiments, cells were pre-treated with zVAD-fmk and/or BV6 for 1h before stimulation.

Glucose free medium was prepared using glucose free DMEM supplemented with 10% FBS (dialysed against PBS to remove glucose) and 100μg/mL L-glutamine. For control conditions, 25mM D-glucose was added to glucose free medium. Cell layers were washed with Hanks Balanced Salts Solution before treatment to remove traces of glucose.

2.2.2 Cell Death Counts, Cell Supernatant Extraction and Lysate Preparation

Cell death counts were carried out in 3 X fields of view/well. Each field of view contained approximately 100 cells (Henry et al., 2013, Hollville and Martin, 2001). Both detached dead cells and adhered cells were lysed using sodium dodecyl sulphate (SDS) lysis buffer (100mM Tris.Cl pH 6.8, 4% SDS, 20% Glycerol, 0.1% Bromophenol Blue, 5% β-mercaptoethanol). Cell supernatants were centrifuged at 500g for 5 minutes to pellet dead cells. Supernatants were removed and kept. 100μl of 1 X SDS lysis buffer was used to lyse and gather adherant cells in the bottom of each well using a cell scraper and combined with the above pellet. Cell lysates were then at a final concentration of approximately 2 x 10^6 cells/mL.

2.2.3 Enzyme-Linked Immunosorbant Assay (ELISA)

Human ELISA kits for IL6, IL8, CXCL1, RANTES were purchased from R&D Systems. Murine ELISA kits for CCL2, CCL5, RANTES, CXCL1 and IL6 were also purchased from R&D Systems. Phosphate-buffered saline (PBS) with 0.05% Tween-20

and PBS with 1% bovine serum albumin (BSA) were prepared as wash buffer and reagent diluent respectively. TMB substrate solution – 40μM TMB and 6.5μM TBABh in DMA – was made and added freshly to 2.5μl H_2O_2 and 7.8mL 205mM potassium citrate (pH 4) directly before use. Finally, 1.8N sulfuric acid was prepared as ELISA stop solution.

The ELISA was performed according to the manufacturer's data sheet. Briefly, 96-well plates were coated with 50μl / well capture antibody overnight. Three washes of 150μl PBST / well were carried out. Wells were blocked for 1h with 150μl reagent diluent, following which 50μl of diluted (or neat) samples and standards were added in triplicate and incubated for 2h. Top standards were 1ng/mL, followed by x6 1:2 dilutions. Final standards were reagent diluent alone. Wells were again washed and 50μl / well detection antibody was added for a further 2h. Following another wash step, 50μl / well streptavidin conjugated to horseradish peroxidase (HRP) was added for 20 minutes (incubated in the dark). After a final wash, 50μl TMB solution was added to the wells. 30μl stop solution was used when the colorimetric change had developed. Absorbance was read at 450nm using a plate reader.

2.2.4 SDS PAGE and Western Blot

Whole cell lysates were fractionated on SDS PAGE gels **(Table 2.1)** and transferred to nitrocellulose membranes using Bio-Rad transfer rigs. Membranes were blocked for 1h in 5% non-fat milk, 0.05% sodium azide in tris-buffered saline (TBS). Membranes were then incubated with antibodies against PERK, IRE1, xBP1, CHOP, ATF4, DR4, DR5, TRAIL, CD95, TRFR1, FADD, Cas 9, IκB, phosphoIκB, p65, phosphop65 (all at 1:1000) and β–actin (at 1:8000) for either 2h (at room temperature) or overnight (at 4^{o}C). Membranes were washed a minimum of three times for 10 minutes, followed by incubation with a 1:2000 dilution of HRP-conjugated anti-mouse or anti-rabbit secondary antibodies for 1h at room temperature. Membranes were washed again, then exposed to SuperSignal chemiluminescent substrate for 2 minutes. Following this, membranes were put in an exposure cassette and exposed to autoradiography film and the film was developed.

Table 2.1: Make-up of SDS PAGE gels.

	12% Resolving Gel	8% Resolving Gel	Stacking Gel
ddH_2O	3.2 mL	4.6 mL	3 mL
30% Accrylamide Mix	4 mL	2.6 mL	0.67 mL
1.5M Tris, pH 8	2.6 mL	2.6 mL	/
1.0M Tris, pH 8.8	/	/	1.25 mL
10 % SDS	100 µl	100 µl	50 µl
10 % APS	100 µl	100 µl	50 µl
TEMED	10 µl	10 µl	5 µl

2.2.5 sgRNA Design

Exon sequences genes of interest were isolated from www.ensembl.org. Exons as close to the 5' end of the gene as possible were used (as the idea is to create a truncated or non-functional protein/transcript). Untranslated regions of exons were avoided. Sequences were checked against the CDS to be found in databeses such as those on NCBI. Exons were searched for targeted Cas 9 targets using the algorithm and sgRNA design tool at http://portals.broadinstitute.org/gpp/public/analysis-tools/sgrna-design (Doench and Fusi, 2016, Doench et al., 2014).

Selected sequences (including an NGG at the end) were Blast n searched against the human genome database to be sure that there are no high specificity off-target matches. The last 3-4 nucleotides (adjacent to the PAM) are the most important to avoid (Doench and Fusi, 2016, Doench et al., 2014). The following overhangs were added to selections, for cloning into pLentiguidePuro or lentiCRISPRv2 plasmids:

Target Sequence: 1 2 3 4 5 6 7 8 9 10 11 12 13 14 15 16 17 18 19 20
Oligo 1 -> 5'- CACCG X X X X X X X X X X X X X X X X X X X X -3'
3'- C X X X X X X X X X X X X X X X X X X X X CAAA -5' <-Oligo 2

Oligos 1 and 2 were sequenced in the 5' to 3' directions.

2.2.6 Preparation of Competent Bacteria (Inoue Method)

Stbl3 bacteria were streaked on lysogeny broth (LB) agar plates (1% bacto-tryptone, 0.5% bacto-yeast extract, 1% NaCl, 1.5% agar) and grown overnight at 37°C. Single colonies were picked and grown in 3mL of LB (1% bacto-tryptone, 0.5% bacto-yeast extract, 1% NaCl) overnight at 37 °C, 280rpm. Bacteria were then grown in 50mL

cultures from an OD_{600} of 0.1 to an OD_{600} of 0.4-0.6 at room temperature, 280rpm in super optimal broth (SOB) (2% bacto trypyone, 0.5% yeast extract, 10mM NaCl, 2.5mM KCl, 10mM $MgCl_2$, 10mM $MgSO_4$, pH 7). Culture chilled on ice for 10 minutes, following which it was centrifuged at 2500g for 10 minutes at 4°C. Cell pellets were resuspended in 20mL of inoue transformation buffer (**ITB**) (10mM PIPES, 55mM $MnCl_2$, 15mM $CaCl_2$, 250mM KCl, pH 6.7) and incubated on ice for a further 10 minutes before another centrifugation step. Pellets were resuspended in 4mL ITB and 7% DMSO, followed by another incubation on ice.

2.2.7 Cloning of sgRNA into Guide Vectors (Figure 2.1)

pLentiguidePuro plasmid was digested with BsmBI and dephosphorylated with alkaline phosphatase for 2h t 37°C as summarised in **Table 2.2**:

Table 2.2: BsmBI digestion reaction of pLentiGuidePuro vector.

	Digestion	Control
pLentiGuidePuro	5 μg	5 μg
FastDigest BsmBI	1 μL	/
Fast Alkaline Phosphatase	3 μL	3 μL
10X Fast Digest Buffer	6 μL	6 μL
100mM DTT	0.6 μL	0.6 μL
ddH_2O	X μL	X μL
Total	60 μL	60 μL

Entire 60μL digestion reactions were mixed with 12μL of 6X loading dye (30% glycerol, 0.25% bromophenol blue) and resolved on 0.6% agarose gels. Gels were stained with ethidium bromide (EtBr).

Linearised, gel-trapped plasmid was extracted and gene-cleaned. Firstly, bands of interest were excised from gel under UV light and weighed. X3 volumes of 6M sodium iodide (NaI) was used to dissolve agarose at 56°C for 10 minutes. A 100μg/mL silica suspension in 6M NaI was used to bind and extract DNA from the solution for 30 minutes at room temperature. A wash buffer (10mM Tris.HCl pH 7.5, 50mM NaCl, 2.5mM EDTA, 50% ethanol) was used to wash the silica pellet twice, 1mL each time. 30μL of DNase/RNase free ddH_2O was used to elute DNA from the silica pellet.

Designed, targeted single-stranded sgRNA oligos were phosphorylated and annealed together to create a double-stranded RNA duplex. 10 X T4 ligation buffer was

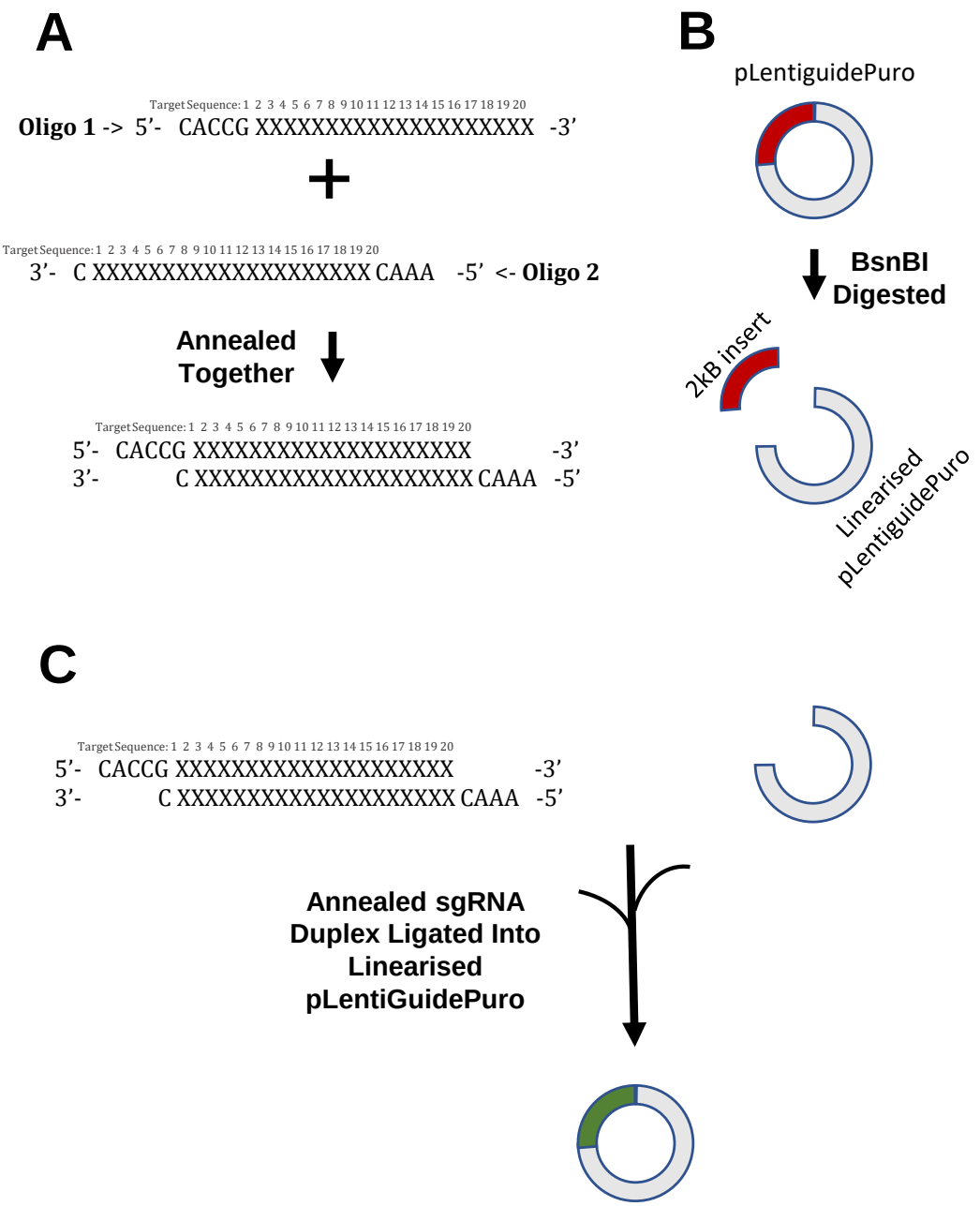

Figure 2.1 Cloning of sgRNA into pLentiGuidePuro

(A) Oligo 1 and oligo 2 are designed with overhangs complimentary to BsmBI digested pLentiGuidePuro. Oligos are annealed together to form an sgRNA duplex.

(B) pLentiGuidePuro is digested to excise a 2kb fragment and linearlise the plasmid. Ends are compatible with the overhangs designated in (A).

(C) Annealed sgRNA duplex from (A) is ligated into BsmBI digested pLentiGuidePuro delivery vector.

use as it contains ATP, which is required for the phosphorylation reaction. Reactions were set up as described in **Table 2.3**:

Table 2.3: Phosphorylation and annealing of sgRNA oligos.

	Annealing Reaction	Control
Oligo 1 (100 μM)	1 μL	/
Oligo 2 (100 μM)	1 μL	/
10X T4 Ligation Buffer	1 μL	1 μL
T4 Polynucleotide Kinase	0.5 μL	0.5 μL
ddH_2O	6.5 μL	8.5 μL
Total	10 μL	10 μL

Reactions were put into a thermocycler set as follows:

37°C for 30 minutes

95°C for 5 minutes

ramp down to 25°C at 5°C/min

Annealed oligos were diluted 1:200 in DNase/RNase free ddH_2O. Double stranded RNA duplexes were then ligated into linearised pLentiGuidePuro overnight at room temperature. Reactions were set up as described in **Table 2.4**:

Table 2.4: Ligation of sgRNA duplexes into linearised pLentiGuidePuro vector.

	Ligation	Control
pLentiGuidePuro	50 ng	50 ng
Diluted Oligo Duplex	1 μL	/
2X Quick Ligase Buffer	5 μL	5 μL
Quick Ligase	0.5 μL	0.5 μL
ddH_2O	X μL	X μL
Total	11 μL	11 μL

Ligations were transformed into 200μL of super competent Stbl3 bacteria by heat shock. Bacteria were incubated on ice with ligation for 30 minutes to allow coating. Bacteria were heat shocked at 42°C for 40 seconds, followed by a 2-minute recovery on ice. 790μL of LB recover media was added and this was incubated at 37°C, 220rpm to allow expression of the ampicillin resistance cassette of the plasmid. 50μL of the

transformation was plated on an LB agar plate containing 100μg/mL ampicillin. Plates were incubated at 37°C overnight.

Single colonies were picked from agar plates (from transformations with sgRNA duplexes of interest) and grown overnight at 37°C, 280rpm in 4mL of LB broth. Entire cultures were used to miniprep plasmid using QIAprep Spin Miniprep Columns. These were used as described in the manufacturers data sheet. Briefly, cultures were pelleted at 6800g for 3 minutes at room temperature. Pellets were resuspended in 250μL of P1 buffer with added 1μg/mL RNase A. 250μL of P2 buffer was added and mixed my inversion, then incubated for 5 minutes. 350μL of P3 buffer was added and also mixed by inversion. Preparations were centrifuged at 6800g for 10 minutes. Supernatant was added to the column, which was then centrifuged at 6800g. The column was washed twice, with 500μL of PB and 750 μL of PE buffers respectively. 30μL of DNase/RNase free ddH_2O was used to elute DNA from the column. 1μg of each preparation was sent to Sigma Aldrich for sequencing to confirm insertion of sgRNAs.

2.2.8 Midi-Plasmid Preparation

Plasmid midi-preps were carried out on successfully ligated sgRNA plasmids using QIAGEN midi-prep columns as described in manufacturers datasheet. Briefly, 50 mL bacterial cultures were grown overnight at 37°C, 280 rpm. Cultures were spun down at 2500g for 10 minutes. Bacterial pellets were resuspended in 4mL of P1 buffer + 1μg/mL RNAse A. 4mL of P2 was added and mixed thoroughly by inversion x 6, followed by incubation at RT for 5 minutes. 4mL of P3 was added and mixed thoroughly by inversion x6, followed by incubation on ice for 20 minutes. Suspensions were centrifuged at 15'000g for 15 minutes at 4°C. QIAGEN midiprep columns were equilibrated with 5mL of equilibration buffer, followed by addition of supernatant from centrifugation step above to the column. Two washes – 10mL of wash buffer each – were carried out. Finally, 5mL of elution buffer was used to elute plasmid DNA from the column. 0.7 volumes of isopropanol – to precipitate plasmid DNA - was added and mixed well by inversion. This was incubated at RT for 20 minutes with inversion every few minutes. Suspensions were centrifuged for 30 minutes at 15'000g at 4°C. Pellets were washed in 1mL 70% ethanol and finally resuspended 1:1 in ddH_2O and Tris-EDTA (10mM Tris, 1mM EDTA).

2.2.9 GenJet Transfection of Plasmids into Mammalian Cells

HeLa cells were plated a density of 10^5 cells/well of 6-well plates and cultured for 24 ho. Medium on cells was replaced 60 minutes before transfection. 1μg of plasmid was gently mixed with 50μL of serum free RPMI or DMEM. 1μL of GenJet transfection

reagent was mixed gently into 50μL serum free media and added immediately to the DNA mixture – mixed gently and incubated at RT for 15 minutes. Complexed lipid mixtures were added dropwise to wells of 6-well plates. Empty, parental pLentiGuidePuro and PAAV-EGFP plasmids were transfected alongside as controls. GFP expression by cells was used to assess transfection efficiency.

2.2.10 Selection of Cells for Uptake of Plasmid

pLentiguidePuro plasmid contains a puromycin selection cassette under a mammalian promoter. Selection with puromycin was carried out over a period of approximately 7 days **(Figure 2.2)**. Cells transfected with parental pLentiguidePuro were retained as a control cell line for future experiments – henceforth denoted as "wild type" cells. Selected cell populations were grown to confluency. Concentrated, untreated cell lysates at a density of 2×10^7 cells / mL were made and western blotted to confirm knock-out at the protein level. In other cases, protein expression was induced with previously verified stimuli before knock-out could be confirmed.

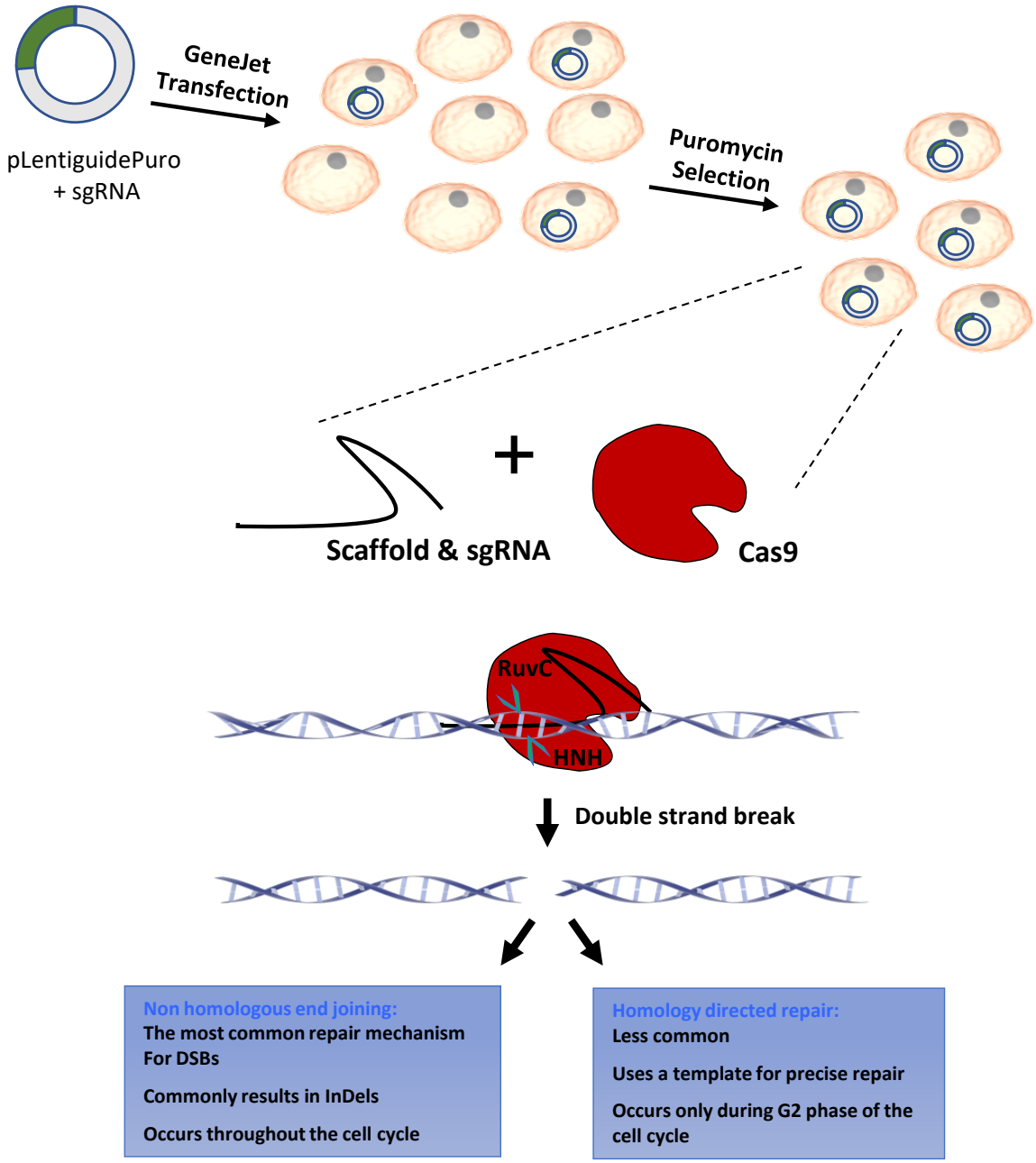

Figure 2.2 Generation of knock-out cell populations using CRISPR

pLentiguidePuro with sgRNA of interest is transfected into mammalian cells that are stably expressing Cas9. Cell populations are then selected with puromycin (as pLentiguidePuro contains a puromycin resistance cassette under a mammalian promoter) in order to select for cells that have taken up plasmid.

Cells then containing Cas9 and an sgRNA template will be subjected to Cas9 cleavage at genomic sites complimentary to the template carried by Cas9. Cas9 nuclease creates double-strand breaks at the target site. The predominant mechanism of DNA repair of double-strand breaks such as these is non-homologous recombination, which is error prone and often leads to Indels being introduced.

Results

3.1 Chapter 1

3.1.1 ER Stress-Inducing Agents Induce Cytokine Production and DR5 Upregulation In HeLa cells

It is well established that cytotoxic agents thapsigargin, brefeldin A and tunicamycin potently induce ER stress in mammalian cells (Ashkenazi et al., 1999). It is well known that these agents are robust inducers of DR5 expression, with cell death in response to some of these agents being DR5 dependent (Ashkenazi et al., 1999). We initially confirmed these results in HeLa cells, as they have been widely used in similar studies **(Figure 3.1 A)**. Consistent with the previous literature, robust phosphorylation and stabilisation respectively of ER membrane-associated sensors PERK and IRE1 was seen upon treatment with these agents. We additionally found substantial upregulation of transcription factors ATF4 and CHOP in response to a range of stimulant concentrations. Finally, we confirmed that while DR4 protein levels remained relatively constant with stimulation, expression levels of both splice variants of DR5 were dramatically upregulated. Preferential formation of a smaller molecular weight form of DR4 and DR5 after treatment with tunicamycin was also observed. This is likely explained by the inhibition of death receptor glycosylation by the drug as both DR4 and DR5 are known to be glycosylated during their synthesis (Wagner et al., 2007).

We wondered, given recent findings by our group (Henry and Martin, 2017, Cullen et al., 2013), whether death receptor upregulation was instrumental in cytokine production in response to these agents. Inflammation has sporadically been associated with an ER stress phenotype and has been shown in response to classical ER stress-inducing agents (Keestra-Gounder et al., 2016, Kim et al., 2012). Initial ELISA results showed that all three classical ER stress-inducing agents induce robust production of the cytokines IL-6 and IL-8 at a number of treatment doses **(Figure 3.1 B)**. It was interesting that cytokine production was seen at drug doses that did not induce a large amount of cell death, suggesting that this was active secretion rather than a passive, death-dependent DAMP response. It was also notable that, particularly with exposure to tunicamycin, cytokines were produced at drug doses that induced the most potent ER stress response. We hypothesised that ER stress-induced cytokine production was fact dependent on upregulation of DR5 and the TRAIL receptor signalling pathway recently described by our group (Henry and Martin, 2017). To test this hypothesis, we used CRISPR technology to knock-out (KO) genes of interest, including: FADD, DR4, DR5 and CHOP.

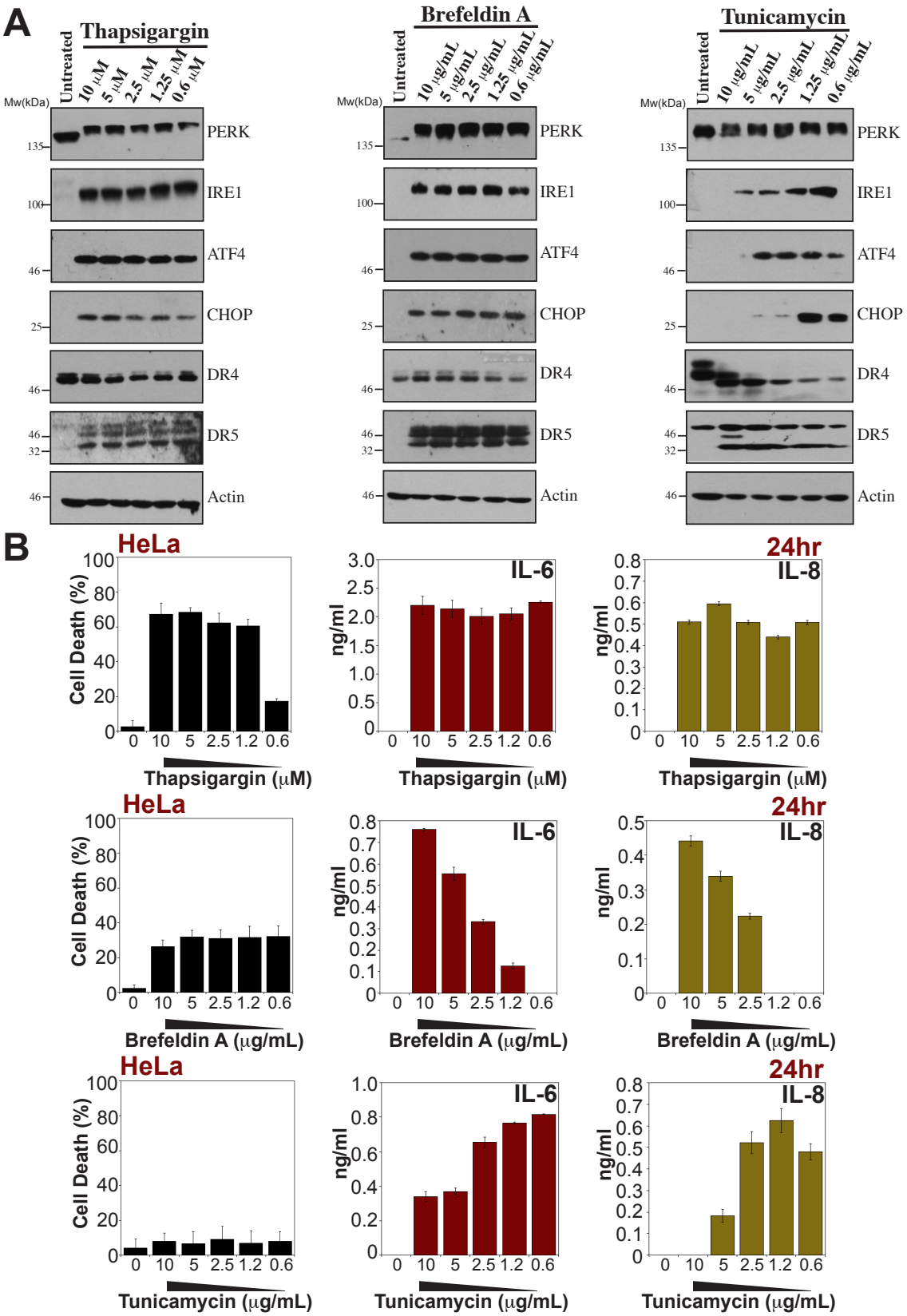

Figure 3.1 ER stress-inducing agents thapsigargin, brefeldin A and tunicamycin trigger DR5 upregulation cytokine production and in HeLa cells

(A) HeLa cells were stimulated for 24hr with the indicated concentrations of Thapsigargin, Brefeldin A or Tunicamycin. Protein expression was analysed by western blot.

(B) HeLa cells were stimulated for 24hr with the indicated concentrations of Thapsigargin, Brefeldin A or Tunicamycin. Cell death was measured based on cell morphology from counts of 3 fields per well (of approximately 100 cells per field). Cytokine concentrations in cell culture supernatants were determined by ELISA. The error bars represent the mean +/- SEM of triplicate samples.

3.1.2 ER Stress-Induced Cytokines Are Dependent On FADD, An Important Adaptor In Death Receptor Signalling

Initially, CRISPR KO cell lines were generated in order to assess the dependency of ER stress-induced cytokines on FADD, an important downstream adaptor in both Fas and TRAIL death receptor signalling. Two FADD-specific sgRNA were designed using the Broad Institute sgRNA design tool. Chosen sequences are described in **Table 3.1**. Separate sgRNAs for each target were designed to remain as close to the beginning of the protein coding sequence as possible. Each sgRNA was designed with complementary overhangs for cloning into linearised sgRNA vector pLentiguidePuro **(Figures 3.2 A & 3.2 B)**. Ligation of targeted sgRNA into pLentiguidePuro was confirmed by sequencing. Results are detailed in **Table 3.2**.

Validated plasmids were transfected into HeLa cells that were stably expressing Cas9 (generated by Dr. Conor M. Henry), alongside parental pLentiguidePuro and pPAAV-EGFP to assess transfection efficiency **(Figure 3.2 C)**. Each plasmid was transfected individually. Cell populations were then selected with puromycin for 5-6 days to enrich for cells that had taken up plasmid. Cells transfected with pLentiguidePuro and subsequently selected with puromycin are hereafter referred to as “wild type” cells and have been used as a control cell line.

Cell lysates were then prepared and used to assess KO of FADD by western blot. As **Figure 3.3 A** illustrates, FADD was successfully deleted in both HeLa sublines. Control treatments were then carried out to confirm that all cell types are responding to stimuli as would be expected. FADD null were initially treated with TNF, versus wild type cells, to confirm that they still actively produced cytokines **(Figure 3.3 B)**. As FADD is an important adaptor in both TRAIL induced death and cytokine production, cells were then treated with a range of doses of TRAIL and as would be expected, both cell death and production of two independent cytokines (IL-6 and IL-8) were ablated in both independent FADD KO populations (**Figure 3.3 C**).

Using a titration of classical ER stress-inducing agents, cell death and production of the cytokines IL-6 and IL-8 were compared in wild-type versus $FADD^{-/-}$ HeLa cells. Specifically, we investigated whether thapsigargin and brefeldin A-induced cytokines were FADD-dependent. In the case of thapsigargin, we found that there was a clear resistance to ER stress-induced cytokine production in the absence of FADD **(Figure 3.4 A)**. With brefeldin A treatment however, while IL-8 production was consistently reduced in the absence of FADD, IL-6 levels were less consistently affected **(Figure 3.4 B)**. However, these data strongly suggest that death receptor signalling is likely to play a role in ER stress-induced cytokine production.

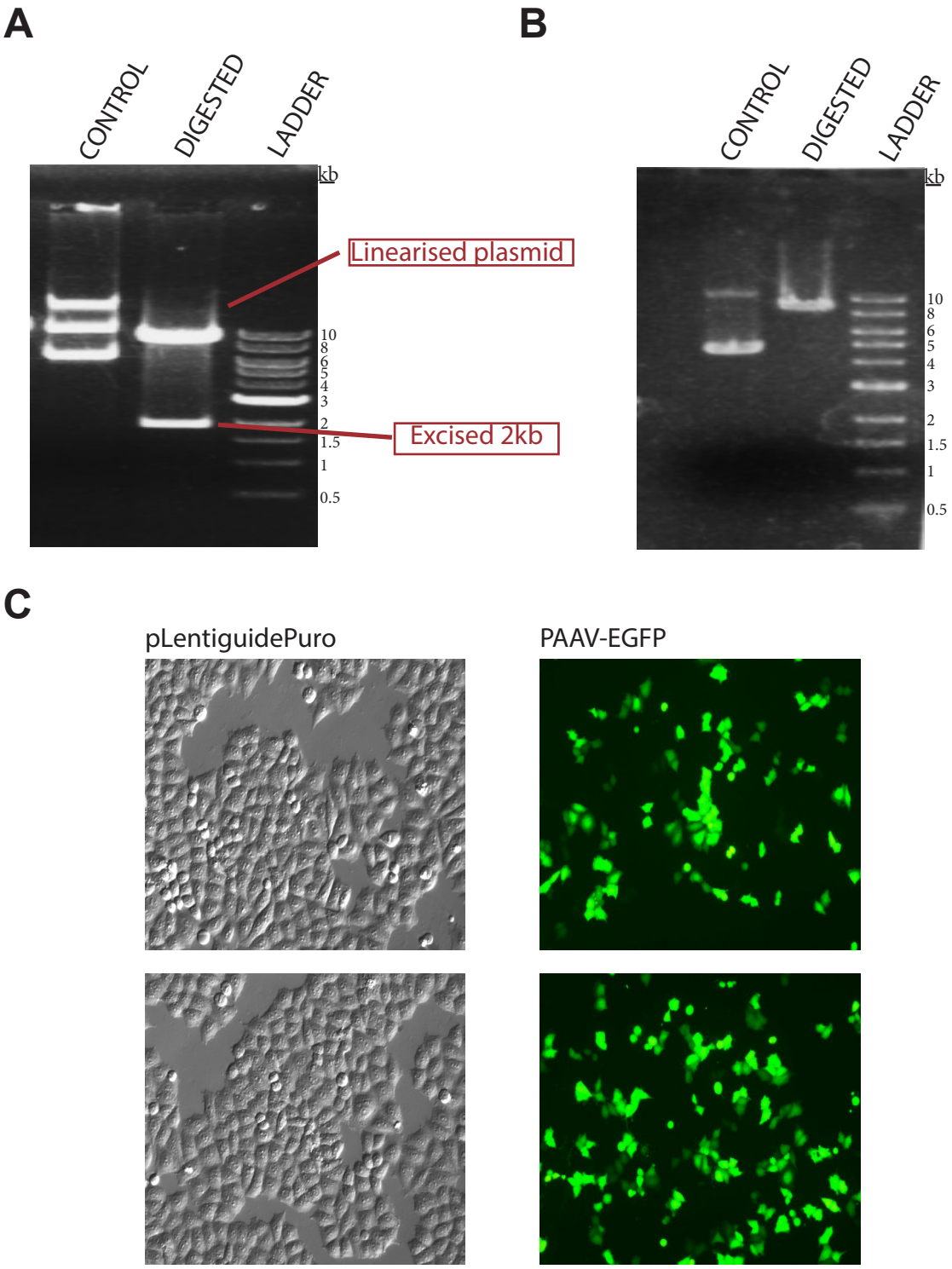

Figure 3.2 Cloning and evaluation of sgRNAa targetting FADD, DR4, DR5 or CHOP.
(A) pLentiguidePuro was digested with BsmBI (DIGESTED) or left untreated (CONTROL). Linearised plasmid and excised 2kb fragment were resolved on a 0.6% agarose gel.
(B) Linearised plasmid from DIGESTED reaction and supercoiled plasmid from CONTROL in (A) were extracted from the agarose gel and gene cleaned. Fragments were resolved and visualised on a 0.6% agarose gel.
(C) Plasmids (parental pLentiguidePuro, sgRNA plasmids & PAAV-EGFP) were transfected into HeLa cells using GenJet. Cells were visualised using phase contrast microscopy to assess cell death and GFP expression. Two representative images of pLentiguidePuro and PAAV-EGFP transfections are shown.

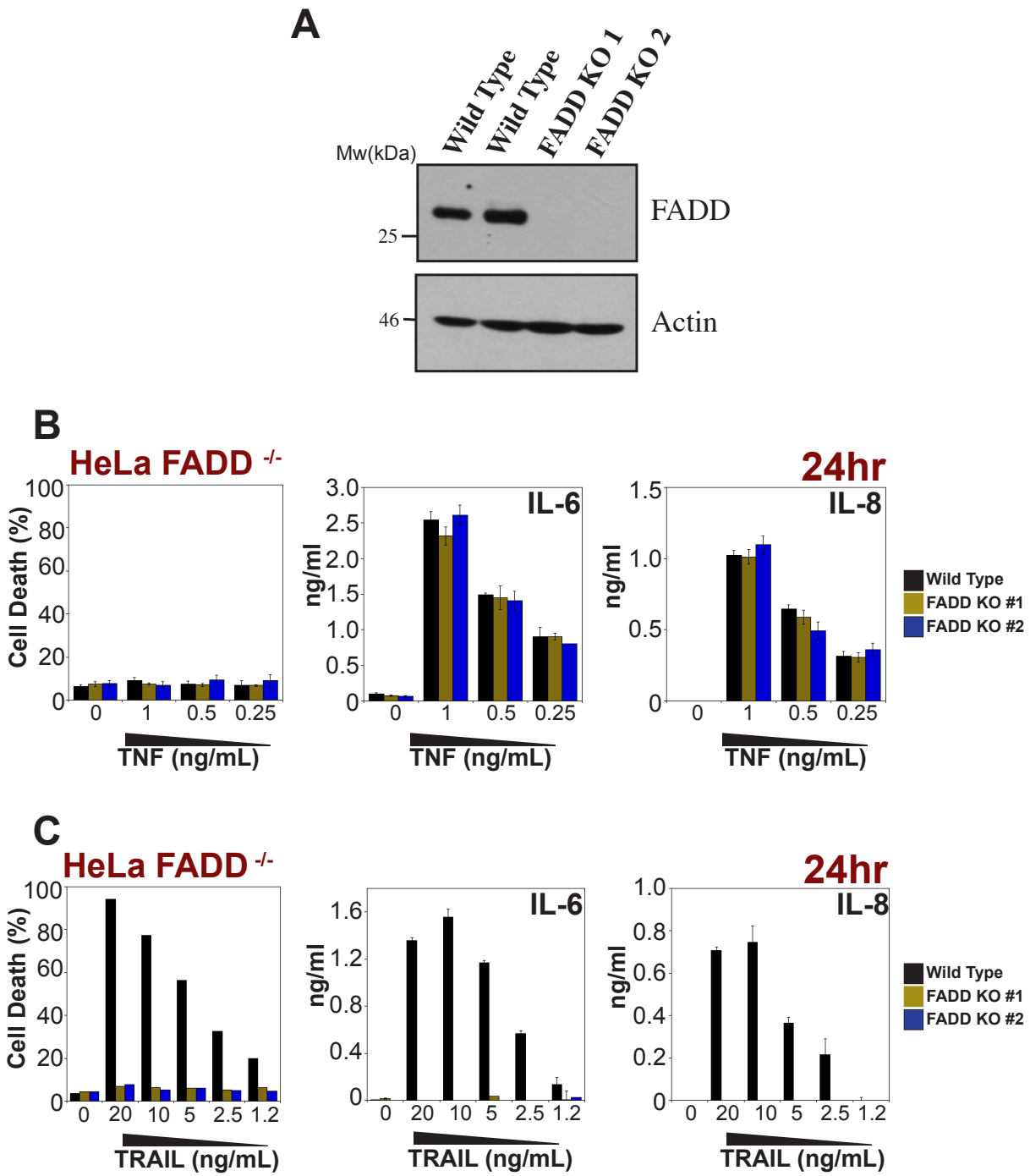

Figure 3.3 CRISPR-mediated deletion of FADD in HeLa cells

(A) Cell populations were puromycin selected after transfection with sgRNA targetting FADD. Cell lysates were prepared and protein expression was analysed by western blot.

(B) HeLa wild type (WT) versus HeLa FADD$^{-/-}$ cells were treated for 24hr with the indicated concentrations of TNF. Cell death was measured based on cell morphology from counts of 3 fields per well (of approximately 100 cells per field). Cytokine concentrations in cell culture supernatants were determined by ELISA.

(C) HeLa WT versus HeLa FADD$^{-/-}$ cells were treated for 24hr with the indicated concentrations of TRAIL. Cell death was measured based on cell morphology from counts of 3 fields per well (of approximately 100 cells per field). Cytokine concentrations in cell culture supernatants were determined by ELISA.

The error bars represent the mean +/- SEM of triplicate samples.

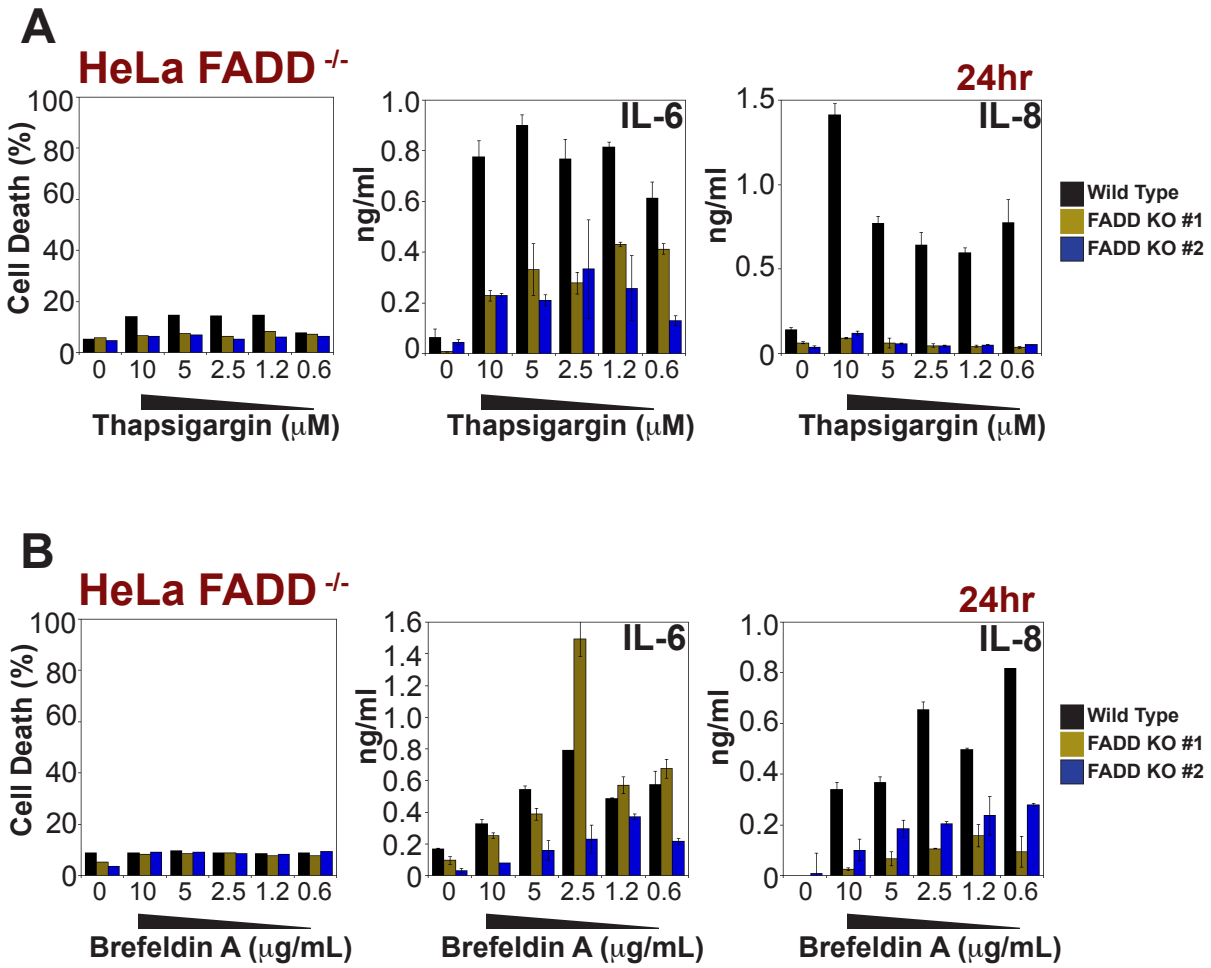

Figure 3.4 ER stress-induced cytokine production is FADD-dependent

(A) HeLa WT wild type versus HeLa FADD$^{-/-}$ cells were treated for 24hr with the indicated concentrations of Thapsigargin. Cell death was measured based on cell morphology from counts of 3 fields per well (of approximately 100 cells per field). Cytokine concentrations in cell culture supernatants were determined by ELISA.
(B) HeLa WT versus HeLa FADD$^{-/-}$ cells were treated for 24hr with the indicated concentrations Brefeldin A. Cell death was measured based on cell morphology from counts of 3 fields per well (of approximately 100 cells per field). Cytokine concentrations in cell culture supernatants were determined by ELISA.
The error bars represent the mean +/- SEM of triplicate samples.

Table 3.1: Summary of sgRNAs designed to target human FADD.

	Sequence	PAM	Exon	Strand
FADD sgRNA 1	GAGGCATAGGAACTTGAGCT	CGG	Exon 1	Antisense
FADD sgRNA 2	GCTCCAGCAGCATGGAGAAG	AGG	Exon 1	Antisense

Table 3.2: Summary of sequencing results to confirm insertion of sgRNA targeting FADD into pLentiGuidePuro vector.

sgRNA	Sequencing Results
FADD sgRNA 1	3969455;Value Read;;**FADD 1.2**;ASM0094025;hU6-F;final result;978;">FADD 12_hU6-F -- 13991 of sequence CAGGCTGTTAGAGAGATAATTAGAATTAATTTGACTGTAAACACAAAGATATTAGTACAAAATACGTGACGT AGAAAGTAATAATTTCTTGGGTAGTTTGCAGTTTTAAAATTATGTTTTAAAATGGACTATCATATGCTTACCG TAACTTGAAAGTATTTCGATTTCTTGGCTTTATATATCTTGTGGAAAGGACGAAACACCGGAGGCATAGGAA CTTGAGCTGTTTTAGAGCTAGAAATAGCAAGTTAAAATAAGGCTAGTCCGTTATCAACTTGAAAAAGTGGC ACCGAGTCGGTGCTTTTTTAAGCTTGGCGTAACTAGATCTTGAGACAAATGGCAGTATTCATCCACAATTTT AAAAGAAAAGGGGGGATTGGGGGGTACAGTGCAGGGGAAAGAATAGTAGACATAATAGCAACAGACAT ACAAACTAAAGAATTACAAAAACAAATTACAAAAATTCAAAATTTTCGGGTTTATTACAGGGACAGCAGAG ATCCACTTTGGCGCCGGCTCGAGGGGGCCCGGGTGCAAAGATGGATAAAGTTTTAAACAGAGAGGAATCT TTGCAGCTAATGGACCTTCTAGGTCTTGAAAGGAGTGGGAATTGGCTCCGGTGCCCGTCAGTGGGCAGAG CGCACATCGCCCACAGTCCCCGAGAAGTTGGGGGGAGGGGTCGGCAATTGATCCGGTGCCTAGAGAAGG TGGCGCGGGGTAAACTGGGAAAGTGATGTCGTGTACTGGCTCCGCCTTTTTCCCGAGGGTGGGGGAGAAC CGTATATAAGTGCAGTAGTCGCCGTGAACGTTCTTTTTCGCAACGGGTTTGCCGCCAGAACACAGGTAAGTG CCGTGTGTGGTTCCCGCGGGCCTGGCCTCTTTACGGGTTATGGCCCTTGCGTGCCTTGATTACTTCACCTGGC TGCAGTACGTGATTCTTGATCCCGAGCTTCGGGTTGGAAGTGGGTGGGAAAATTCA"; 3969455;Value Read;;**FADD 2.1**;ASM0094026;hU6-F;final result;950;">FADD 21_hU6-F -- 15965 of sequence AGGCTGTTAGAGAGATAATTAGAATTAATTTGACTGTAAACACAAAGATATTAGTACAAAATACGTGACGTAG AAAGTAATAATTTCTTGGGTAGTTTGCAGTTTTAAAATTATGTTTTAAAATGGACTATCATATGCTTACCGTAAC TTGAAAGTATTTCGATTTCTTGGCTTTATATATCTTGTGGAAAGGACGAAACACCGGCTCCAGCAGCATGGAG AAGGTTTTAGAGCTAGAAATAGCAAGTTAAAATAAGGCTAGTCCGTTATCAACTTGAAAAAGTGGCACCGAGT CGGTGCTTTTTTAAGCTTGGCGTAACTAGATCTTGAGACAAATGGCAGTATTCATCCACAATTTTAAAAGAAAA GGGGGGATTGGGGGGTACAGTGCAGGGGAAAGAATAGTAGACATAATAGCAACAGACATACAAACTAAAGA ATTACAAAAACAAATTACAAAAATTCAAAATTTTCGGGTTTATTACAGGGACAGCAGAGATCCACTTTGGCGCC GGCTCGAGGGGGCCCGGGTGCAAAGATGGATAAAGTTTTAAACAGAGAGGAATCTTTGCAGCTAATGGACCT TCTAGGTCTTGAAAGGAGTGGGAATTGGCTCCGGTGCCCGTCAGTGGGCAGAGCGCACATCGCCCACAGTCCC CGAGAAGTTGGGGGGAGGGGTCGGCAATTGATCCGGTGCCTAGAGAAGGTGGCGCGGGGTAAACTGGGAA AGTGATGTCGTGTACTGGCTCCGCCTTTTTCCCGAGGGTGGGGGAGAACCGTATATAAGTGCAGTAGTCGCCG TGAACGTTCTTTTTCGCAACGGGTTTGCCGCCAGAACACAGGTAAGTGCCGTGTGTGGTTCCCGCGGGCCTGG CCTCTTTACGGGTTATGGCCCTTGCGTGCCTTGAATTACTTCCACCTGGCTGCAGTACGTGATTCTTGATCCGAACT";

3.1.3 ER Stress-Induced Cytokine Production Is Dependent On DR4 and DR5

We next asked whether ablation of TRAIL death receptors (DR4/TRAIL-R1 or DR5/TRAIL-R2) would reduce cytokine production seen in response to ER stress. sgRNAs targeting human TNFRSF10A (DR4) and TNFRSF10B (DR5) genes were designed using the same methods described for FADD and are summarised in **Table 3.3**.

Table 3.3: Summary of sgRNAs designed to target human DR4 and DR5.

	Sequence	PAM	Exon	Strand
DR4 sgRNA 1	GCGGGGAGGATTGAACCACG	AGG	Exon 1	Sense
DR4 sgRNA 2	AAGTGTGGGGCTCTTCCGCG	GGG	Exon 2	Sense
DR5 sgRNA 1	CCAGGACCCAGGGAGGCGCG	GGG	Exon 1	Sense
DR5 sgRNA 2	CCTAGCTCCCCAGCAGAGAG	CGG	Exon 2	Sense

sgRNA sequences were similarly cloned into pLentiguidePuro and plasmids were sent for sequencing to confirm insertion. Results have been summarised in **Table 3.4**.

DR4 and DR5 were deleted, either alone or in combination, from HeLa cells using CRISPR. Cell lysates were prepared and protein expression was analysed to confirm KO of DR4 and DR5 respectively **(Figures 3.5 A & 3.6 A-C)**. As DR5 has previously been implicated as an important molecule in thapsigargin-induced death, cells were then treated with a titration of thapsigargin and cell death was analysed. Surprisingly, both DR4 an DR5 null cell populations were protected from thapsigargin-induced cell death, though DR5 ablation was substantially more effective **(Figure 3.5 B)**. We next measured cytokines in the cell supernatants from this experiment and found that deletion of DR4 or DR5 protected from thapsigargin-induced production of inflammatory cytokines IL-6 and IL-8 **(Figure 3.5 C)**. DR5 deletion supressed thapsigargin-induced cytokine production to a greater extent than loss of DR4. Interestingly, IL-8 production was affected more than IL-6.

Control treatments were then carried out to confirm that all cell types responded to stimuli as would be expected. Wild-type, DR4, DR5 and DR4/DR5 KO cells were initially treated with TNF, versus wild type cells, to confirm that they were still producing cytokines as expected **(Figures 3.7 A)**. DR4/DR5 KO cells were treated with a range of doses of TRAIL. As expected, both cell death and production of two independent cytokines (IL-6 and IL-8) in response to TRAIL was ablated in both DR4/DR5 null cell populations (**Figures 3.7 B & 3.7 C**).

Table 3.4: Summary of sequencing results to confirm insertion of sgRNA targeting DR4 and DR5 into pLentiGuidePuro vector.

sgRNA	Sequencing Results
DR4 sgRNA 1	3906695;Value Read;;**pLentiguidePuro +DR4sgRNA 1.1**;ASM000IH99;hU6-F;final result;981;"> pLentiguidePuro +DR4sgRNA 11_hU6-F -- 12993 of sequence ACACGCTGTTAGAGAGATAATTAGAATTAATTTGACTGTAAACACAAAGATATTAGTACAAAATACGTGACG TAGAAAGTAATAATTTCTTGGGTAGTTTGCAGTTTTAAAATTATGTTTTAAAATGGACTATCATATGCTTACCG TAACTTGAAAGTATTTCGATTTCTTGGCTTTATATATCTTGTGGAAAGGACGAAACACCG**GCGGGGAGGATT** **GAACCACG**GTTTTAGAGCTAGAAATAGCAAGTTAAAATAAGGCTAGTCCGTTATCAACTTGAAAAAGTGGCA CCGAGTCGGTGCTTTTTTAAGCTTGGCGTAACTAGATCTTGAGACAAATGGCAGTATTCATCCACAATTTTAAA AGAAAAGGGGGGATTGGGGGGTACAGTGCAGGGGAAAGAATAGTAGACATAATAGCAACAGACATACAAA CTAAAGAATTACAAAAACAAATTACAAAAATTCAAAATTTTCGGGTTTATTACAGGGACAGCAGAGATCCACT TTGGCGCCGGCTCGAGGGGGCCCGGGTGCAAAGATGGATAAAGTTTTAAACAGAGAGGAATCTTTGCAGCTA ATGGACCTTCTAGGTCTTGAAAGGAGTGGGAATTGGCTCCGGTGCCCGTCAGTGGGCAGAGCGCACATCGCC CACAGTCCCCGAGAAGTTGGGGGGAGGGGTCGGCAATTGATCCGGTGCCTAGAGAAGGTGGCGCGGGGTA AACTGGGAAAGTGATGTCGTGTACTGGCTCCGCCTTTTTCCCGAGGGTGGGGGAGAACCGTATATAAGTGCA GTAGTCGCCGTGAACGTTCTTTTTCGCAACGGGTTTGCCGCCAGAACACAGGTAAGTGCCGTGTGTGGTTCCC GCGGGCCTGGCCTCTTTACGGGTTATGGCCCTTGCGTGCCTTGAATTACTTCCACCTGGCTGCAGTACGTGAT TCTTGATCCCGAGCTTCGGGTTGGAAGTGGGTGGGGAAAATTCA"; 3906695;Value Read;;**pLentiguidePuro +DR4sgRNA 2.2**;ASM0094001;hU6-F;final result;983;"> pLentiguidePuro +DR4sgRNA 22_hU6-F -- 12995 of sequence TACAGGCTGTTAGAGAGATAATTAGAATTAATTTGACTGTAAACACAAAGATATTAGTACAAAATACGTGAC GTAGAAAGTAATAATTTCTTGGGTAGTTTGCAGTTTTAAAATTATGTTTTAAAATGGACTATCATATGCTTAC CGTAACTTGAAAGTATTTCGATTTCTTGGCTTTATATATCTTGTGGAAAGGACGAAACACCGAAGTGTGGGG CTCTTCCGCGGTTTTAGAGCTAGAAATAGCAAGTTAAAATAAGGCTAGTCCGTTATCAACTTGAAAAAGTGG CACCGAGTCGGTGCTTTTTTAAGCTTGGCGTAACTAGATCTTGAGACAAATGGCAGTATTCATCCACAATTTT AAAAGAAAAGGGGGGATTGGGGGGTACAGTGCAGGGGAAAGAATAGTAGACATAATAGCAACAGACATA CAAACTAAAGAATTACAAAAACAAATTACAAAAATTCAAAATTTTCGGGTTTATTACAGGGACAGCAGAGAT CCACTTTGGCGCCGGCTCGAGGGGGCCCGGGTGCAAAGATGGATAAAGTTTTAAACAGAGAGGAATCTTTG CAGCTAATGGACCTTCTAGGTCTTGAAAGGAGTGGGAATTGGCTCCGGTGCCCGTCAGTGGGCAGAGCGCA CATCGCCCACAGTCCCCGAGAAGTTGGGGGGAGGGGTCGGCAATTGATCCGGTGCCTAGAGAAGGTGGCG CGGGGTAAACTGGGAAAGTGATGTCGTGTACTGGCTCCGCCTTTTTCCCGAGGGTGGGGGAGAACCGTATA TAAGTGCAGTAGTCGCCGTGAACGTTCTTTTTCGCAACGGGTTTGCCGCCAGAACACAGGTAAGTGCCGTGT GTGGTTCCCGCGGGCCTGGCCTCTTTACGGGTTATGGCCCTTGCGTGCCTTGAATTACTTCCACCTGGCTGC AGTACGTGATTCTTGATCCCGAGCTTCGGGTTGGAAGTGGGTGGGAAAGTTCGA"
DR5 sgRNA 1	3906695;Value Read;;**pLentiguidePuro +DR5sgRNA 1.1**;ASM0094006;hU6-F;final result;980;"> pLentiguidePuro +DR5sgRNA 11_hU6-F -- 14994 of sequence CAGGCTGTTAGAGAGATAATTAGAATTAATTTGACTGTAAACACAAAGATATTAGTACAAAATACGTGACGT AGAAAGTAATAATTTCTTGGGTAGTTTGCAGTTTTAAAATTATGTTTTAAAATGGACTATCATATGCTTACCGT AACTTGAAAGTATTTCGATTTCTTGGCTTTATATATCTTGTGGAAAGGACGAAACACCG**CCAGGACCCAGGG** **AGGCGCG**GTTTTAGAGCTAGAAATAGCAAGTTAAAATAAGGCTAGTCCGTTATCAACTTGAAAAAGTGGCA CCGAGTCGGTGCTTTTTTAAGCTTGGCGTAACTAGATCTTGAGACAAATGGCAGTATTCATCCACAATTTTAA AAGAAAAGGGGGGATTGGGGGGTACAGTGCAGGGGAAAGAATAGTAGACATAATAGCAACAGACATACA AACTAAAGAATTACAAAAACAAATTACAAAAATTCAAAATTTTCGGGTTTATTACAGGGACAGCAGAGATCC ACTTTGGCGCCGGCTCGAGGGGGCCCGGGTGCAAAGATGGATAAAGTTTTAAACAGAGAGGAATCTTTGCA GCTAATGGACCTTCTAGGTCTTGAAAGGAGTGGGAATTGGCTCCGGTGCCCGTCAGTGGGCAGAGCGCACA TCGCCCACAGTCCCCGAGAAGTTGGGGGGAGGGGTCGGCAATTGATCCGGTGCCTAGAGAAGGTGGCGCG GGGTAAACTGGGAAAGTGATGTCGTGTACTGGCTCCGCCTTTTTCCCGAGGGTGGGGGAGAACCGTATATAA GTGCAGTAGTCGCCGTGAACGTTCTTTTTCGCAACGGGTTTGCCGCCAGAACACAGGTAAGTGCCGTGTGTG GTTCCCGCGGGCCTGGCCTCTTTACGGGTTATGGCCCTTGCGTGCCTTGAATTACTTCCACCTGGCTGCAGTAC GTGATTCTTGATCCCGAGCTTCGGGTTGGAAGTGGGTGGGAAAATTCA";
DR5 sgRNA 2	3906695;Value Read;;**pLentiguidePuro +DR5sgRNA 2.1**;ASM0094006;hU6-F;final result;980;"> pLentiguidePuro +DR5sgRNA 21_hU6-F -- 14994 of sequence CAGGCTGTTAGAGAGATAATTAGAATTAATTTGACTGTAAACACAAAGATATTAGTACAAAATACGTGACGT AGAAAGTAATAATTTCTTGGGTAGTTTGCAGTTTTAAAATTATGTTTTAAAATGGACTATCATATGCTTACC GTAACTTGAAAGTATTTCGATTTCTTGGCTTTATATATCTTGTGGAAAGGACGAAACACCG**CCTAGCTCCCC** **AGCAGAGAG**GTTTTAGAGCTAGAAATAGCAAGTTAAAATAAGGCTAGTCCGTTATCAACTTGAAAAAGTG GCACCGAGTCGGTGCTTTTTTAAGCTTGGCGTAACTAGATCTTGAGACAAATGGCAGTATTCATCCACAATT TTAAAAGAAAAGGGGGGATTGGGGGGTACAGTGCAGGGGAAAGAATAGTAGACATAATAGCAACAGACA TACAAACTAAAGAATTACAAAAACAAATTACAAAAATTCAAAATTTTCGGGTTTATTACAGGGACAGCAGAG ATCCACTTTGGCGCCGGCTCGAGGGGGCCCGGGTGCAAAGATGGATAAAGTTTTAAACAGAGAGGAATCTT TGCAGCTAATGGACCTTCTAGGTCTTGAAAGGAGTGGGAATTGGCTCCGGTGCCCGTCAGTGGGCAGAGCG CACATCGCCCACAGTCCCCGAGAAGTTGGGGGGAGGGGTCGGCAATTGATCCGGTGCCTAGAGAAGGTGG CGCGGGGTAAACTGGGAAAGTGATGTCGTGTACTGGCTCCGCCTTTTTCCCGAGGGTGGGGGAGAACCGTA TATAAGTGCAGTAGTCGCCGTGAACGTTCTTTTTCGCAACGGGTTTGCCGCCAGAACACAGGTAAGTGCCGT GTGTGGTTCCCGCGGGCCTGGCCTCTTTACGGGTTATGGCCCTTGCGTGCCTTGAATTACTTCCACCTGGCTG CAGTACGTGATTCTTGATCCCGAGCTTCGGGTTGGAAGTGGGTGGGAAAATTCA;

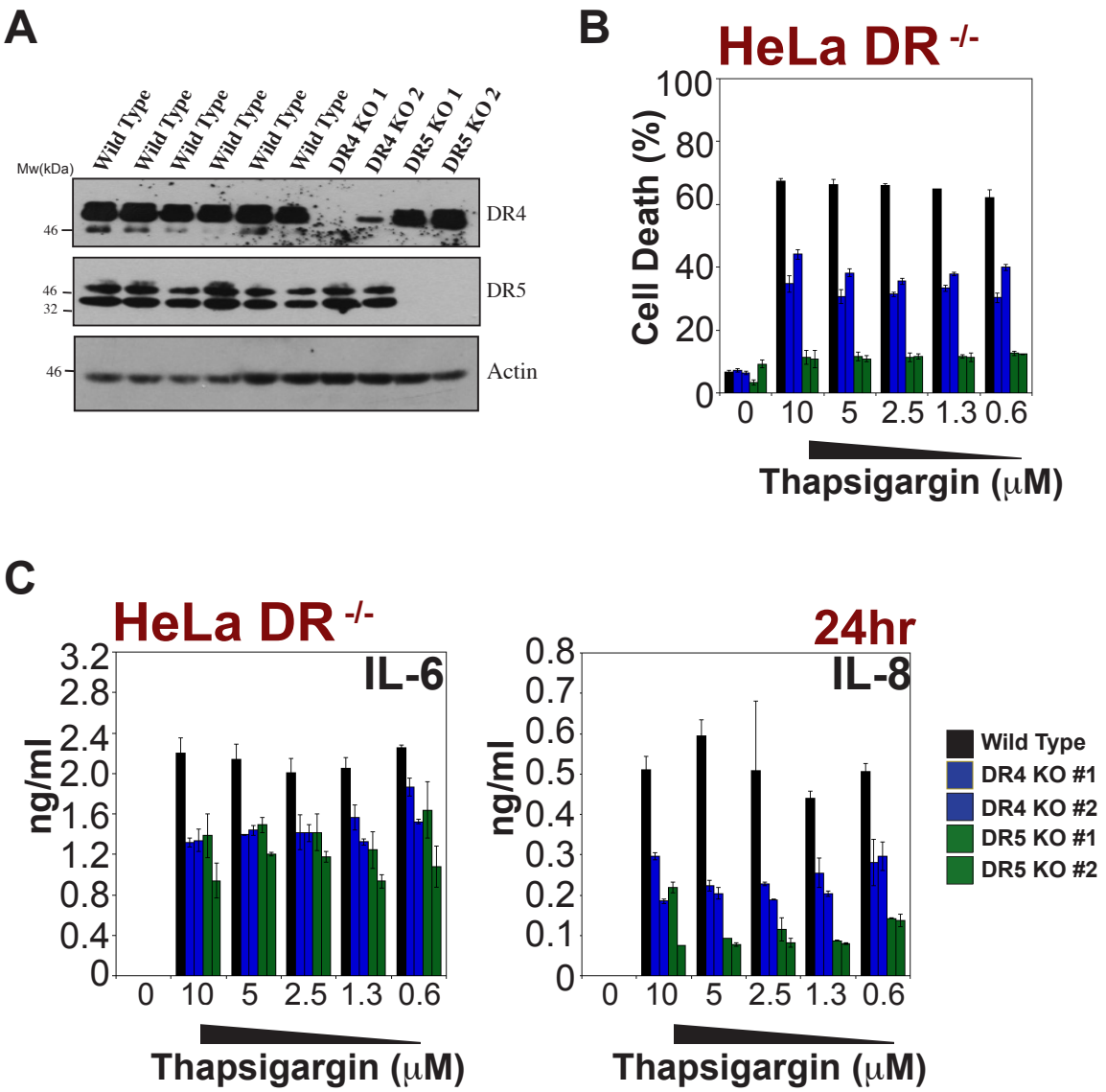

Figure 3.5 ER stress-induced cytokine production is dependent on death receptors DR4 and DR5
(A) Cell populations were puromycin selected after transfection with sgRNA targetting DR4 or DR5. Cell lysates were prepared and protein expression was analysed by western blot.
(B) HeLa WT versus HeLa DR4$^{-/-}$ and HeLa DR5$^{-/-}$ cells were treated for 24hr with the indicated concentrations of Thapsigargin. Cell death was measured based on cell morphology from counts of 3 fields per well (of approximately 100 cells per field).
(C) Cytokine concentrations in cell culture supernatants from cell supernatants in (B) were determined by ELISA.
The error bars represent the mean +/- SEM of triplicate samples.

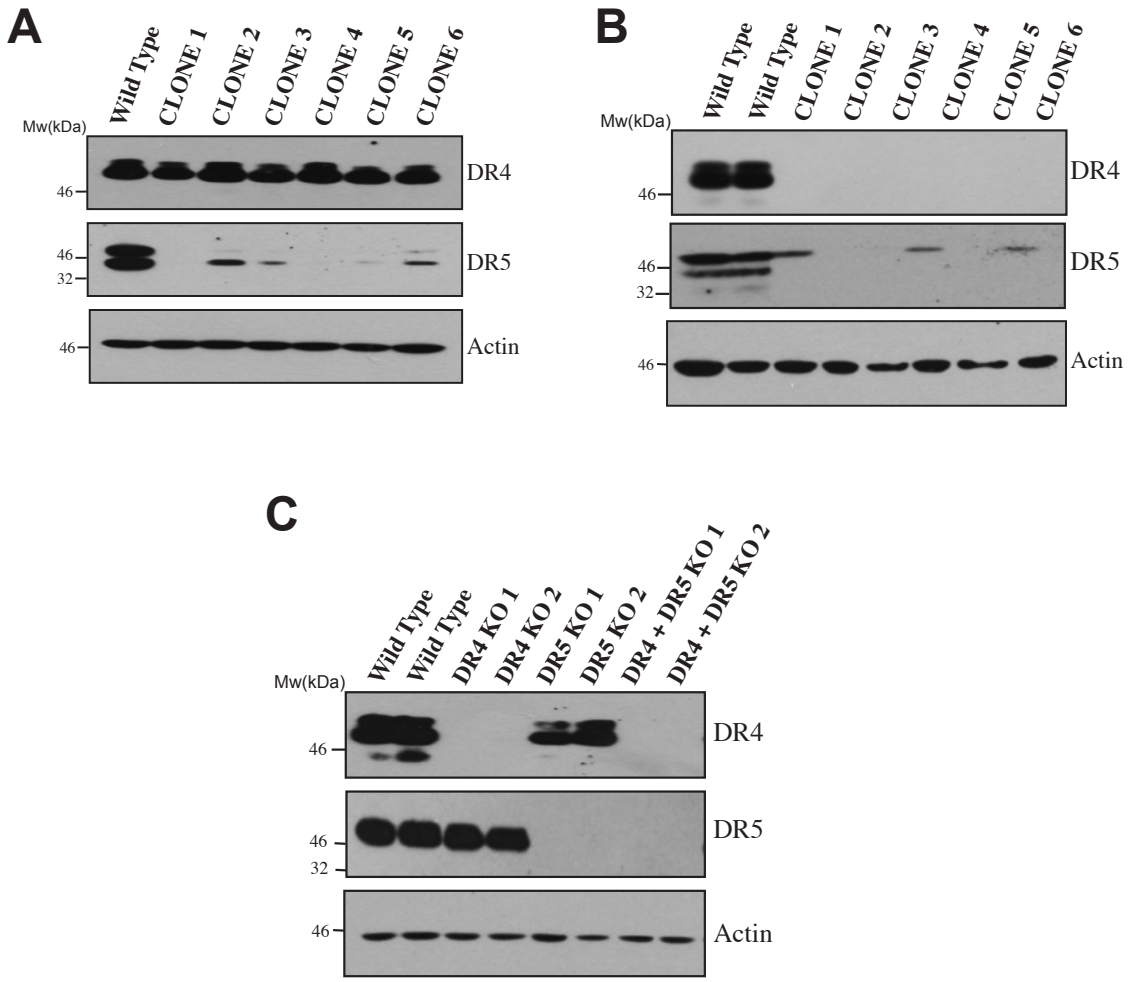

Figure 3.6 Generation of DR4, DR5 and DR4/DR5 null cell lines

(A) HeLa CRISPR KO were generated by GenJet transfection of sgRNA targetting DR4 or DR5, followed by selection using puromycin. DR5 KO clones were expanded from a single cell using limited dilution cloning.
(B) HeLa CRISPR KO were generated by GenJet transfection of sgRNA targetting both DR4 and DR5, followed by selection using puromycin. DR4/DR5 KO clones were expanded from a single cell using limited dilution cloning.
(C) Wild type HeLa cells and DR4, DR5 and DR4/DR5 DKO cell populations were grown up.
In (A-C) cell lysates were prepared and protein expression was analysed by western blot.

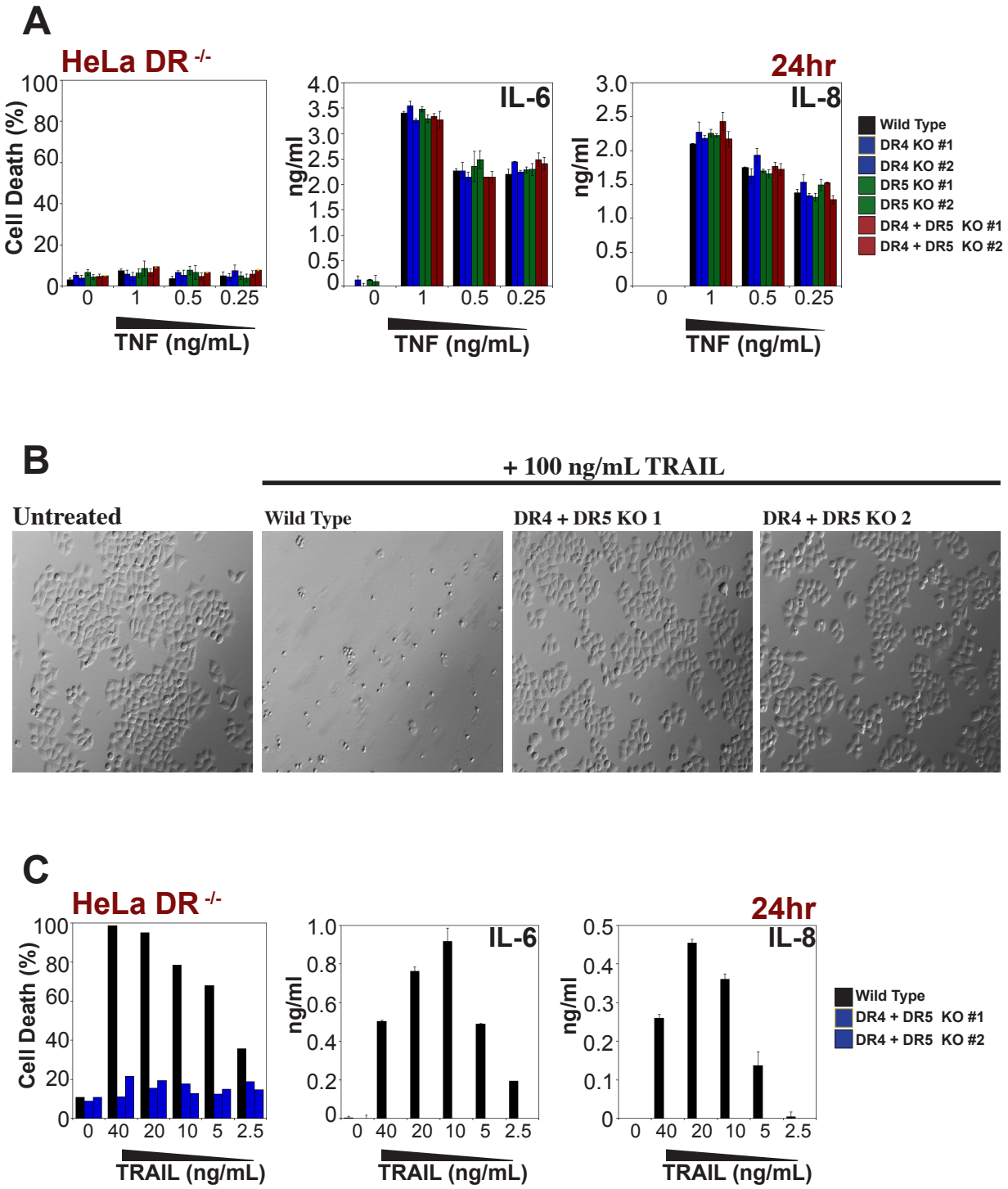

Figure 3.7 DR4/DR5 DKO HeLa cells are protected from TRAIL-induced cell death and cytokine production

(A) HeLa WT versus HeLa DR4/DR5$^{-/-}$ cells were treated for 24hr with the indicated concentrations of TNF. Cell death was measured based on cell morphology from counts of 3 fields per well (of approximately 100 cells per field). Cytokine concentrations in cell culture supernatants were determined by ELISA.
(B) HeLa WT versus HeLa DR4/DR5$^{-/-}$ cells were treated for 24hr with the indicated concentration of TRAIL. Cells were visualised using phase contrast microscopy.
(C) HeLa WT versus HeLa DR4/DR5$^{-/-}$ cells were treated for 24hr with the indicated concentrations of TRAIL. Cell death was measured based on cell morphology from counts of 3 fields per well (of approximately 100 cells per field). Cytokine concentrations in cell culture supernatants were determined by ELISA.
The error bars represent the mean +/- SEM of triplicate samples.

We next explored what effect this more comprehensive disruption of TRAIL signalling had on cytokine production in response to ER stress. Quite strikingly, KO of both DR4 and DR5 again conferred protection against cell death and cytokine production in response to thapsigargin treatment, with DR5 ablation having a marginally more impressive effect. Consistent with this, DR4/DR5 double KO cell populations showed a synergistic protective effect **(Figures 3.8 A & 3.8 B)**. With regards to cytokine production in response to brefeldin A, a similar protective effect was seen in DR4/DR5 KO cells **(Figure 3.8 C)**.

3.1.4 ER Stress-Induced Cytokines Are Independent of TRAIL Ligand

Thapsigargin, brefeldin A and tunicamycin treatments were carried out in the presence of a TRAILR2-Fc fusion protein in order to assess whether ER stress-induced cytokine production was dependent on autocrine or paracrine TRAIL ligand. However, neutralisation of TRAIL ligand has no effect on death or cytokine production seen in response to ER stress-inducing agents thapsigargin, brefeldin A or tunicamycin **(Figures 3.9 A-3.9 C)**.

3.1.5 ER Stress-Induced Cytokines Are CHOP Dependent.

As CHOP has been implicated in DR5 upregulation in response to ER stress, we next asked whether ER stress induced-cytokine production was CHOP-dependent. CHOP KO cell populations were generated in the same manner as described above for FADD KO cells. Two sgRNAs targeted against the human GADD153 (CHOP) gene were designed. These are summarised in **Table 3.5**. sgRNA sequences were cloned into pLentiguidePuro and plasmids were sent for sequencing to confirm insertion. Results are summarised in **Table 3.6**.

Cells were treated with brefeldin A in order to upregulate the transcription factor CHOP so that KO could be confirmed at the protein level by western blot **(Figure 3.10 A)**. Control treatments were then carried out to confirm that all cell types responded to TNF as would be expected. Cells were initially treated with a titration of TNF versus wild type cells, to confirm that they still produced cytokines as expected **(Figure 3.10 B)**. Using a titration of all three classical ER stress inducing agents, cell death and production of IL-6 and IL-8 in CHOP KO cells were compared to wild type HeLa cells **(Figures 3.11 A-3.11 C)**. A striking reduction in cytokine production was seen in the CHOP KO cells when compared with the wild type cells with all three stimuli and at all doses. Interestingly, in the case of thapsigargin, a marked protection from cell death was seen in the absence of CHOP, while a very marginal protection was seen with brefeldin A-induced death. In conclusion, we have identified a CHOP/DR4/DR5/FADD-dependent

signalling pathway which links ER stress to inflammatory signalling in this context **(Figure 3.12)**.

Table 3.5: Summary of sgRNAs designed to target human CHOP.

	Sequence	PAM	Exon	Strand
CHOP sgRNA 1	CCAGCTGGACAGTGTCCCGA	GGG	Exon 1	Sense
CHOP sgRNA 2	AGCACATCTGCAGGATAATG	CGG	Exon 2	Sense

Table 3.6: Summary of sequencing results to confirm insertion of sgRNA targeting CHOP into pLentiGuidePuro vector

sgRNA	Sequencing Results
CHOP sgRNA 1	3969455;Value Read;;**CHOP 1.1**;ASM0094022;hU6-F;final result;951;">CHOP 11_hU6-F – 14965 of sequence AGGCTGTTAGAGAGATAATTAGAATTAATTTGACTGTAAACACAAAGATATTAGTACAAAATACGTGA CGTAGAAAGTAATAATTTCTTGGGTAGTTTGCAGTTTTAAAATTATGTTTTAAAATGGACTATCATATGCT TACCGTAACTTGAAAGTATTTCGATTTCTTGGCTTTATATATCTTGTGGAAAGGACGAAACACCGCCAGCT GGACAGTGTCCCGAGTTTTAGAGCTAGAAATAGCAAGTTAAAATAAGGCTAGTCCGTTATCAACTTGAAA AAGTGGCACCGAGTCGGTGCTTTTTTAAGCTTGGCGTAACTAGATCTTGAGACAAATGGCAGTATTCATC CACAATTTTAAAAGAAAAGGGGGGATTGGGGGGTACAGTGCAGGGGAAAGAATAGTAGACATAATAGC AACAGACATACAAACTAAAGAATTACAAAAACAAATTACAAAAATTCAAAATTTTCGGGTTTATTACAGG GACAGCAGAGATCCACTTTGGCGCCGGCTCGAGGGGGCCCGGGTGCAAAGATGGATAAAGTTTTAAACA GAGAGGAATCTTTGCAGCTAATGGACCTTCTAGGTCTTGAAAGGAGTGGGAATTGGCTCCGGTGCCCGTC AGTGGGCAGAGCGCACATCGCCCACAGTCCCCGAGAAGTTGGGGGGAGGGGTCGGCAATTGATCCGGTG CCTAGAGAAGGTGGCGCGGGGTAAACTGGGAAAGTGATGTCGTGTACTGGCTCCGCCTTTTTCCCGAGGG TGGGGGAGAACCGTATATAAGTGCAGTAGTCGCCGTGAACGTTCTTTTTCGCAACGGGTTTGCCGCCAGAA CACAGGTAAGTGCCGTGTGTGGTTCCCGCGGGCCTGGCCTCTTTACGGGTTATGGCCCTTGCGTGCCTTGAA TTACTTCCACCTGGCTGCAGTACGTGATTCTTGATCCCAAGCT";
CHOP sgRNA 2	3969455;Value Read;;**CHOP 2.2**;ASM0094023;hU6-F;final result;979;">CHOP 22_hU6-F – 15994 of sequence AGGCTGTTAGAGAGATAATTAGAATTAATTTGACTGTAAACACAAAGATATTAGTACAAAATACGTGACGT AGAAAGTAATAATTTCTTGGGTAGTTTGCAGTTTTAAAATTATGTTTTAAAATGGACTATCATATGCTTACC GTAACTTGAAAGTATTTCGATTTCTTGGCTTTATATATCTTGTGGAAAGGACGAAACACCGAGCACATCTGC AGGATAATGGTTTTAGAGCTAGAAATAGCAAGTTAAAATAAGGCTAGTCCGTTATCAACTTGAAAAAGTGG CACCGAGTCGGTGCTTTTTTAAGCTTGGCGTAACTAGATCTTGAGACAAATGGCAGTATTCATCCACAATTT TAAAAGAAAAGGGGGGATTGGGGGGTACAGTGCAGGGGAAAGAATAGTAGACATAATAGCAACAGACA TACAAACTAAAGAATTACAAAAACAAATTACAAAAATTCAAAATTTTCGGGTTTATTACAGGGACAGCAGA GATCCACTTTGGCGCCGGCTCGAGGGGGCCCGGGTGCAAAGATGGATAAAGTTTTAAACAGAGAGGAAT CTTTGCAGCTAATGGACCTTCTAGGTCTTGAAAGGAGTGGGAATTGGCTCCGGTGCCCGTCAGTGGGCAG AGCGCACATCGCCCACAGTCCCCGAGAAGTTGGGGGGAGGGGTCGGCAATTGATCCGGTGCCTAGAGAA GGTGGCGCGGGGTAAACTGGGAAAGTGATGTCGTGTACTGGCTCCGCCTTTTTCCCGAGGGTGGGGGAG AACCGTATATAAGTGCAGTAGTCGCCGTGAACGTTCTTTTTCGCAACGGGTTTGCCGCCAGAACACAGGTA AGTGCCGTGTGTGGTTCCCGCGGGCCTGGCCTCTTTACGGGTTATGGCCCTTGCGTGCCTTGAATTACTTCC ACCTGGCTGCAGTACGTGATTCTTGATCCCGAGCTTCGGGTTGGAAGTGGGTGGGGAAAGTTCG";

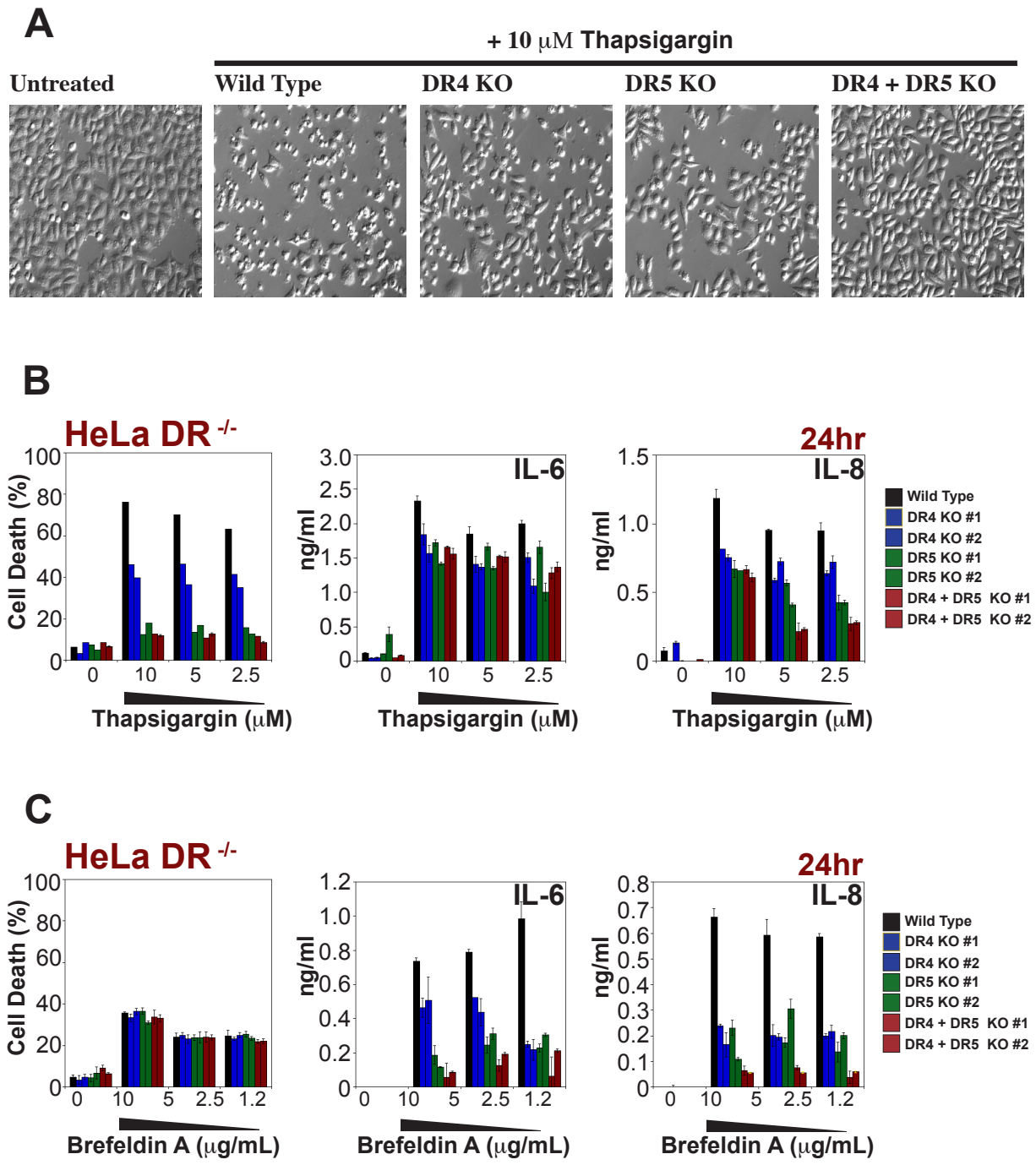

Figure 3.8 ER stress-induced cytokines are dependent on death receptors DR4 and DR5

(A) HeLa WT versus HeLa DR4$^{-/-}$, DR5$^{-/-}$ and DR4/DR5$^{-/-}$ cells were treated for 24hr with the indicated concentration of Thapsigargin. Cells were visualised using phage contrast microscopy.

(B)HeLa WT versus HeLa DR4$^{-/-}$, DR5$^{-/-}$ and DR4/DR5$^{-/-}$ cells were treated for 24hr with the indicated concentrations of Thapsigargin.

(C) HeLa WT versus HeLa DR4$^{-/-}$, DR5$^{-/-}$ and DR4/DR5$^{-/-}$ cells were treated for 24hr with the indicated concentrations of Brefeldin A.

In (B & C), cell death was measured based on cell morphology from counts of 3 fields per well (of approximately 100 cells per field). Cytokine concentrations in cell culture supernatants were determined by ELISA. The error bars represent the mean +/- SEM of triplicate samples.

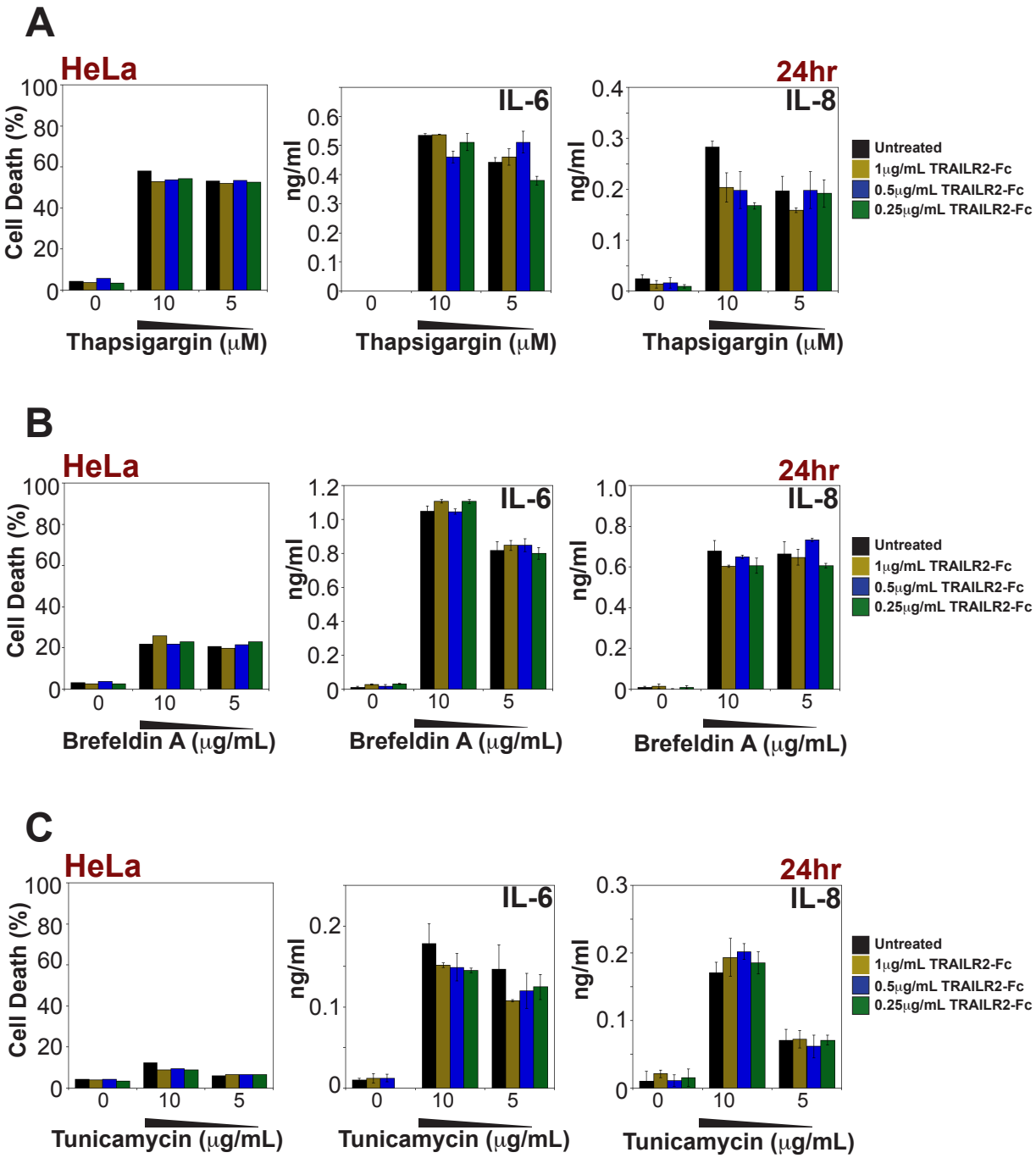

Figure 3.9 ER stress-induced cytokines are independent of TRAIL ligand

(A) HeLa cells were treated for 24hr with the indicated doses of Thapsigargin +/- the indicated doses of TRAIL-R2Fc.

(B) HeLa cells were treated for 24hr with the indicated doses of BrefeldinA +/- the indicated doses of TRAIL-R2Fc.

(C) HeLa were treated for 24hr with the indicated doses of Tunicamycin +/- the indicated doses of TRAILR2Fc.

In (A-C), cell death was measured based on cell morphology from counts of 3 fields per well (of approximately 100 cells per field). Cytokine concentrations in cell culture supernatants were determined by ELISA.

The error bars represent the mean +/- SEM of triplicate samples.

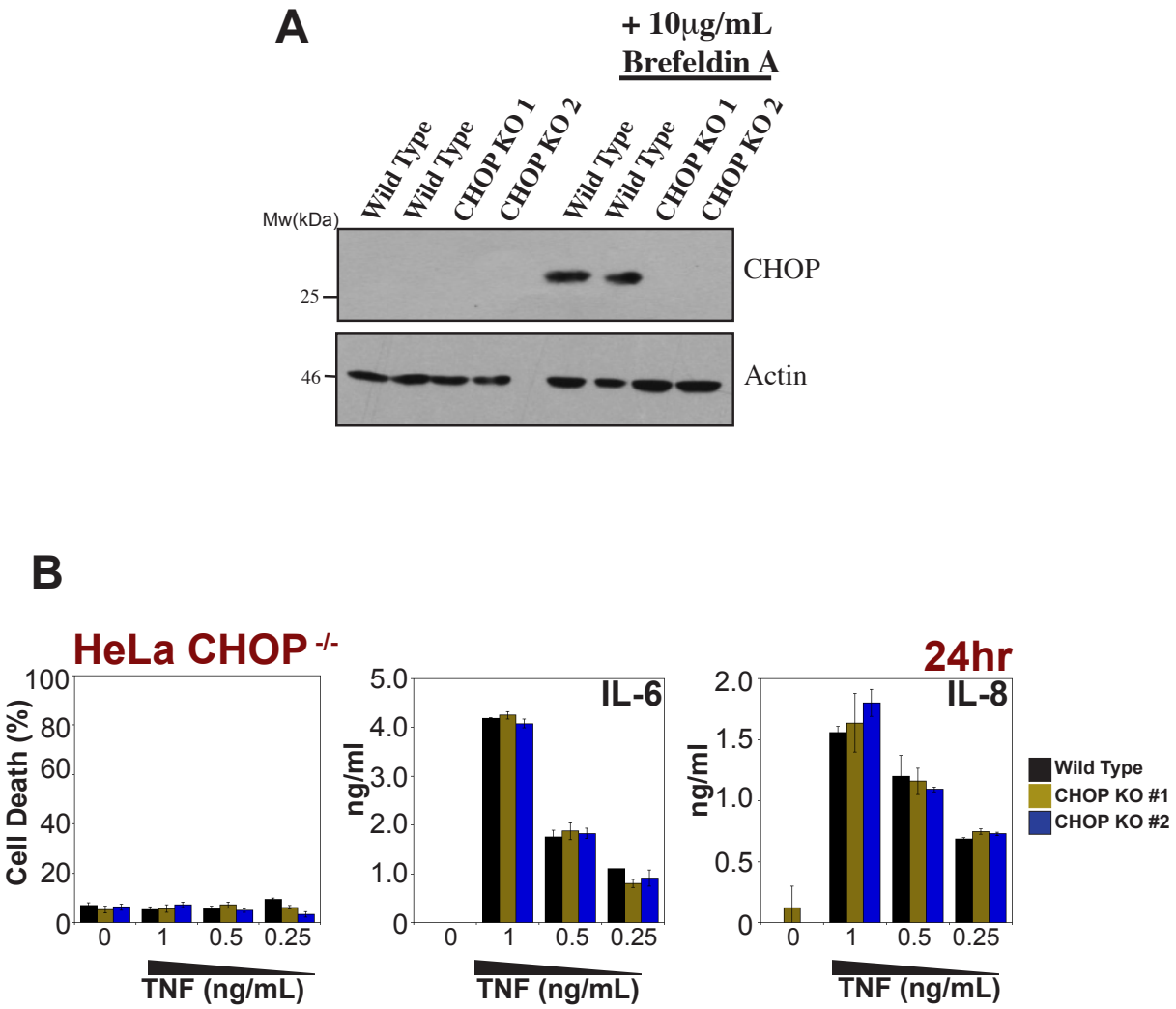

Figure 3.10 Generation of CHOP KO HeLa cells using CRISPR

(A) HeLa CRISPR KO were generated by GenJet transfection of sgRNA targetting CHOP, followed by selection using puromycin. Selected cell populations were treated for 24hr with the indicated concentration of Brefeldin A. Cell lysates were prepared and protein expression was analysed by western blot.

(B) HeLa WT versus HeLa CHOP$^{-/-}$ cells were treated for 24hr with the indicated concentrations of TNF. Cell death was measured based on cell morphology from counts of 3 fields per well (of approximately 100 cells per field). Cytokine concentrations in cell culture supernatants were determined by ELISA.

The error bars represent the mean +/- SEM of triplicate samples.

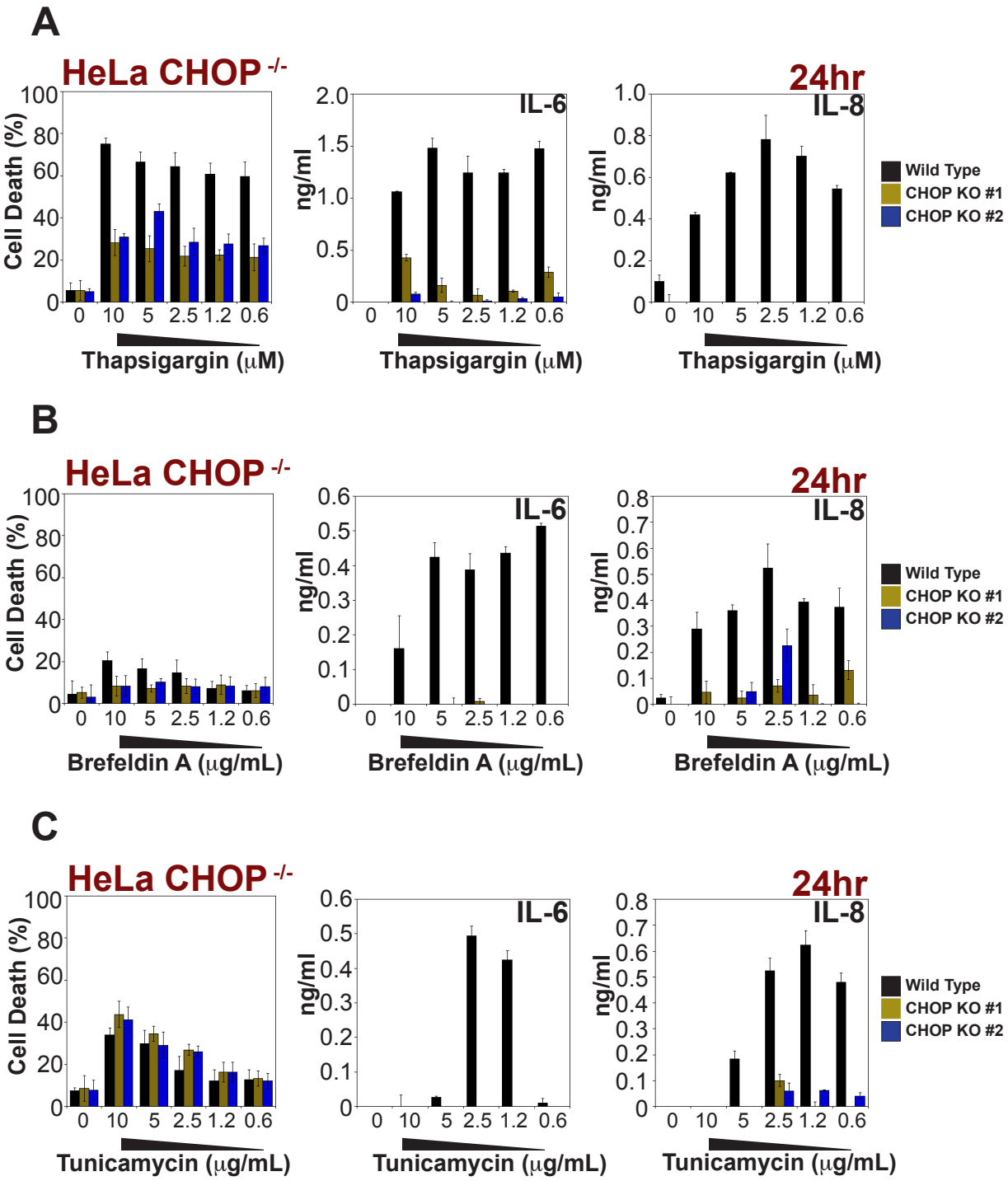

Figure 3.11 ER stress-induced cytokines are CHOP-dependent

(A) HeLa WT versus HeLa CHOP$^{-/-}$ cells were treated for 24hr with the indicated doses of Thapsigargin.
(B) HeLa WT versus HeLa CHOP$^{-/-}$ cells were treated for 24hr with the indicated doses of BrefeldinA.
(C) HeLa WT versus HeLa CHOP$^{-/-}$ cells were treated for 24hr with the indicated doses of Tunicamycin.
In (A-C), cell death was measured based on cell morphology from counts of 3 fields per well (of approximately 100 cells per field). Cytokine concentrations in cell culture supernatants were determined by ELISA.
The error bars represent the mean +/- SEM of triplicate samples.

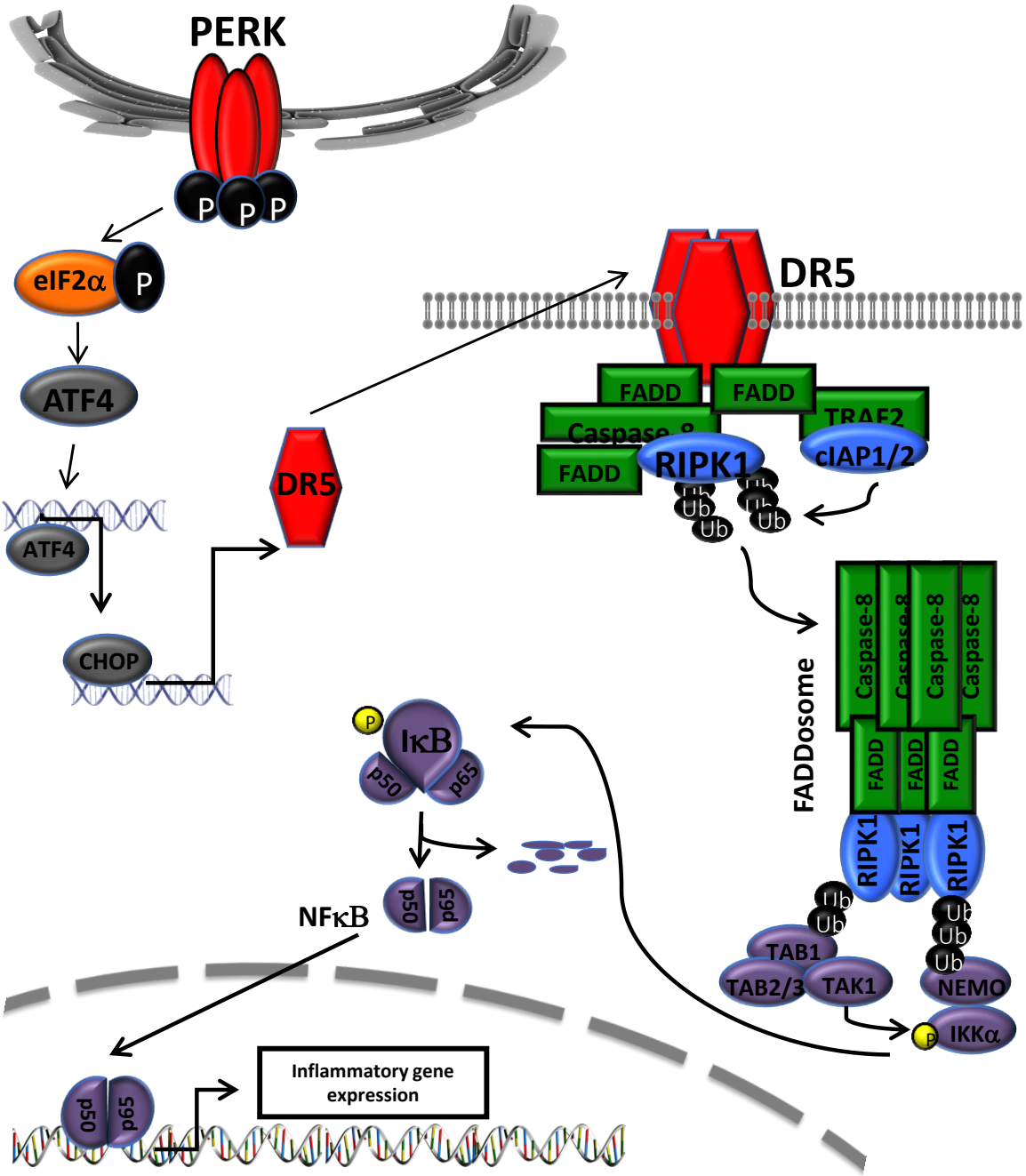

Figure 3.12 ER stress-induced cytokines in a death receptor dependent manner

ER stress-induced sequestration of BiP away from ER membrane-associated receptor PERK allows for oligomerisation and autophosphorylation of PERK. Activated PERK leads to transcriptional upregulation of the transcription factor CHOP. In turn, CHOP transcriptionally upregulates DR5, leading to receptor aggregation and ligand-independent activation of signalling downstream of DRs.

FADD is recruited to the DISC via its DD, while caspase-8 is recruited downstream via its DEDs. RIPK1 associates with the receptor-associated complex via DD interactions with FADD. Oligomerisation of caspase-8 occurs, allowing for the formation of a soluble aggregate that act as a scaffold. Stabilised FADD associates with caspase-8 and facilitates the successive recruitment of RIPK1 to form what has been dubbed the "FADDosome" complex. TRAF2 binding to FADD allows for IAP association with the complex and subsequent addition of ubiquitin chains to RIPK1. Modified RIPK1 can recruit the TAB/TAK1 and IKK complexes, ultimately leading to the phosphorylation and degradation of IkB. The p50 and p65 NFkB subunits are then free to translocate to the nucleus, leading to downstream activation of inflammatory signalling.

3.1.6 Glucose Deprivation-Induced Cell Death Is Death Receptor and FADD-Dependent.

As metabolic stress (which can induce ER stress), particularly nutrient deprivation frequently occurs in tumours, it is plausible that ER stress pathway activation under these circumstances may lead to death receptor upregulation. KO cells generated earlier in this study were used in order to assess whether ER stress-induced cell death in response to glucose deprivation was dependent on death receptor upregulation and downstream signalling. Mild protection from cell death seen in response to glucose deprivation was seen in the absence of DR4, with a more marked protection seen in the absence or DR5 or of both receptors **(Figure 3.13 A & 3.13 B)**. Ablation of FADD also provided a similar protective effect to that seen in DR4/DR5 double KO cells. These results suggest that death receptors are relevant in physiologically relevant ER stress contexts. While glucose deprivation-induced cytokine induction was not analysed in this study, this analysis may give interesting results.

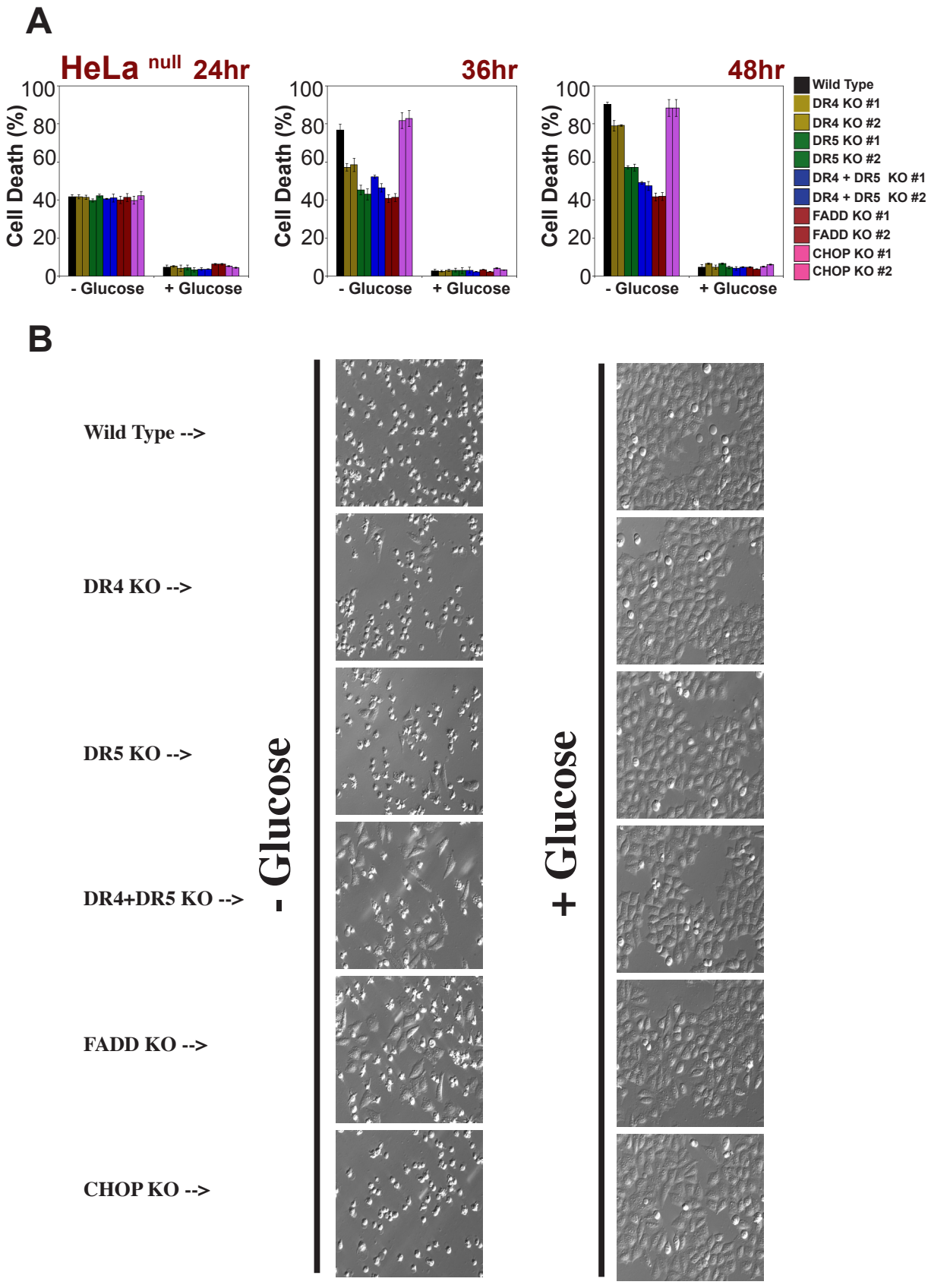

Figure 3.13 Glucose deprivation-induced cell death is TRAIL-R and FADD-dependent
(A) HeLa WT versus the indicated HeLa knockouts were incubated in glucose free DMEM (-glucose) or DMEM supplemented with 25mM glucose for 24, 36 and 48 hr. Cell death was measured based on cell morphology from counts of 3 fields per well (of approximately 100 cells per field).
(B) Cells from (A) were visualised using phase contrast microscopy.
The error bars represent the mean +/- SEM of triplicate samples.

3.2 Chapter 2

3.2.1 Taxanes Induce Cytokine Production, ER Stress and DR5 Upregulation

Taxanes, paclitaxel and docetaxel, have previously been shown to induce cytokines in sporadic studies and have classically been associated with secondary inflammation and metastasis (Javeed, 2009, Kajiyama, 2007, Penson, 2000, Pusztai, 2004). They have also been associated with DR4 and DR5 upregulation (Dorsey et al., 2009, Nimmanapalli et al., 2001). Initial experiments carried out by our group (Henry C.M. & Sullivan G. personal communication) showed that DR5 is important for taxane-induced cytokine production. To investigate further whether taxane-induced inflammation is dependent on DR signalling, we first confirmed that both paclitaxel and docetaxel robustly induce cytokines in HeLa cells over a range of doses **(Figure 3.14 A)**. Surprisingly, both taxanes also induce a robust ER stress response – causing phosphorylation of PERK, stabilisation and upregulation of IRE1 and upregulation of transcription factors CHOP and ATF4. Additionally, upregulation of both the long and short forms of DR5 was observed **(Figure 3.14 B)**. Interestingly, sporadic associations between taxanes and ER stress have been made previously (Notte, 2015). Paclitaxel treatment in breast cancer cells has been shown to induce ATF4-dependent UPR (Notte et al., 2015). ER stress genes have additionally been implicated in paclitaxel induced apoptosis (Liao et al., 2008). In line with this, treatment with thapsigargin has been shown to increase the cell killing potency of paclitaxel or docetaxel by 10- to 12-fold (Wu et al., 2009). Given that taxanes have been associated tenuously with ER stress as well as death receptor upregulation, we wondered whether ER stress was in fact causative to death receptor upregulation in this case. It is plausible that ER stress acts more universally than is realised in this respect. We initially showed that taxanes induce NFκB activation, manifesting in degradation of IκBα and accumulation of phospho-IκBα. Similarly, accumulation of phospho-p65 was seen, while p65 remained relatively constant **(Figure 3.14 C)**.

To confirm that this phenomenon was not limited to HeLa cells. We additionally tested the colon cancer cell line HCT116, which has previously been shown to produce cytokines in response to TRAIL stimulation (Henry and Martin, 2017). Treatment with a range of concentrations of paclitaxel or docetaxel robustly induced cytokine production in these cells, particularly IL-8 **(Figure 3.15 A)**. Similar to the response seen in HeLa cells, activation and upregulation of classic ER stress-associated markers was detected, as was a robust upregulation of DR5 **(Figure 3.15 B)**.

Two additional human cell lines were also tested – the NSCLC cell line A549 and the colon carcinoma cell line SKOV3, both of which have previously been shown to

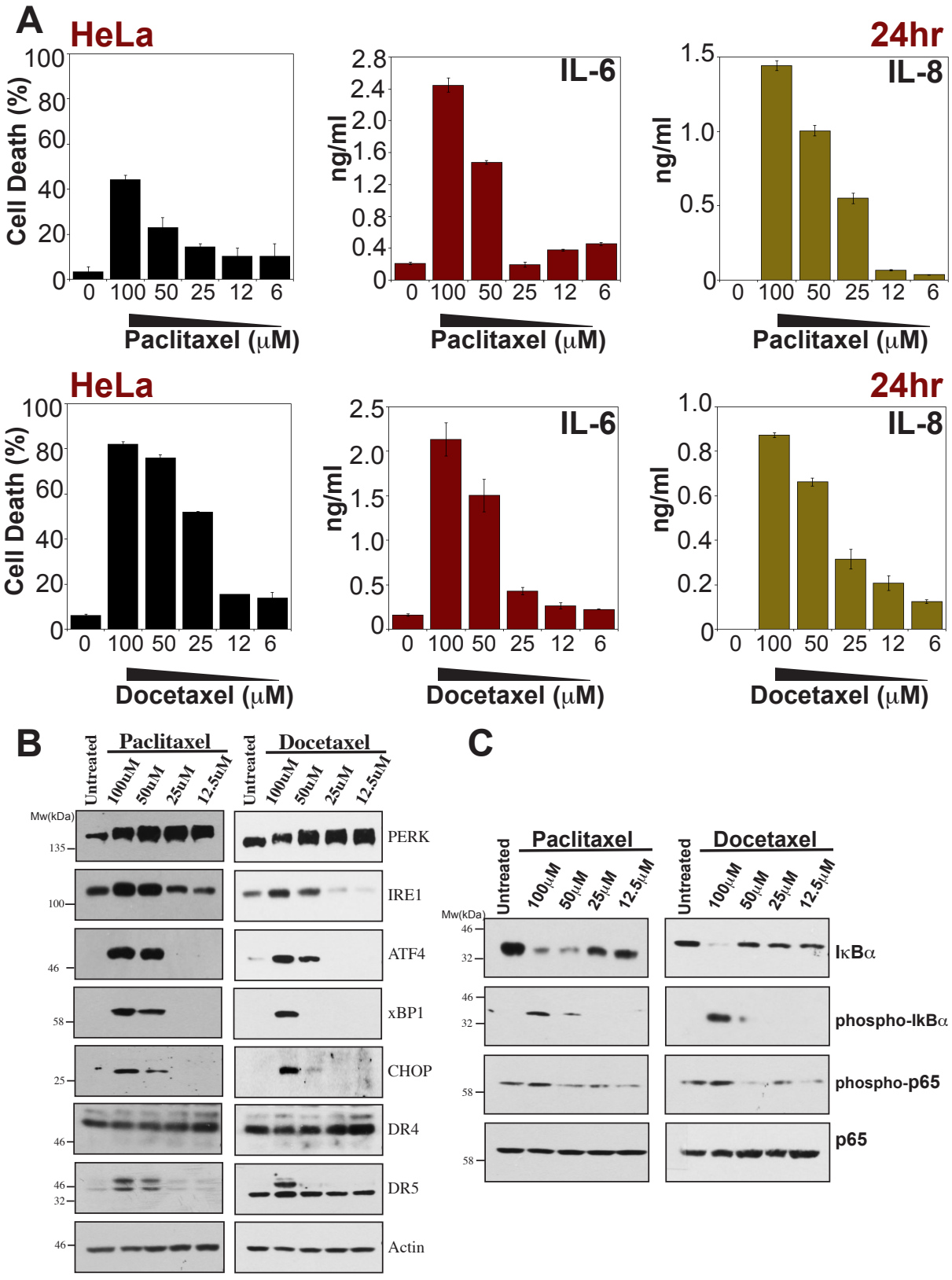

Figure 3.14 Taxanes Paclitaxel and Docetaxel induce cytokines and DR5 upregulation in HeLa cells
(A) HeLa cells were stimulated for 24hr with the indicated concentrations of Paclitaxel or Docetaxel. Cell death was measured based on cell morphology from counts of 3 fields per well (of approximately 100 cells per field). Cytokine concentrations in cell culture supernatants were determined by ELISA.
(B & C) HeLa cells were stimulated for 24hr with the indicated concentrations of Paclitaxel or Docetaxel for 24. Cell lysates were prepared and protein expression was analysed by western blot.
The error bars represent the mean +/- SEM of triplicate samples.

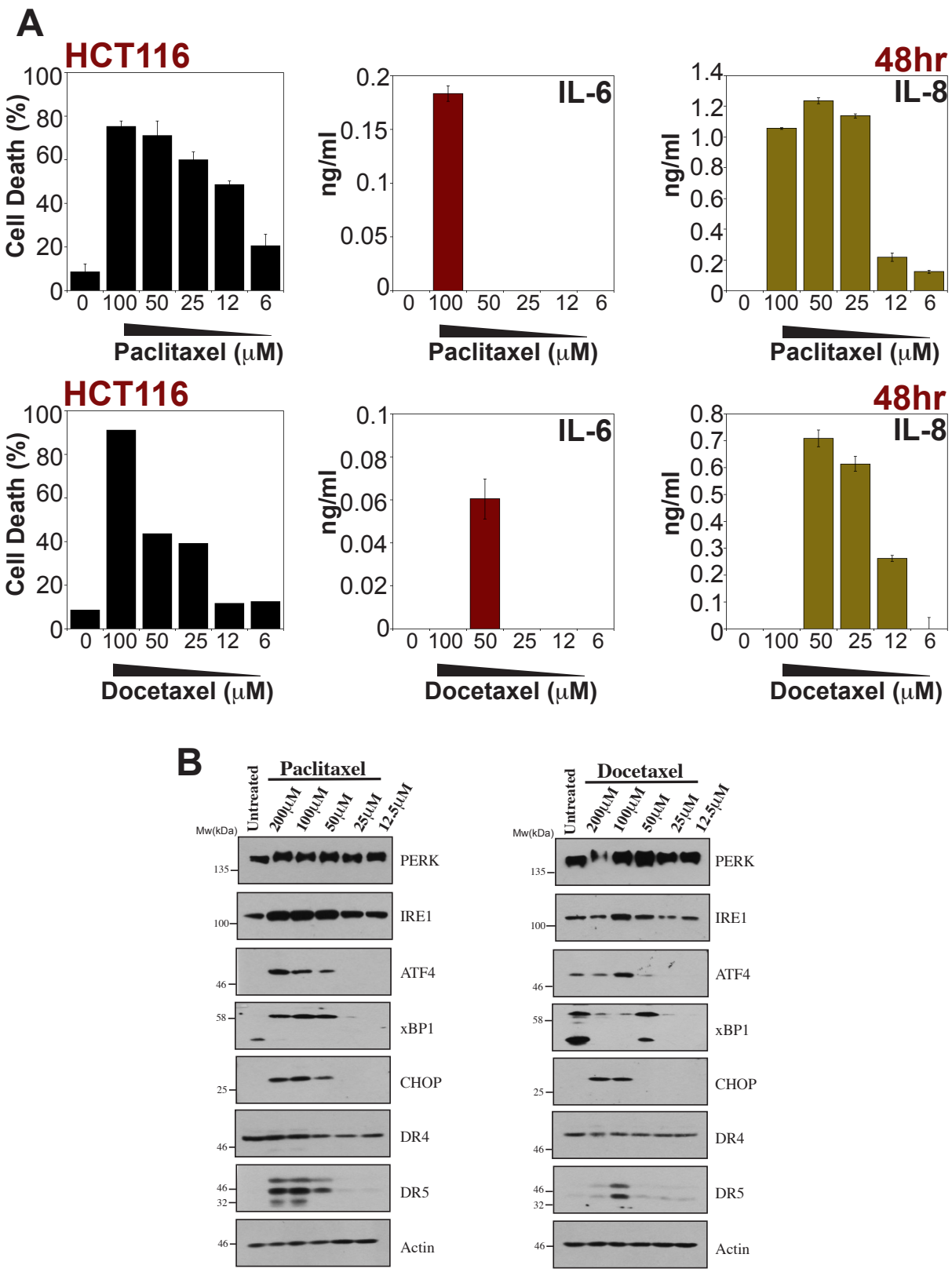

Figure 3.15 Taxanes Paclitaxel and Docetaxel induce cytokines and DR5 upregulation in HCT116 colon cancer cells

(A) HCT116 cells were stimulated for 48hr with the indicated concentrations of Paclitaxel or Docetaxel. Cell death was measured based on cell morphology from counts of 3 fields per well (of approximately 100 cells per field). Cytokine concentrations in cell culture supernatants were determined by ELISA.

(B) HCT116 cells were stimulated for 24hr with the indicated concentrations of Paclitaxel or Docetaxel. Cell lysates were prepared and protein expression was analysed by western blot.

The error bars represent the mean +/- SEM of triplicate samples.

respond to paclitaxel (Penson et al., 2000, Pal et al., 2013). It was found that both cell lines additionally produce cytokines in response to both paclitaxel and docetaxel **(Figures 3.16 A & 3.17 A)**. IL-6, RANTES and CXCL1 were among the cytokines produced. We additionally observed an ER stress response and DR5 upregulation upon taxane treatment in the SKOV3 cell line **(Figures 3.16 B)**.

Finally, we tested the two murine cell lines CT26 and 3LL. Both were found to be potent responders to treatment with paclitaxel. CT26 cells produced an abundance of CCL2, CXCL1 and RANTES **(Figure 3.18 A)**, while 3LL cells produced CXCL1, RANTES and CXCL2 in response to taxanes **(Figure 3.18 D)**. In both cases, doses that induced cytokine production did not induce much cell death **(Figure 3.18 B & 3.18 F)**. While little death was seen at these doses, it was noted that cells had undergone a morphological change – appearing more rounded and condensed **(Figures 3.18 C & 3.18 F)**.

3.2.2 Taxane-Induced Cytokine Production Is Dependent On Signalling Downstream Of Death Receptors.

FADD and caspase-8 are important effector molecules downstream of the TRAIL receptors. FADD KO cell populations generated earlier in this study and caspase-8 KO cells that were generated by Conor M. Henry (and used in a study published in early 2017 by our group (Henry and Martin, 2017)) were used to assess the importance of FADD and caspase-8 in paclitaxel-induced inflammatory cytokines. There was no apparent change in the induction/stabilisation/resting levels of ER stress-associated molecules PERK, IRE1, ATF4 or CHOP or death receptors DR4 and DR5 in the FADD KO cells **(Figure 3.19 A)**. This suggests, as would be expected, that FADD may operate downstream of ER stress and CHOP induced DR5. A role for FADD in paclitaxel-induced cytokines was confirmed **(Figure 3.19 B)**, with dramatic protection being observed in the FADD KO cells when compared to wild-type cells. Caspase-8 KO showed conflicting results – while levels of RANTES and IL-8 were reduced, high background levels of IL-6 in caspase-8 null cells made this result inconclusive **(Figure 3.19 C)**. There interestingly appears to be less DR5 at basal levels and less DR5 accumulating in response to paclitaxel treatment in these cells, while levels of ER stress-associated transcription factors CHOP and ATF4 remained constant **(Figure 3.19 D)**. We concluded that signalling downstream of death receptors is indeed important for taxane-induced cytokine production.

We next wanted to analyse what dependence taxane-induced cytokines have on effectors downstream of TRAIL receptors. Treatment with SMAC mimetic BV6 in combination with paclitaxel caused an increase in cell death and a concurrent decrease

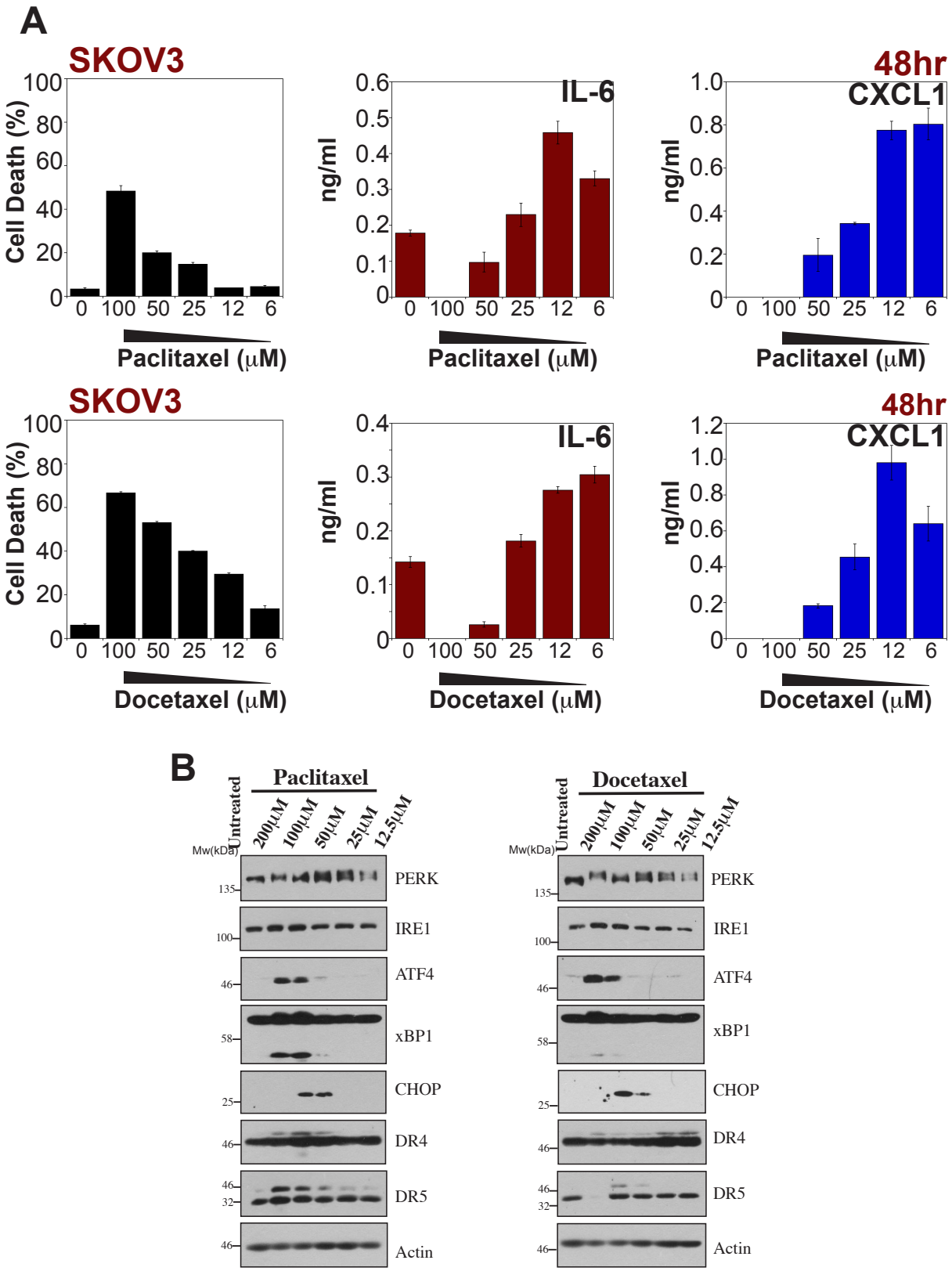

Figure 3.16 Taxanes Paclitaxel and Docetaxel induce cytokines and DR5 upregulation in SKOV3 ovarian carcinoma cells

(A) SKOV3 cells were stimulated for 48hr with the indicated concentrations of Paclitaxel or Docetaxel. Cell death was measured based on cell morphology from counts of 3 fields per well (of approximately 100 cells per field). Cytokine concentrations in cell culture supernatants were determined by ELISA.

(B) SKOV3 cells were stimulated for 24hr with the indicated concentrations of Paclitaxel or Docetaxel. Cell lysates were prepared and protein expression was analysed by western blot.

The error bars represent the mean +/- SEM of triplicate samples.

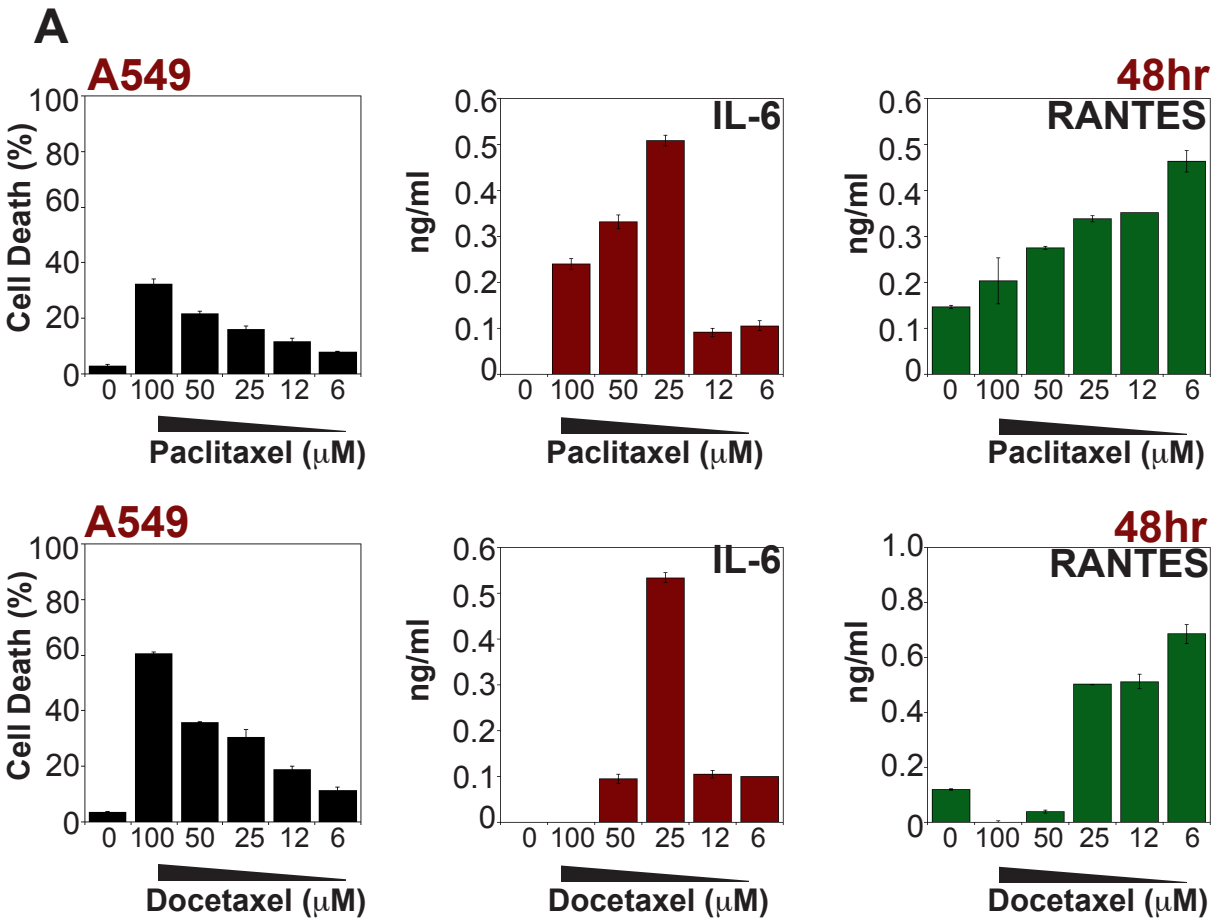

Figure 3.17 Taxanes Paclitaxel and Docetaxel induce cytokines production in A549 NSCLC cells
(A) A549 cells were stimulated for 48hr with the indicated concentrations of Paclitaxel or Docetaxel. Cell death was measured based on cell morphology from counts of 3 fields per well (of approximately 100 cells per field). Cytokine concentrations in cell culture supernatants were determined by ELISA.
The error bars represent the mean +/- SEM of triplicate samples.

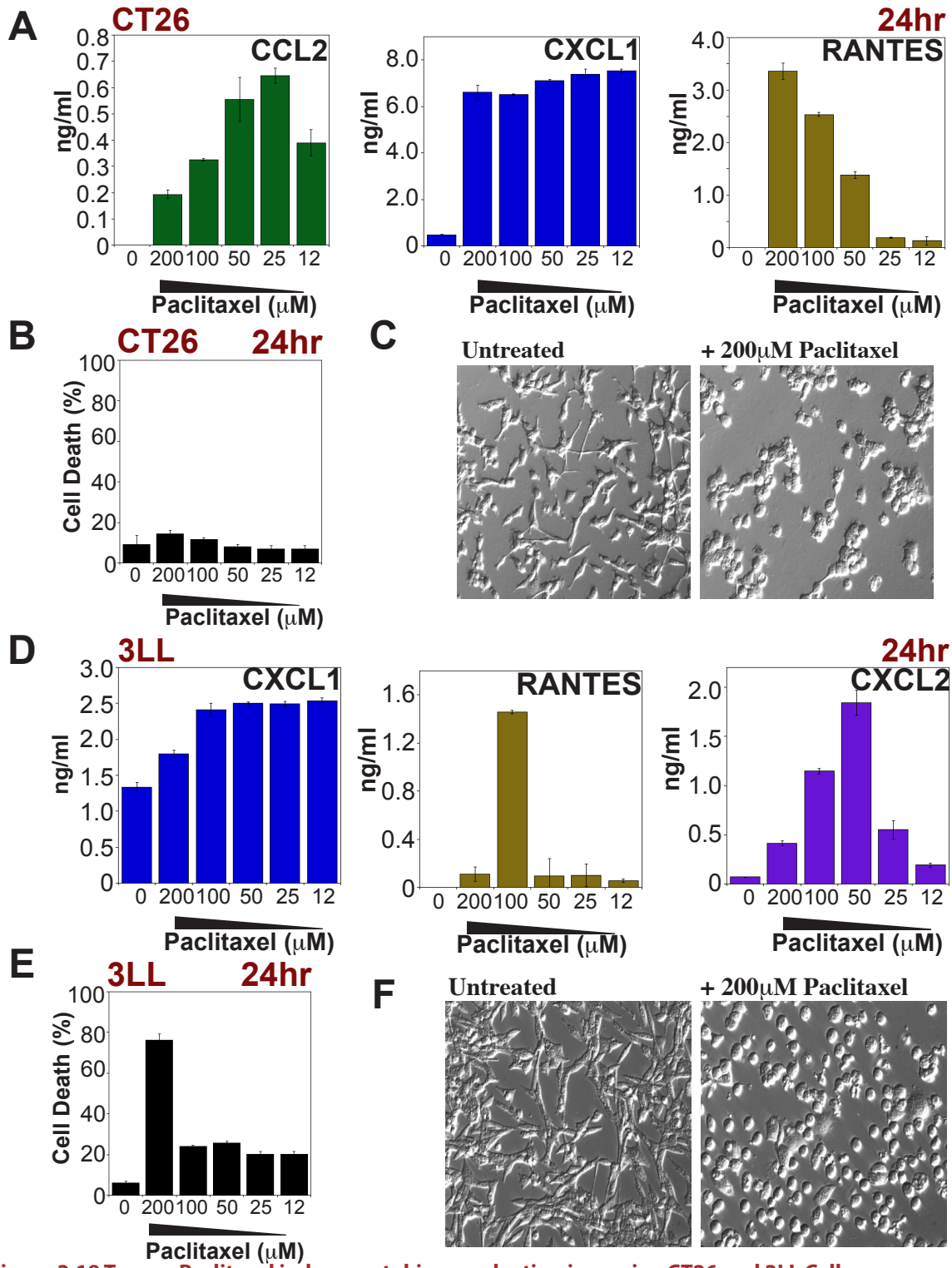

Figure 3.18 Taxane Paclitaxel induces cytokine production in murine CT26 and 3LL Cells

(A) CT26 cells were stimulated for 24hr with the indicated concentrations of Paclitaxel or Docetaxel. Cytokine concentrations in cell culture supernatants were determined by ELISA.

(B) CT26 cells were stimulated for 24hr with the indicated concentrations of Paclitaxel or Docetaxel. Cell death was measured based on cell morphology from counts of 3 fields per well (of approximately 100 cells per field).

(C) Cells from (B) were visualised using phage contrast microscopy.

(D) 3LL cells were stimulated for 24hr with the indicated concentrations of Paclitaxel or Docetaxel. Cytokine concentrations in cell culture supernatants were determined by ELISA.

(E) 3LL cells were stimulated for 24hr with the indicated concentrations of Paclitaxel or Docetaxel. Cell death was measured based on cell morphology from counts of 3 fields per well (of approximately 100 cells per field).

(F) Cells from (E) were visualised using phage contrast microscopy.

The error bars represent the mean +/- SEM of triplicate samples.

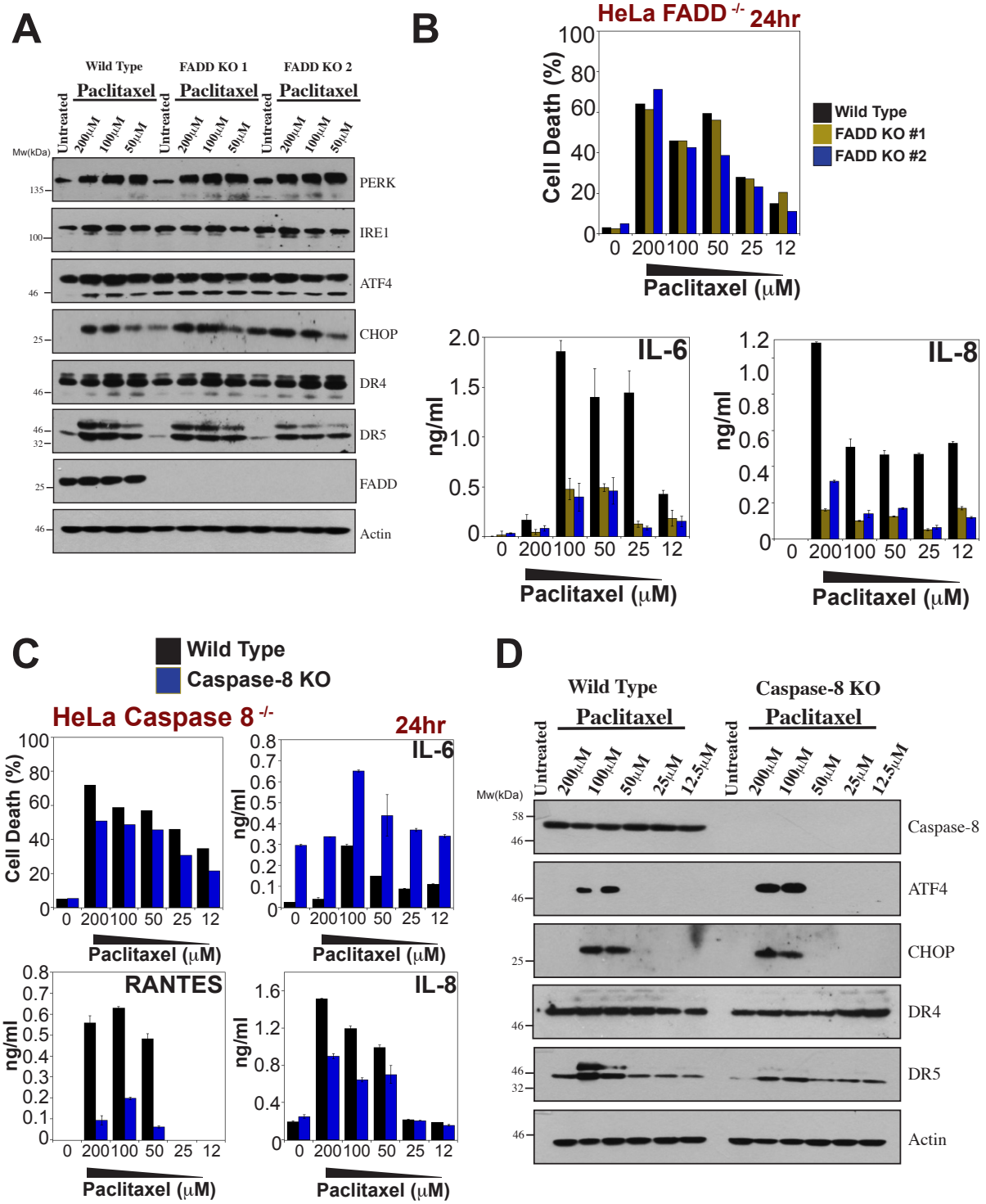

Figure 3.19 Taxane-induced cytokine production is dependent on signalling downstream of TRAIL-Rs
(A) HeLa WT versus HeLa FADD$^{-/-}$ cells were treated for 24hr with the indicated concentrations of Paclitaxel.
(B) Cells treated as in (A).
(C) HeLa WT versus HeLa FADD$^{-/-}$ cells were treated for 24hr with the indicated concentrations of Paclitaxel.
(D) HeLa WT versus HeLa FADD$^{-/-}$ cells were treated for 24hr with the indicated concentrations of Paclitaxel.
In (A & D), protein expression was analysed by western blot.
In (B & C), cell death was measured based on cell morphology from counts of 3 fields per well (of approximately 100 cells per field). Cytokine concentrations were determined by ELISA.
The error bars represent the mean +/- SEM of triplicate samples.

in induced cytokines IL-6 and IL-8 **(Figure 3.20 A)**. This may be explained by IAP antagonism preventing ubiquitination of RIPK1 downstream of TRAIL receptors, leading to the preferential formation of a soluble cell death-inducing ripoptosome-like complex II, as has been described downstream of the TNF receptor (Feoktistova et al., 2011, Tenev et al., 2011). Treatment with pan caspase inhibitor zVAD-fmk ablated cell death seen in response to paclitaxel, but dramatically increased production of IL-6 and IL-8 **(Figure 3.20 B)**. That a caspase-inhibitor would ablate cell death seen in response to paclitaxel is unsurprising as the intrinsic apoptotic pathway has been previously implicated (Wang et al., 2000). Increased cytokine production observed in the presence of zVAD may be due to caspase stabilisation and has been observed previously in the context of TRAIL-induced cytokine and chemokine production (Henry and Martin, 2017). This suggests that cytokine production is an active process, rather than just being a passive side-effect of necrotic cell release of intracellular cytokines. Dual treatment with both BV6 and zVAD-fmk ablated cytokine production and cell death seen in response to paclitaxel **(Figure 3.20 B)**. Under these conditions, where both caspases and IAPs have been inhibited, TRAIL receptor signalling appears to be ineffectual, as would be expected.

3.2.3 Generation of Fas KO Cells To Assess Whether Fas Plays A Role In Taxane-Induced Cytokine Production

Given that the adaptor molecule FADD is an important downstream effector of both Fas and TRAIL receptors, we wanted to assess whether Fas receptor plays also a role in taxane-induced cytokines. Targeted sgRNA were designed for the human CD95 gene (Fas), using the Broad Institute design tool. Chosen sequences are summarised in **Table 3.7**. sgRNAs for each target were deliberately designed to target different exons, while remaining as close to the beginning of the protein coding sequence as possible. Each sgRNA was sequenced with complementary overhangs for cloning into linearised sgRNA vector pLentiguidePuro **(Figures 3.2 A & 3.2 B).** Insertion of targeted sgRNA into pLentiguidePuro was confirmed by sequencing. Sequencing results are summarised below in **Table 3.8**

Plasmids were transfected into HeLa cells that are stably expressing Cas9 (generated by CMH), alongside parental pLentiguidePuro and PAAV-EGFP. Cells were then selected with puromycin to enrich for cells that had taken up plasmids. KO was validated by western blot **(Figure 3.21 A)**. Cells were treated, versus wild type cells, with a titration of CH11 to confirm that they no longer underwent apoptosis in response to anti-Fas stimulation **(Figure 3.21 B & 3.21 C)**. It was also confirmed that these cells do not produce cytokines IL-6 and IL-8 in response to CH11 **(Figure 3.21 D)**. Finally, KO

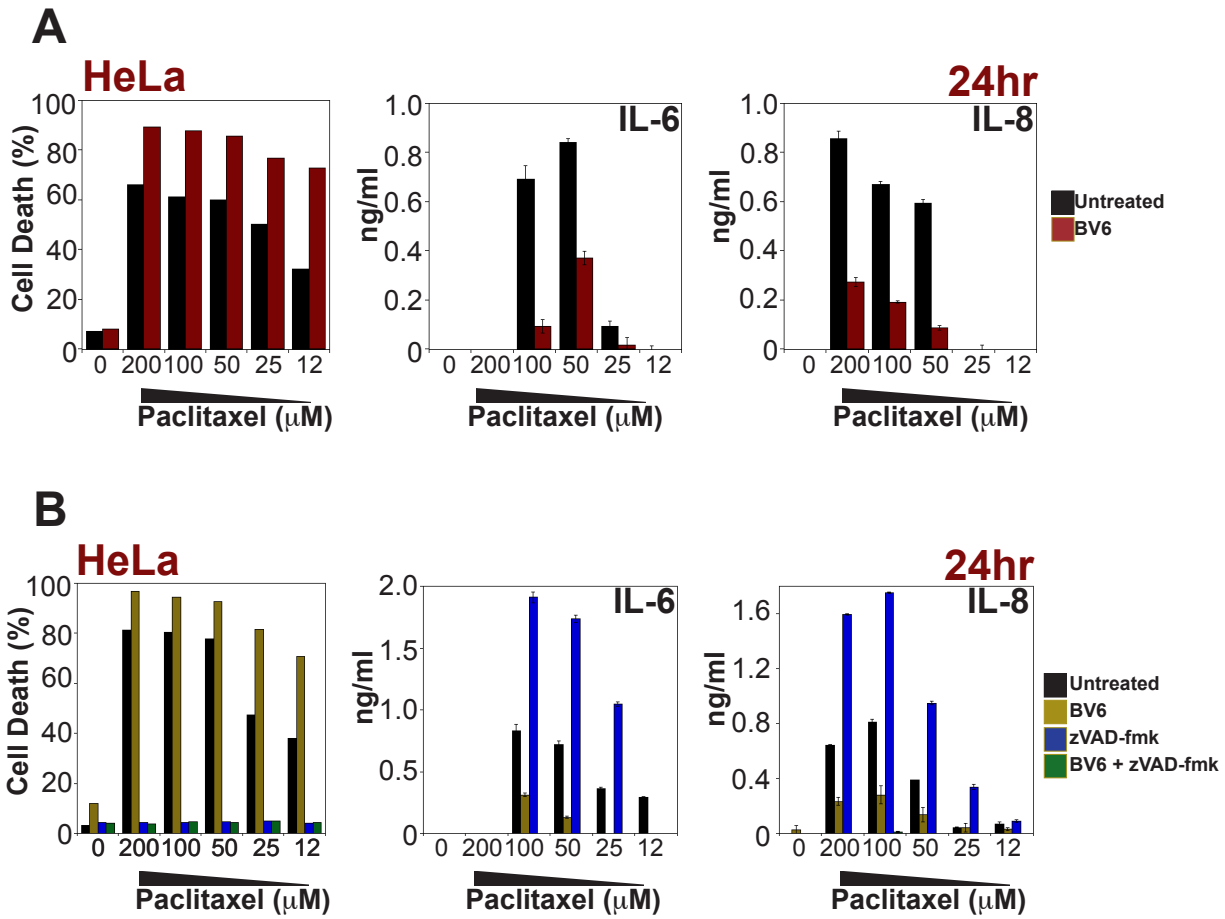

Figure 3.20 Taxane-induced cytokine production is dependent on signalling downstream of TRAIL-Rs
(A) Hela cells were treated with the indicated concentrations of Paclitaxel +/- 10μM BV6 for 24 hr. Cell death was measured based on cell morphology from counts from 3 fields of view per well (of approximately 100 cells per field). Cytokine concentrations in cell culture supernatants were determined by ELISA.
(B) Hela cells were treated with the indicated concentrations of Paclitaxel +/- 10μM BV6 and/or 10μM zVAD-fmk for 24 hr. Cell death was measured based on cell morphology from counts from 3 fields of view per well (of approximately 100 cells per field). Cytokine concentrations in cell culture supernatants were determined by ELISA.
The error bars represent the mean +/- SEM of triplicate samples.

cell populations were treated with TRAIL to confirm that TRAIL signalling had not been effected **(Figure 3.21E)**.

Table 3.7: Summary of sgRNAs designed to target human Fas.

	Sequence	PAM	Exon	Strand
Fas sgRNA 1	GTGACTGACATCAACTCCAA	GGG	Exon 2	Sense
Fas sgRNA 2	ACTGCGTGCCCTGCCAAGAA	GGG	Exon 3	Sense

Table 3.8: Summary of sequencing results to confirm insertion of sgRNA targeting Fas into pLentiGuidePuro vector.

sgRNA	Sequencing Results
Fas sgRNA 1	6069959;Value Read;;3.5 **FAS 1**;ASM0094134;hU6-F;final result;1020;">35 FAS 1_hU6-F – 141034 of sequence CGATACAGGCTGTTAGAGAGATAATTAGAATTAATTTGACTGTAAACACAAAGATATTAGTACAAAATACGTG ACGTAGAAAGTAATAATTTCTTGGGTAGTTTGCAGTTTTAAAATTATGTTTTAAAATGGACTATCATATGCTTAC CGTAACTTGAAAGTATTTCGATTTCTTGGCTTTATATATCTTGTGGAAAGGACGAAACACCGGTGACTGACATCA ACTCCAAGTTTTAGAGCTAGAAATAGCAAGTTAAAATAAGGCTAGTCCGTTATCAACTTGAAAAAGTGGCACC GAGTCGGTGCTTTTTTAAGCTTGGCGTAACTAGATCTTGAGACAAATGGCAGTATTCATCCACAATTTTAAAAG AAAAGGGGGGATTGGGGGGTACAGTGCAGGGGAAAGAATAGTAGACATAATAGCAACAGACATACAAACTA AAGAATTACAAAAACAAATTACAAAAATTCAAAATTTTCGGGTTTATTACAGGGACAGCAGAGATCCACTTTGG CGCCGGCTCGAGGGGGCCCGGGTGCAAAGATGGATAAAGTTTTAAACAGAGAGGAATCTTTGCAGCTAATGG ACCTTCTAGGTCTTGAAAGGAGTGGGAATTGGCTCCGGTGCCCGTCAGTGGGCAGAGCGCACATCGCCCACAG TCCCCGAGAAGTTGGGGGGAGGGGTCGGCAATTGATCCGGTGCCTAGAGAAGGTGGCGCGGGGTAAACTGGG AAAGTGATGTCGTGTACTGGCTCCGCCTTTTTCCCGAGGGTGGGGGAGAACCGTATATAAGTGCAGTAGTCGCC GTGAACGTTCTTTTTCGCAACGGGTTTGCCGCCAGAACACAGGTAAGTGCCGTGTGTGGTTCCCGCGGGCCTGG CCTCTTTACGGGTTATGGCCCTTGCGTGCCTTGAATTACTTCCACCTGGCTGCAGTACGTGATTCTTGATCCCGAG CTTCGGGTTGGAAGTGGGTGGGAAAATTCCAAGGCCTTGCGCTTAAGGAGCCCCTTCCCCTCGGG"; 6069959;Value Read;;3.6 **FAS 2**;ASM0094135;hU6-F;final result;973;">36 FAS 2_hU6-F – 13986 of sequence GAAACAGGCTGTTAGAGAGATAATTAGAATTAATTTGACTGTAAACACAAAGATATTAGTACAAAATACGTGAC GTAGAAAGTAATAATTTCTTGGGTAGTTTGCAGTTTTAAAATTATGTTTTAAAATGGACTATCATATGCTTACCGT AACTTGAAAGTATTTCGATTTCTTGGCTTTATATATCTTGTGGAAAGGACGAAACACCGACTGCGTGCCCTGCCA AGAAGTTTTAGAGCTAGAAATAGCAAGTTAAAATAAGGCTAGTCCGTTATCAACTTGAAAAAGTGGCACCGAGT CGGTGCTTTTTTAAGCTTGGCGTAACTAGATCTTGAGACAAATGGCAGTATTCATCCACAATTTTAAAAGAAAAG GGGGGATTGGGGGGTACAGTGCAGGGGAAAGAATAGTAGACATAATAGCAACAGACATACAAACTAAAGAAT TACAAAAACAAATTACAAAAATTCAAAATTTTCGGGTTTATTACAGGGACAGCAGAGATCCACTTTGGCGCCGGC TCGAGGGGGCCCGGGTGCAAAGATGGATAAAGTTTTAAACAGAGAGGAATCTTTGCAGCTAATGGACCTTCTA GGTCTTGAAAGGAGTGGGAATTGGCTCCGGTGCCCGTCAGTGGGCAGAGCGCACATCGCCCACAGTCCCCGAG AAGTTGGGGGGAGGGGTCGGCAATTGATCCGGTGCCTAGAGAAGGTGGCGCGGGGTAAACTGGGAAAGTGAT GTCGTGTACTGGCTCCGCCTTTTTCCCGAGGGTGGGGGAGAACCGTATATAAGTGCAGTAGTCGCCGTGAACGT TCTTTTTCGCAACGGGTTTGCCGCCAGAACACAGGTAAGTGCCGTGTGTGGTTCCCGCGGGCCTGGCCTCTTTAC GGGTTATGGCCCTTGCGTGCCTTGAATTACTTCCACCTGGCTGCAGTACGTGATTCTTGATCCCGAGCTTCGGGT TGGAATGGGGT";

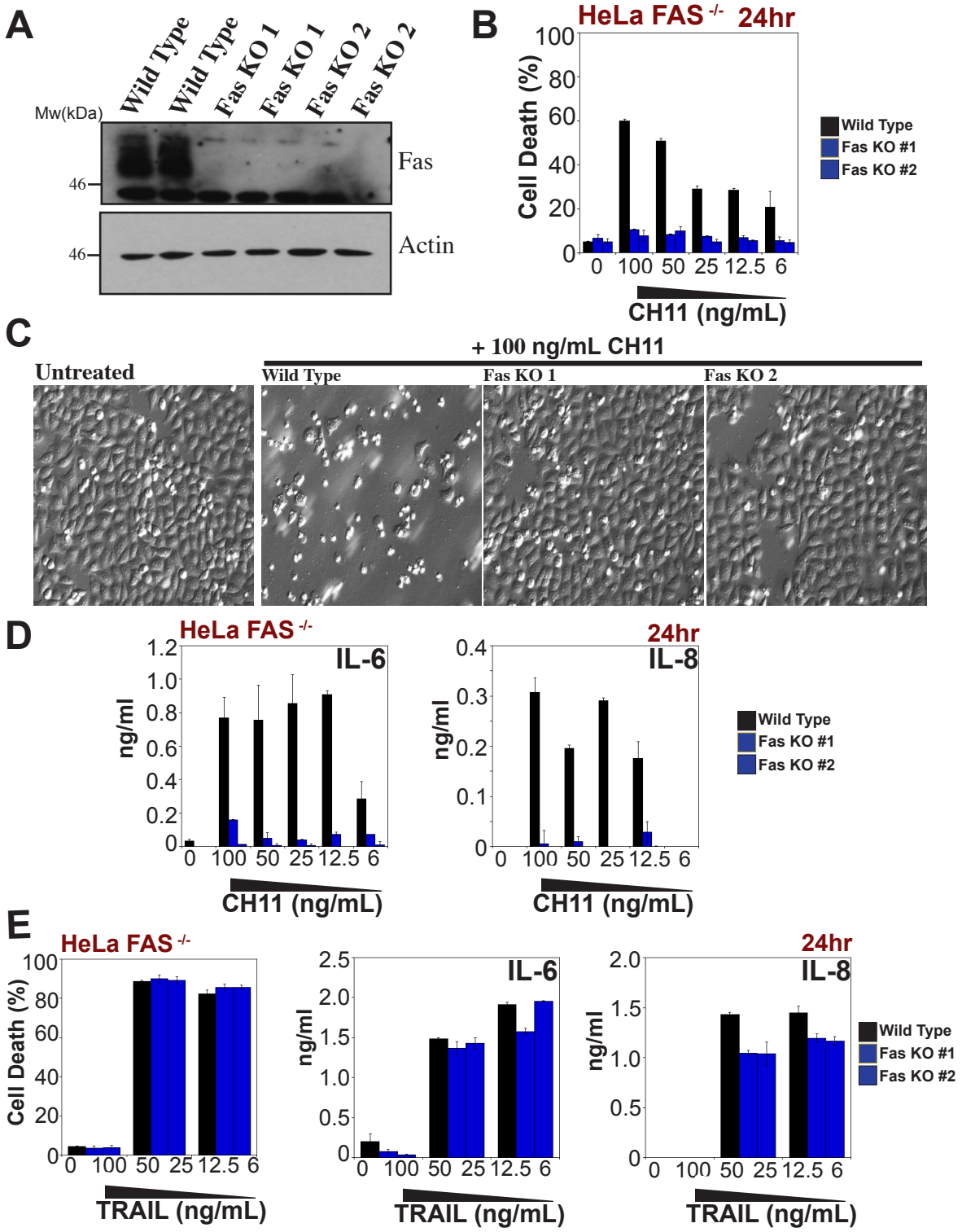

Figure 3.21 Generation of Fas null HeLa cells using CRISPR

(A) HeLa CRISPR KO were generated by GenJet transfection of sgRNA targetting Fas, followed by selection using puromycin. Cell lysates were prepared and protein expression was analysed by western blot.
(B) HeLa WT versus HeLa Fas$^{-/-}$ cells were treated for 24hr with the indicated doses of CH-11. Cell death was measured based on cell morphology from counts of 3 fields per well (of approximately 100 cells per field).
(C) Cells from (B) were visualised using phase contrast microscopy.
(D) HeLa WT versus HeLa Fas$^{-/-}$ cells were treated for 24hr with the indicated doses of CH-11. Cytokine concentrations in cell culture supernatants were determined by ELISA.
(E) HeLa WT versus HeLa Fas$^{-/-}$ cells were treated for 24hr with the indicated doses of TRAIL. Cell death was measured based on cell morphology from counts of 3 fields per well (of approximately 100 cells per field). Cytokine concentrations in cell culture supernatants were determined by ELISA.
The error bars represent the mean +/- SEM of triplicate samples.

3.2.4 Taxane-Induced Cytokines Are Fas-Independent

Treatment of wild type cells versus Fas null cells showed that taxane-induced death and cytokine production was independent of the death receptor Fas **(Figures 3.22 A & 3.22 B)**. What was unexpected however, was that IL-8 production in response to paclitaxel was enhanced in the absence of Fas. This perhaps suggests that Fas may play a protective role from taxane-induced cytokines, though this would need to be investigated further.

3.2.5 Taxane-Induced Cytokines Are Death Receptor Dependent

We next investigated whether the absence of DR4 or DR5 may affect taxane induced cytokine production. We initially treated wild-type, DR4 and DR5 KO HeLa cells with paclitaxel to test this, finding that while DR5 ablation may provide a marginal protection, the result was not particularly convincing **(Figure 3.23 A)**. We next tested both DR4/DR5 double KO cells with paclitaxel. Strikingly, DR4/DR5 DKO reduced paclitaxel-induced cytokines, while induced cell death remained unaffected **(Figure 3.23 B)**. This suggests that DR4 plays a role additionally, though this wasn't seen in the single KO population. Perhaps DR4 is only important when there is no DR5 present. We additionally tested these cell lines with docetaxel treatment **(Figure 3.23 C)** and observed a similar result, with DR4/DR5 DKO cell populations showing a drastic protective effect, while death remained remarkably unaffected.

Paclitaxel drug treatments were carried out in the presence of a TRAILR2-Fc fusion in order to assess whether taxane-induced cytokine production was dependent on autocrine or paracrine TRAIL ligand. Results conclusively showed that neutralisation of TRAIL ligand has no effect on death or cytokine production seen in response to paclitaxel, though the Fc-fusion dramatically protected from TRAIL-induced cytokine production **(Figure 3.23 D)**.

To assess this important observation in a more physiologically relevant experiment, we tested whether HeLa cells produce cytokines in response to shorter pulse treatments with paclitaxel, then following the cells until a 24 hr endpoint **(Figure 3.24 A)**. We found that 2 hr, 4hr and 8hr pulse treatments did indeed induce cytokine production. Indeed, at some doses, pulse treatments yielded more cytokines than 24 hr continuous treatment. This may be explained by the reduction in associated cell death when cells were pulse treated rather than exposed to cytotoxic drug continuously. We tested death receptor KO cell populations with an 8 hr pulse treatment of paclitaxel and found an even greater protective effect from taxane-induced cytokines than that seen with continuous treatments **(Figure 3.24 B)**. We finally tested DR4 and DR5 upregulation in response to an 8-hour pulse treatment with paclitaxel and found robust induction of

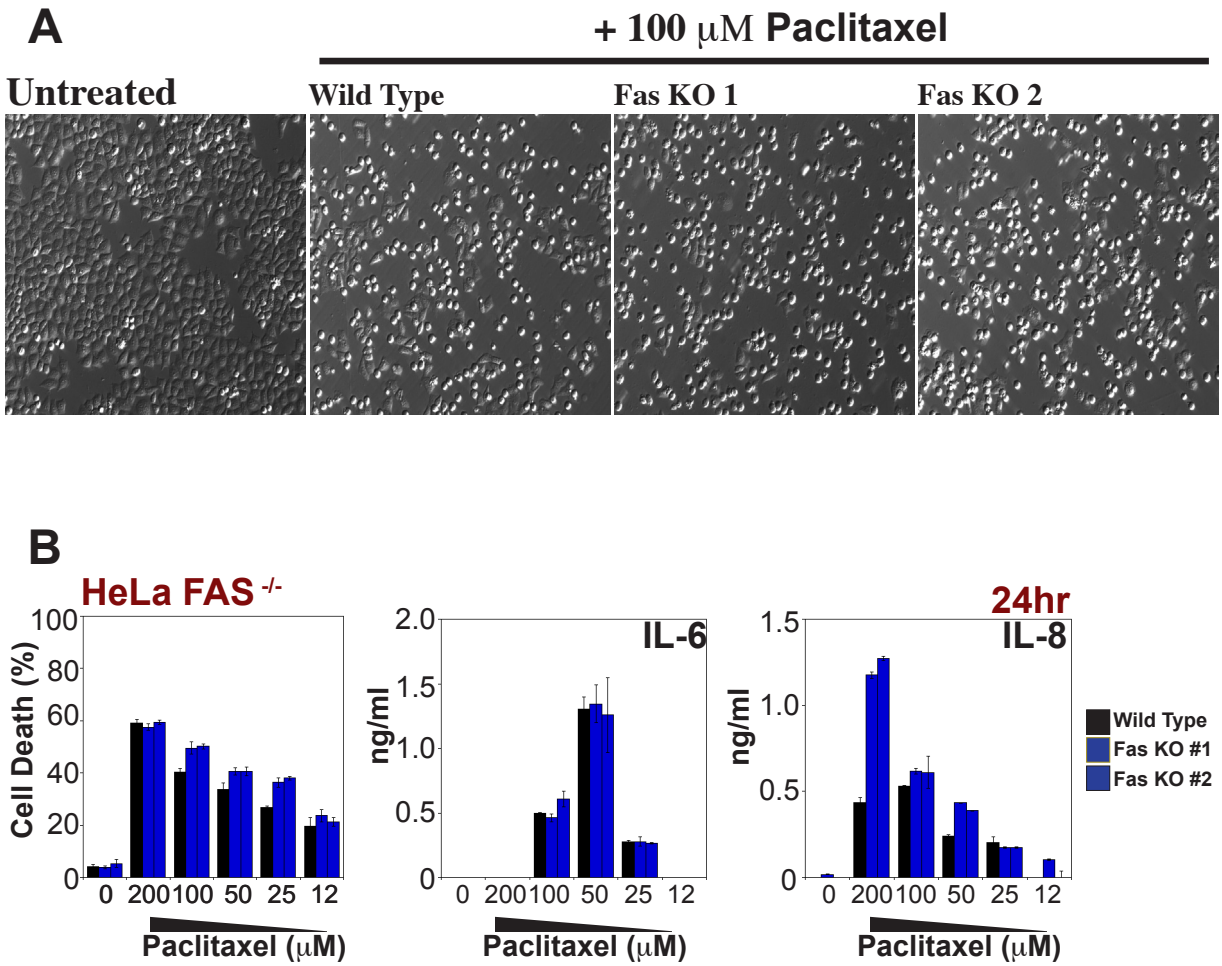

Figure 3.22 Taxane-induced cytokine production is Fas-independent

(A) HeLa WT versus HeLa Fas$^{-/-}$ cells were treated for 24hr with the indicated doses of Paclitaxel. Cells were visualised by phase contrast microscopy.

(B) HeLa WT versus HeLa Fas$^{-/-}$ cells were treated for 24hr with the indicated doses of Paclitaxel. Cell death was measured based on cell morphology from counts of 3 fields per well (of approximately 100 cells per field). Cytokine concentrations in cell culture supernatants were determined by ELISA.

The error bars represent the mean +/- SEM of triplicate samples.

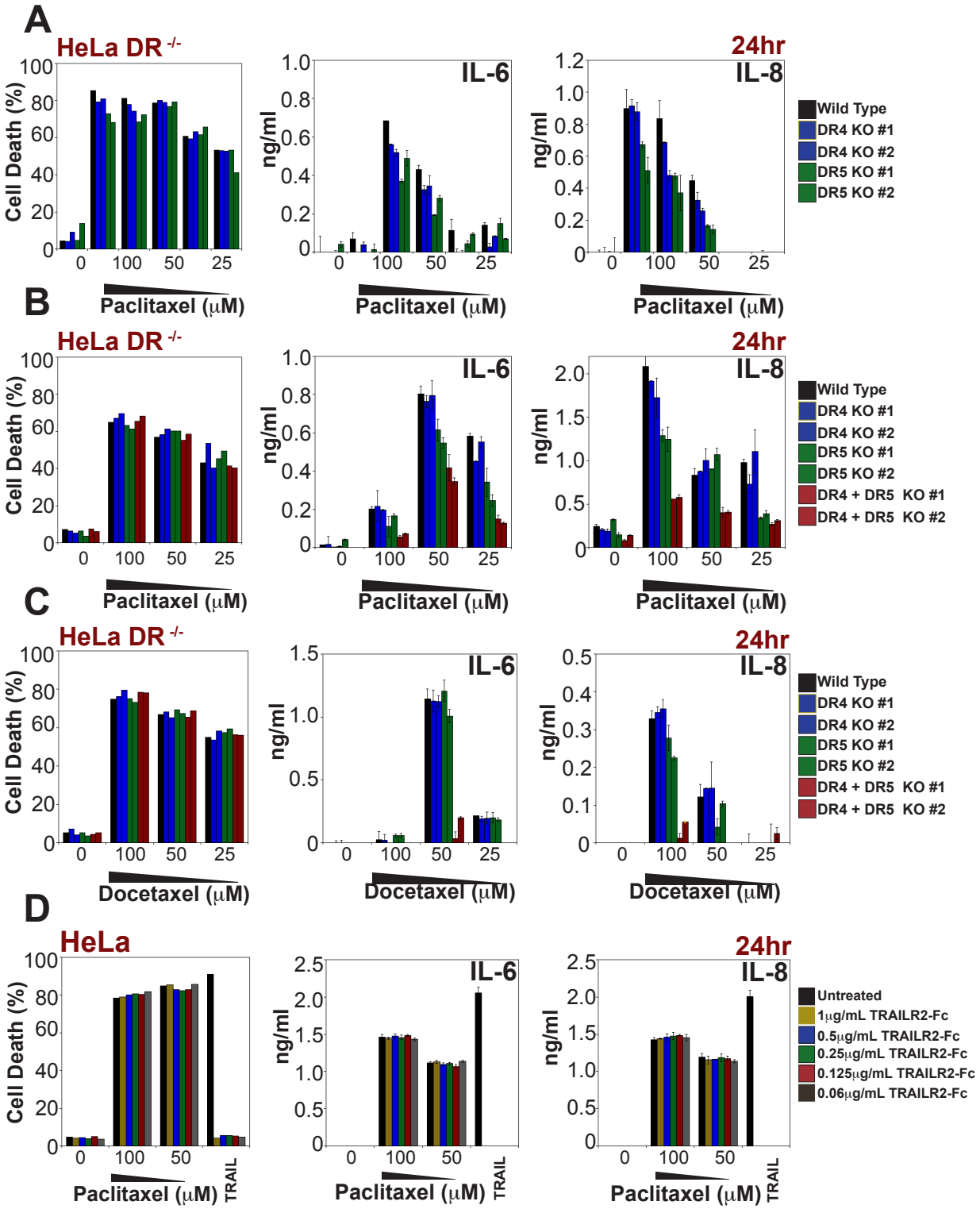

Figure 3.23 Taxane-induced cytokine production is TRAIL-R-dependent

(A) HeLa WT versus HeLa DR4$^{-/-}$ and DR5$^{-/-}$ cells were treated for 24hr with the indicated concentrations of Paclitaxel.

(B) HeLa WT versus HeLa DR4$^{-/-}$, DR5$^{-/-}$ and DR4/DR5$^{-/-}$ cells were treated for 24hr with the indicated concentrations of Paclitaxel.

(C) HeLa WT versus HeLa DR4$^{-/-}$, DR5$^{-/-}$ and DR4/DR5$^{-/-}$ cells were treated for 24hr with the indicated concentrations of Docetaxel.

(D) HeLa WT, DR4, DR5 and DR4 + DR5 KO cells were treated for 24hr with the indicated concentrations of Paclitaxel +/- the indicated doses of TRAILR2-Fc

In (A-C) cell death was measured based on cell morphology from counts of 3 fields per well (of approximately 100 cells per field). Cytokine concentrations in cell culture supernatants were determined by ELISA.

The error bars represent the mean +/- SEM of triplicate samples.

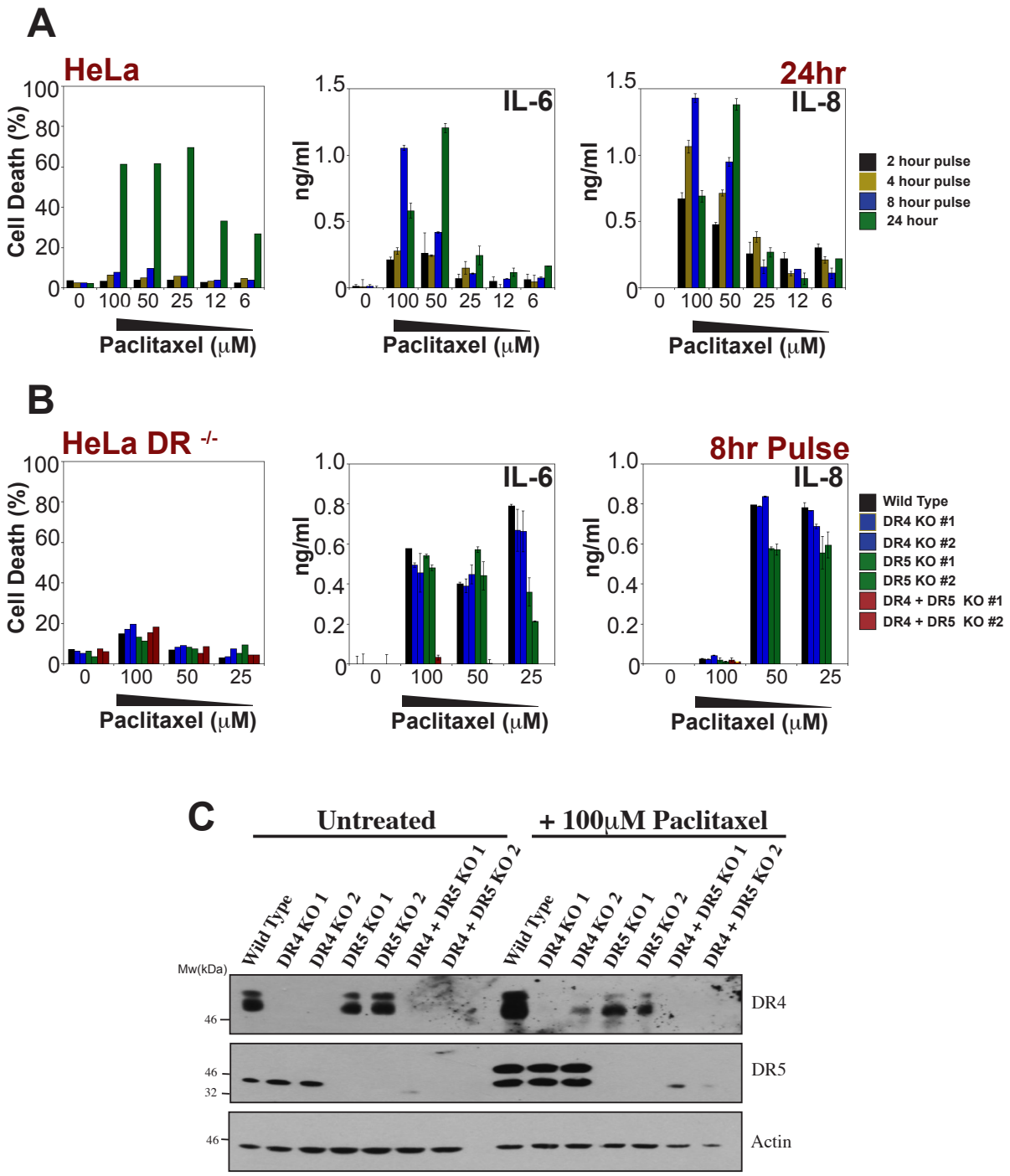

Figure 3.24 Taxane-induced cytokine production is TRAIL-R-dependent

(A) HeLa cells were treated for 2, 4 and 8hr with the indicated concentrations of Paclitaxel. After the indicated duration, the paclitaxel was removed, cell monolayers were washed and media was replenished with fresh media for 24hr. Cells were additionally treated for a further 24 hrs without replensihing media.

(B) HeLa WT versus HeLa DR4$^{-/-}$, DR5$^{-/-}$ and DR4/DR5$^{-/-}$ cells were treated for 8hr with the indicated concentrations of Paclitaxel. After the indicated duration, the paclitaxel was removed, cell monolayers were washed and media was replenished with fresh media for 24hr. Cells were additionally treated for a further 24 hrs without replensihing media.

In (A & B) cell death was measured based on cell morphology from counts of 3 fields per well (of approximately 100 cells per field). Cytokine concentrations in cell culture supernatants were determined by ELISA.

(C) HeLa WT versus HeLa DR4$^{-/-}$, DR5$^{-/-}$ and DR4/DR5$^{-/-}$ cells were treated for 8hr with the indicated concentration of Paclitaxel. Protein expression was analysed by western blot.

The error bars represent the mean +/- SEM of triplicate samples.

DR5, as is seen with 24 hour continuous treatment **(Figure 3.24 C)**. It was also observed that DR4 or DR5 induction was not seen in the respective null cell populations.

3.2.6 Taxane-Induced Cytokines Are CHOP-Dependent

Finally, we explored whether taxane-induced cytokines were dependent on the previously elucidated CHOP-DR5-FADD pathway. We tested whether taxane-induced cytokines were dependent on ER stress-induced CHOP by comparing taxane treated CHOP KO cells to wild type cells. Interestingly, western blot analysis showed that DR5 upregulation in response to paclitaxel was ablated in CHOP KO cells **(Figure 3.25 A)**. This suggests that DR5 upregulation is CHOP-dependent in this context. We then tested cell supernatants from taxane treated wild type versus CHOP null cells and found that in the absence of CHOP, paclitaxel induced IL-6 and IL-8 were dramatically reduced **(Figure 3.25 B)**. Consistent with this, we found that docetaxel induced IL-6 was very much CHOP-dependent, though IL-8 was noticeably less so **(Figure 3.25 C)**. In conclusion, we have uncovered an ER-stress-induced CHOP-DR4/DR5-cytokine signalling pathway that occurs in response to taxane exposure **(Figure 3.26)**. This pathway may lead to unwanted cytokine production in response to taxane chemotherapy that is likely to facilitate tumour survival and/or progression.

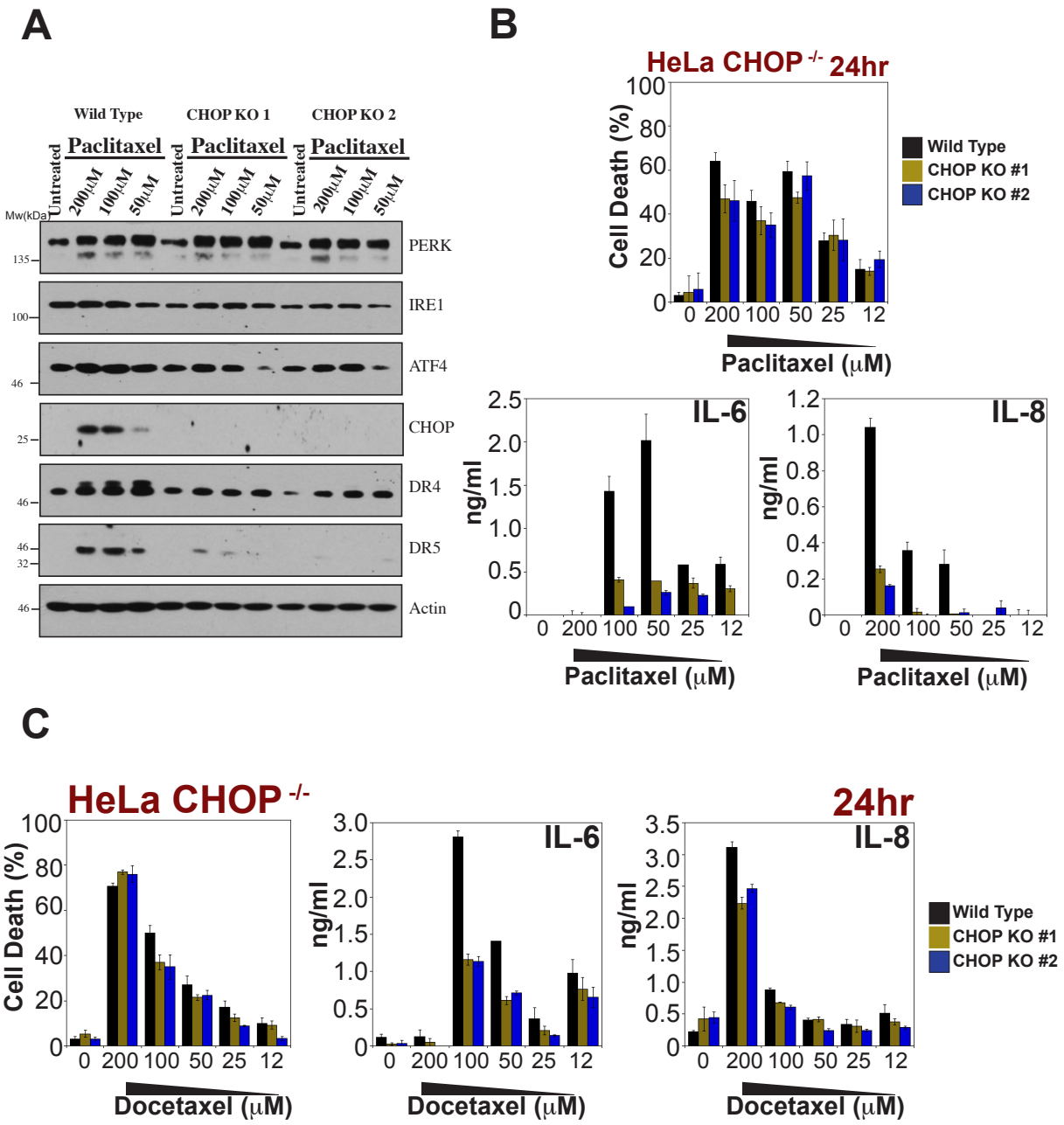

Figure 3.25 Taxane-induced cytokine production is CHOP-dependent

(A) HeLa WT versus HeLa CHOP$^{-/-}$ cells were treated for 24hr with the indicated concentration of Paclitaxel. Cell lysates were prepared and protein expression was analysed by western blot.

(B) HeLa WT versus HeLa CHOP$^{-/-}$ cells were treated for 24hr with the indicated concentration of Paclitaxel. Cell death was measured based on cell morphology from counts of 3 fields per well (of approximately 100 cells per field). Cytokine concentrations in cell culture supernatants were determined by ELISA.

(C) HeLa WT versus HeLa CHOP$^{-/-}$ cells were treated for 24hr with the indicated concentration of Docetaxel. Cell death was measured based on cell morphology from counts of 3 fields per well (of approximately 100 cells per field). Cytokine concentrations in cell culture supernatants were determined by ELISA.

The error bars represent the mean +/- SEM of triplicate samples.

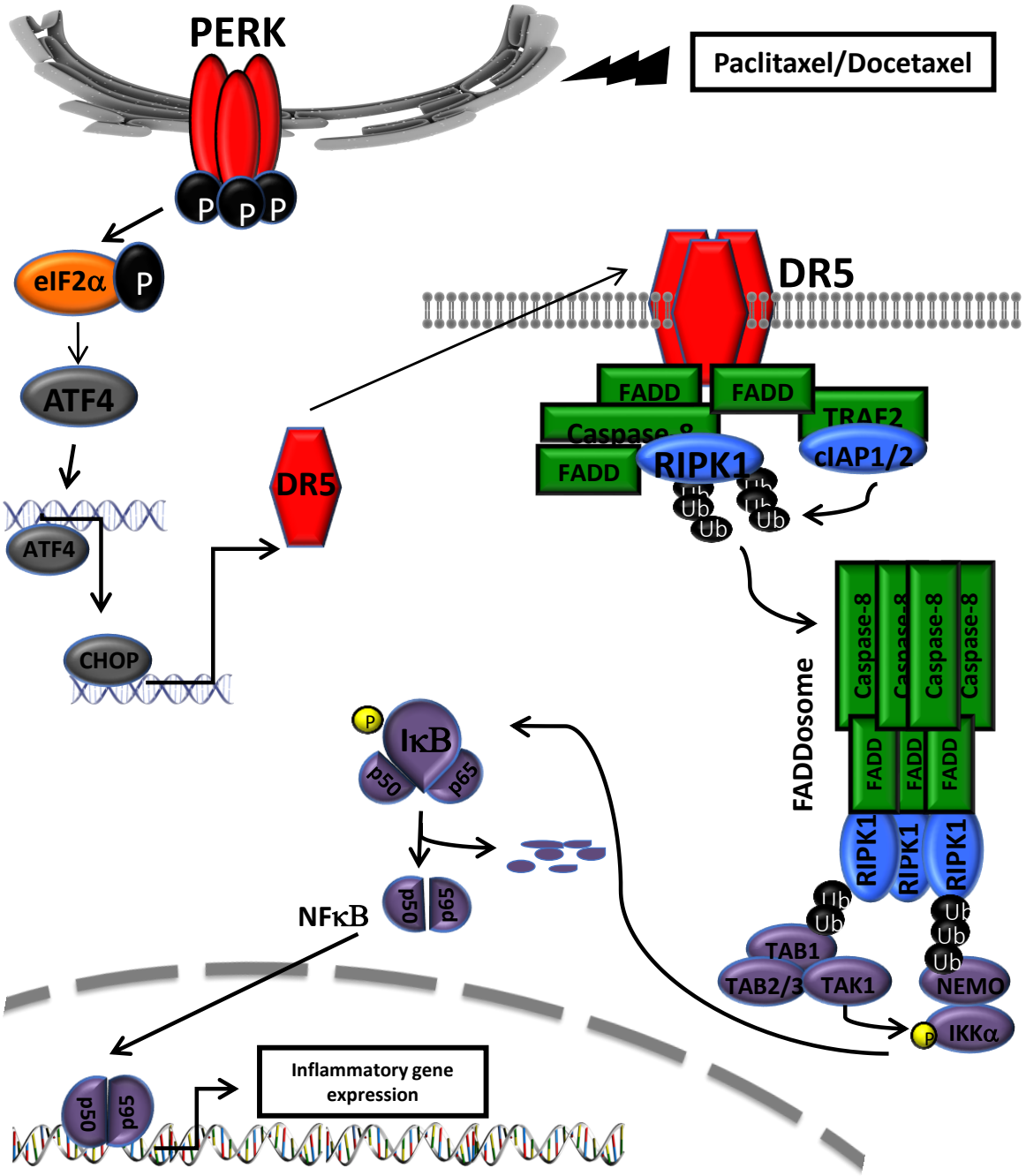

Figure 3.26 Taxanes induce cytokine production in an ER stress-associated, DR5-dependent manner

Taxnae-induced ER stress leads to activation of ER membrane-associated receptor PERK. Activated PERK leads to transcriptional upregulation of the transcription factor CHOP. In turn, CHOP transcriptionally upregulates DR5, leading to receptor aggregation and ligand-independent activation of signalling downstream of DRs. FADD is recruited to the DISC via its DD, while caspase-8 is recruited downstream via its DEDs. RIPK1 associates with the receptor associated complex via DD interactions with FADD. Oligomerisation of caspase-8 occurs, allowing for the formation of a soluble aggregate that act as a scaffold. Stabilised FADD associates with caspase-8 and facilitates the successive recruitment of RIPK1 to form what has been dubbed the "FADDosome" complex. TRAF2 binding to FADD allows for IAP association with the complex and subsequent addition of ubiquitin chains to RIPK1. Modified RIPK1 can recruit the TAB/TAK1 and IKK complexes, ultimately leading to the phosphorylation and degradation of IkB. The p50 and p65 NFkB subunits are then free to translocate to the nucleus, leading to downstream activation of inflammatory signalling.

Discussion

4.1 Chapter 1

In this study, we have identified physiological contexts where TRAIL-induced inflammation may occur. To begin, ER stress-induced DR upregulation contributes to spontaneous and ligand-independent TRAIL receptor inflammatory signalling. While it was surprising that DR activation and signalling occurred in the absence of ligand stimulation, it has been shown previously that TRAIL receptor aggregation can lead to activation of death receptor signalling (Chan et al., 2000), so it is plausible that something similar may be happening here due to the robust upregulation of DR5 seen in our experiments. Regardless of previous controversy regarding the main mechanism of cell death induction in response to ER stress, and while ER stress-induced cell death was inconsistently associated with death receptors here, ER stress-induced cytokines are clearly death receptor-dependent. We have clearly illustrated an alternative output of the widely studied DR upregulation seen in response to ER stress. Inflammatory cytokine production was dependent on FADD, DR4 (somewhat), DR5 and CHOP. It is possible that this pathway mimics the CHOP-dependent DR5 upregulation that has been studied in some contexts of stress induced apoptosis, however this would need to be further elucidated as we have not shown here that DR5 upregulation in response to ER stress in CHOP dependent (Lu et al., 2014a). These results can be extrapolated to speculate as to what role DR upregulation and subsequent inflammation play in more specific contexts. Here we will focus on solid tumour-associated ER stress as an example.

The importance of ER stress and death receptor-dependent death in malignant tissues has been explored for some time (Yamaguchi and Wang, 2004). However, more recently this ER stress pathway has been described in a number of specific physiological contexts including under conditions of glucose or nutrient deprivation or hypoxia (Iurlaro et al., 2017, Jiang et al., 2017). As solid tumours grow, cells become cut off from the vasculature and can become hypoxic and depleted of necessary nutrients. However, tumours adapt to these stresses, and particularly, adaptive ER stress responses have been observed in many different types of cancer – including breast, lung, prostate, skin and pancreatic cancers (Wang and Kaufman, 2014). Cancer initiation is classically attributed to loss-of-function mutations in tumour suppressor genes (such as p53 and PTEN) and gain-of-function mutations in oncogenes (such as HRAS and BRAF) – ultimately leading to uncontrolled proliferation and progression (Obeng et al., 2006). Loss-of-function and gain-of-function mutations have both been shown to lead to

increased protein synthesis rates and ultimately induce an ER stress response (Corazzari et al., 2015).

Hypoxia leads to the production of ROS in mitochondria and the ER. During ER stress, this is contributed to by the increased disulphide bond formation and oxidative folding promoted by ERO1α (a transcriptional target of CHOP) during the ISR. It has been suggested that this increased capacity for withstanding oxidative stress is beneficial for tumour growth (Clarke et al.), with ERO1α being put forward as a predictor of poor prognosis in breast cancer models (Kutomi et al., 2013). In line with this, it has been shown that ablation of PERK in breast carcinoma cells results in impaired tumour growth and a reduction in the accumulation of ROS (Bobrovnikova-Marjon et al., 2010).

Glucose deprivation and hypoxia have been linked to VEGF production and neovascularisation. Inhibition of PERK results in reduced tumour growth, vascularity and perfusion, with the UPR being proposed as the link between nutrient deprivation, hypoxia and the angiogenic switch (Wang et al., 2012). TRAIL DRs have very recently been shown to be important for glucose deprivation induced apoptosis in an ATF4-dependent, CHOP-independent manner – suggesting that regulation of DRs in this context is mainly at the transcriptional level. Nutrient deprivation in this manner was shown to upregulate both DR4 and DR5 TRAIL receptors (Iurlaro et al., 2017). It is plausible that, similar to what we have seen in our experiments, ER stress-induced death receptor upregulation under nutrient deprivation conditions may contribute to inflammatory outcomes. It is plausible that either nutrient excess and nutrients in short supply may in either instance contribute to TRAIL-dependent inflammation. Indeed, TRAIL receptor deletion in mice suppresses the inflammation of nutrient excess (Idrissova et al., 2015).

Metastasis, or the process by which cancerous cells migrate from the primary tumour site to foreign body tissues, characteristically involves epithelial-to-mesenchymal transition (EMT) of cells and infiltration first into the tissue extracellular matrix and secondly into the two main mammalian circulatory systems – the lymphatic and cardiovascular systems (Nieto et al.). EMT is characterised by decreased expression of epithelial cell marker E-cadherin, with concurrent increased expression of mesenchymal markers such as fibronectin and vimentin. EMT-induced migration and extracellular matrix protein secretion has been shown to be dependent on ER stress and can be inhibited using pharmacological PERK inhibitors or by silencing ATF4 (Feng et al., 2014, Dey et al., 2015). IRE1 has additionally been shown to be a key regulator in the malignant switch of human gliomas, being required for the production of angiogenic factors IL-6, IL-8 and VEGF (Auf et al., 2010). Indeed, the production of proinflammatory cytokines and chemokines has been observed in a range of cancerous tissues

(Mahadevan et al., 2010, Marjon et al., 2004). Consistent with the production of this inflammatory milieu, excessive ER stress has been shown to increase tumour immunosurveilance and thus indirectly reduce tumour burden (Kepp et al., 2013). Knock-out tumour models have highlighted the importance of ER stress effectors such as CHOP and ATF4 in tumour growth. In the N-diethylnitrosamine (DEN)-induced hepatocellular carcinoma model, knock-out of CHOP has been shown to reduce carcinogenesis (Scaiewicz et al., 2013). The PERK arm of the UPR has been implicated in the promotion of cancer cell growth and proliferation on several occasions (Bobrovnikova-Marjon et al., 2010, Blais et al., 2006).

Here we have elucidated a key role for FADD in ER stress-induced cytokines, downstream of TRAIL receptors DR4 and DR5. However, we consistently saw that FADD ablation afforded a greater protection from ER stress-induced cytokine production than did ablation of DR4 and DR5. Thus, it is possible that alternative death receptors that use FADD as an adaptor (such as Fas) also play a role here. Caspase-8 and FADD, both important adaptor molecules in the TRAIL signalling pathway, have also been characterised in a number of studies as pro-tumorigenic molecules (Terlizzi et al., 2015, Fan et al., 2013). In many cases, null tumours or the deletion of these molecules appears to be beneficial for tumour clearance. One convincing study by Terlizzi and colleagues in a NSCLC model showed that pharmacological inhibition of caspase-8 limited both tumour growth and metastasis (Terlizzi et al., 2015). Strikingly, this correlated with a concurrent reduction in the release of proinflammatory cytokines such as IL-6 and IL-8 into the tumour microenvironment (Terlizzi et al., 2015). Similarly, high expression levels of DR5, caspase-8 and FADD has been linked to poor prognostic outcomes in head and neck cancer patients with lymph node metastasis (Fan et al., 2013). Hartwig et al. additionally showed that deletion of FADD or shRNA stable knockdown of TRAIL-R2 substantially reduced tumour burden in NSCLC and Lewis Lung Carcinoma mouse models. Importantly, cytokine levels (CCL2, IL-8 and IL-6) measured from lung homogenates were reduced in FADD deficient mice (Hartwig et al., 2017). It seems plausible that the absence of mTRAILR2, FADD or caspase-8, naturally occurring and tumour associated ER stress-induced inflammation is somewhat ablated.

Conversely, mutant forms of caspase-8 which are found in numerous cancers have shed further light on the role of this molecule (Soung et al., 2005, Soung et al., 2004). Spontaneous mutations favour the formation and progression of tumours, assumably due to the selection of mutant caspase-8 which can no longer promote apoptosis but can still bind to FADD, with an increased ability to activate NFκB (Ando et al., 2013, Liu et al., 2002). Indeed, one study of head and neck cancers found that such a mutant caspase-8 was found to be constitutively bound to FADD (Li et al., 2014).

Tumour-associated overexpression of phosphorylated, cytoplasmic FADD has been associated with cell proliferation, NFkB activation and aggressive forms of lung cancer with a bad prognostic outcome (Bhojani et al., 2005, Chen et al., 2005).

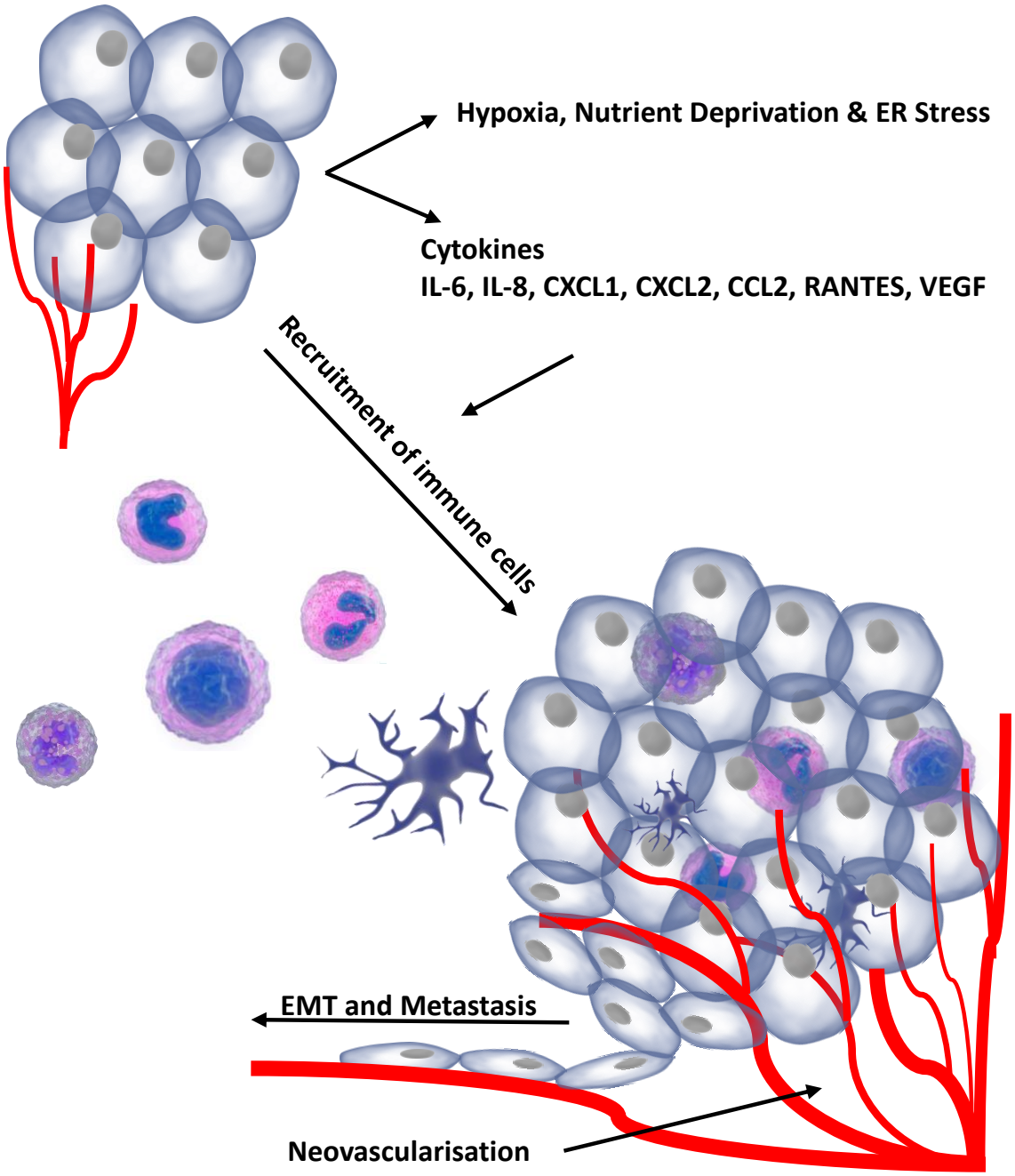

Figure 4.1 ER stress-induced progression of solid tumours
Unregulated tumour growth induces hypoxia, nutrient deprivation and ultimately ER stress. ER stress concurrently induces DR5-dependent upregulation of cytokine such as IL-6, IL-8, CXCL1, RANTES and CCL2. Cytokine and chemokine-dependent recruitment of tumour-associated immune cells occurs, ultimately facilitating tumour growth, angiogenesis, EMT and metastasis.

4.2 Chapter 2

We have shown that taxanes induce numerous cytokines in a range of different cell types. Previous studies have shown that taxanes induce activation of NFκB and a number of inflammatory mediators (including IL-6, IL-8, IL-1β and VEGF) in various tumour cell types (White et al., 1998, Lee et al., 1997, Pusztai et al., 2004, Volk et al., 2008). An analysis of the functions of these cytokines in tumour biology paints an interesting picture. IL-8, CXCL1 and CXCL2 have been shown to be important players in early stage neutrophil recruitment to sites of tissue inflammation (De Filippo et al., 2013). When dysregulated or chronically expressed following constitutive NFκB activation in solid tumours, these chemokines have been implicated in tumour formation - causing angiogenesis, tissue damage and ultimately being beneficial for tumour growth (Dhawan and Richmond, 2002). Particularly, enhanced proliferation and invasion of numerous malignant tissues has been attributed to CXCL1/CXCL2 signalling (Singh et al., 2009, Wang et al., 2006). Observed correlations of poor prognosis and IL-8 overexpression has been attributed to cancer stem cell formation and an invasive phenotype (Chen et al., 2014). Other cytokines of interest, such as IL-6 and RANTES, have also been implicated in tumour progression. Chronic IL-6 expression is seen in malignant tissues in mouse models as well as human disease and it acts to support tumour growth and survival, while also being linked to angiogenesis. Conversely, IL-6 has been shown to reorganise the T-cell response of the tumour microenvironment, particularly playing a role in the activation and survival of these leukocytes so that they may effectively act to clear tumour burden (Fisher et al., 2014). Previous studies also report the induction of markers associated with metastasis in response to paclitaxel, including mitogen activated protein kinase (MAPK) activation (Shtil et al., 1999). The invasive phenotype known as EMT has been observed following paclitaxel treatment in ovarian carcinoma models (Kajiyama et al., 2007). Similarly, paclitaxel has been shown to enhance liver metastasis in breast cancer mouse models (Li et al., 2016). Collectively, this suggests that taxane-induced cytokines are very likely to be protumorigenic.

While taxane induced cytokines induce immune cell infiltration and concurrent angiogenesis and metastasis, taxanes also induce cell death via their role as microtubule disruptors. Microtubule disruptors, while exerting their effects on rapidly dividing cancer cells, also affect dividing non-cancerous cells – thus leading to the observed toxicity with which they are widely associated. It is therefore plausible that taxanes may act on tumour cells, tumour stroma and additionally on recruited immune cells to globally activate an immune response that leads to unwanted effects such as metastasis and invasion. Indeed, a compelling study by Liu and colleagues illustrates that chemotherapeutic

agents such as paclitaxel induce cytokines and angiogenic factors from both tumour and stromal cells, ultimately promoting an invasive phenotype (Liu et al., 2015).

Immune cell infiltration and diverse activation of immune cell effector functions is commonly seen in patients treated with taxanes as well as in *in vitro* and *in vivo* models. Paclitaxel has been proposed to stimulate tumour-associated macrophage (TAM) cytotoxicity directly and induce the secretion of IL-12 and TNF-α and inducible nitric oxide synthase (iNOS). This activation has been linked to the activation of dendritic cells, natural killer cells and CD8+ T-cells by TAMs, resulting in tumour regression (Park et al., 2013, Javeed et al., 2009). Conversely, in separate studies, paclitaxel-induced influx of TAMs was shown to be detrimental to chemotherapy response in mouse mammary carcinoma and breast cancer patients (Shree et al., 2011, DeNardo et al., 2011). Paclitaxel was additionally shown to promote the ability of murine BM–DCs to present antigens to T-cells *in vitro* by upregulating antigen-processing machinery gene components, costimulatory molecules and IL-12p70 (Shurin et al., 2009). Exposure to paclitaxel sustained the ability of 6-sulfo LacNAc dendritic cells (slanDCs) to produce proinflammatory cytokines and their potential to activate T-lymphocytes and NK cells (Wehner et al., 2013).

Docetaxel has also been shown to polarize immunosuppressive myeloid derived suppressor cells (MDSCs) toward an inflammatory M1-like phenotype, and to selectively kill MDSCs while sparing the M1-like cells (Kodumudi et al., 2010). A previous study in a murine melanoma model has attributed the anti-tumour activities of paclitaxel to a decreased accumulation and immunosuppressive activities of tumour-infiltrating MDSCs. The authors also interestingly noted the restoration of cytotoxic CD8+ T-cell effector functions in the tumour microenvironment (Sevko et al., 2013). This skewing towards a cytotoxic T-cell response has also been previously observed with docetaxel (Hodge et al., 2013). It is also interesting that immune cell profiles tend to differ between patients with favourable or unfavourable prognoses. A highly responsive to taxane chemotherapy group of breast carcinomas characterized by a high CD4, CD68 and CD20 and a low CD8 infiltration were identified by Garcia-Martinez and colleagues. The study also illustrated a rearrangement of the tumour infiltrating lymphocyte population after treatment with paclitaxel – while numbers of immunoregulatory CD4 and T-regulatory lymphocytes were reduced, numbers of cytotoxic CD8+ lymphocytes were again significantly up (Garcia-Martinez et al., 2014). In a similar response, paclitaxel augments Th1 cellular immunity in patients with advanced non-small cell lung cancer by increasing the levels of circulating IFN-γ-secreting CD8 T-cells and IL-2-secreting CD4 T-cells (Zhang et al., 2008). Paclitaxel specifically impairs viability and cytokine production in FOXP3+Treg cells, but not in FOXP3−CD4 effector cells (Zhu et al., 2011).

In line with this, treatment of mice bearing pre-existing squamous cell carcinomas with B cell-depleting αCD20 monoclonal antibodies improved response to paclitaxel-based chemotherapy. Improved responsiveness was dependent on altered chemokine expression by immunosuppressive macrophages that ultimately fostered tumour infiltration of activated CD8+ T cells via CCR5-dependent mechanisms (Affara et al., 2014). The authors interestingly noted an increase in the expression levels of RANTES, CCL9, MCP3, CCL2, and CCL3 with combined treatment. It has previously been shown that B-cell responses, including the production of antibodies targeting tumour-associated antigens, in-fact facilitate tumour growth by promoting protumour immune responses and protecting tumour cells from cytotoxic CD8+ T-cell mediated killing (Gunderson and Coussens, 2013).

Paclitaxel has very recently shown greater efficacy in several preclinical models – including NSCLS and triple-negative breast cancer - in combination with checkpoint blockade therapies (Lu et al., 2017, McArthur and Page, 2016). It is well known that cancer cells can be eliminated by cytotoxic CD8+ T-cells and infiltration of these T-cells into tumours is associated with a positive prognosis (Gajewski et al., 2013, Schreiber et al., 2011, Fridman et al., 2012). However, quite often in patients with established tumours, immune suppression has occurred and acts as a barrier to tumour clearance. CD8+ T-cells can be supressed in this context after their activation by increasing expression of immune checkpoint receptors such as cytotoxic T lymphocyte antigen-4 (CTLA-4) and programmed death-1 (PD-1), increasing their susceptibility to apoptosis from ligation of these receptors. Within the tumour microenvironment, tumour cells and infiltrating regulatory lymphocytes are often seen to overexpress PD-L1, the main ligand for PD-1 (Keir et al., 2008). Unsurprisingly, therapies targeting T-cell inhibitory checkpoint signalling pathways with specific antibodies in order to re-establish an anti-tumour response have been a success (Topalian et al., 2012). Checkpoint blockade therapies can be extremely effective but unfortunately some tumours which have not been pre-infiltrated by CD8+ T-cells appear to be resistant (Topalian et al., 2012, Schreiber et al., 2011). A recent study showed that immunogenic chemotherapy using agents such as cyclophosphamide can instigate T-cell infiltration into tumours and sensitise them to checkpoint inhibitor therapy (Pfirschke et al., 2016), and assumably paclitaxel acts similarly, as it is certainly immunogenic and capable of immune priming the tumour microenvironment (Swart et al., 2016, Soliman, 2017).

While there is a plethora of studies clarifying the inflammatory outputs of paclitaxel, the mechanisms which promote this inflammation were previously unclear. In this study, we have shown that taxane-induced cytokine production in our explored context is dependent on TRAIL DRs and downstream DR signalling. Similarly to the ER

stress-induced inflammatory phenotype observed, DR aggregation due to robust upregulation is the likely cause of inflammatory signalling engagement (Chan et al., 2000), inducing robust cytokine production. Downstream effectors FADD and caspase-8 were also (and unsurprisingly) found to be important. While zVAD-fmk co-treatment blocked taxane induced cell death and concurrently increased cytokine production, SMAC mimetic BV6 had converse effects. Protection from taxane induced inflammatory outputs while concurrently increasing its killing ability may be beneficial therapeutically. Indeed, SMAC mimetics have been shown to sensitise to the cell death-inducing capacity of chemotherapeutic agents (Probst et al., 2010). SMAC mimetics such as Brinaprint have been shown to sensitise chemoresistant triple negative breast cancer cells to paclitaxel, suggesting that combination therapies may be a mechanism to overcome resistance (Panayotopoulou et al., 2017). Synergistic effects have also been seen in models of hepatocellular carcinoma and NSCLC (Tian et al., 2014, Greer et al., 2011). It is interesting that these results have not previously been understood in terms of what we now know about TRAIL receptor signalling, but is clear that the DR-dependent inflammatory signalling induced by taxanes will be effected by SMAC mimetic dual therapies.

Surprisingly however, ablation of ER stress-associated transcription factor CHOP also lended protection against taxane-induced inflammatory outputs. While taxanes have previously been associated sporadically with an ER stress response (Notte et al., 2015), we show here an important physiological outcome of this response. CHOP ablation concurrently reduced expression of DR5, a molecule which we have additionally shown to be important. It can be speculated that CHOP-induced DR5 upregulation contributes to engagement of DR signalling in this context. Additionally, while we have shown here that taxanes induce an ER stress response, the mechanism of this induction is unknown. It is possible that microtubule disruption by taxanes directly causes changes in the curvature of the ER and induced activation of the ER membrane associated sensors (Schwarz and Blower, 2016). It is also possible that taxanes engage the ER stress response in a similar manner previously described for other xenobiotics – as the ER contains the majority of cytochrome P450 enzymes involved in xenobiotic metabolism and under conditions of prolonged exposure to xenobiotics, ER stress and apoptosis are initiated (Cribb et al., 2005).

Importantly, elucidation of this signalling pathway introduces new possibilities for therapy. Despite this inflammatory phenotype, it is clear that taxanes are effective at killing and initially reducing tumour burden, yet they are often associated with secondary inflammation, drug resistance, relapse and tumour reoccurrence (Makker et al., 2013, Markman and Bookman, 2000). Liu and colleagues showed that in their *in vitro* and *in*

vivo models, cytokine blockade of molecules which they had found to be upregulated in response to paclitaxel dramatically protected from chemotherapy induced metastasis, while prolonging the median survival time of mice by approximately 40% (Liu et al., 2015). With humans showing similar cytokine responses in response to taxane therapies, cytokine blockade combination therapies may prove fruitful in the context of taxane chemotherapy.

While taxanes have exclusively been studied here, there are a number of other chemotherapeutic drugs which have classically been associated with inflammatory effects, as well as DR upregulation. As examples, etoposide, doxorubicin, cisplatin and 5-flourouracil all warrant study. The use of each of these drugs has been linked to inflammatory cytokine production, metastasis, chemoresistance and ultimately tumour recurrence (Vyas et al., 2014). Additionally, as has been described above, these agents have been linked with death receptor upregulation, though Fas DR may prove to be more important in these contexts. In a manner similar to taxanes, it is plausible that this upregulation may lead to receptor aggregation and activation of inflammatory signalling.

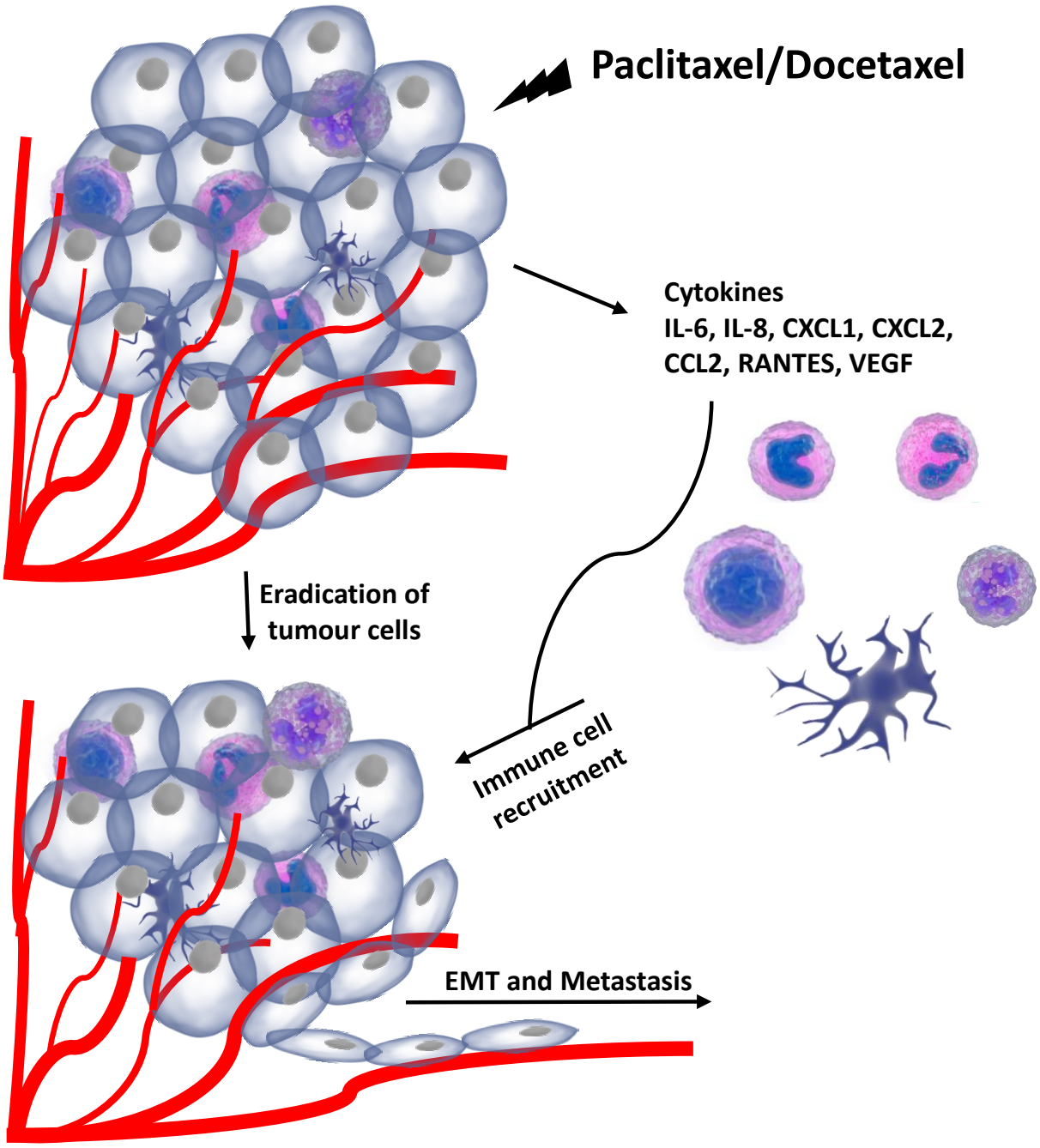

Figure 4.2 Taxanes induce inflammation via a DR5 and ER stress-dependent pathway
Taxane chemotherapy on established tumours leads to ER stress and death receptor-dependent production of cytokines and chemokines such as IL-6, IL-8, CXCL1, CXCL2, CCL2, RANTES and VEGF, as well as eradication of tumour cells via microtubule disruption, cell cycle arrest and ultimately apoptosis. Cytokine and chemokine release leads to immune cell recruitment in the tumour microenvironment and ultimately, angiogenesis, EMT and metastasis.

4.3 Conclusions and Future Perspectives

Following the reinvigoration of interest in TRAIL induced NFkB activation and inflammatory signalling earlier this year by our group, the physiological contexts where TRAIL-induced inflammation is important remained to be explored. It is clear that while this aspect of TRAIL signalling had until now been remarkably overlooked, it is an exciting area to be studied. A picture of a globally relevant pathway of ER stress induced inflammation via DRs has been highlighted here. Providing the link between chemotherapy-induced inflammation and via ER stress-associated death receptor upregulation, as we have done in our study, will prove pivotal in taking the next step to understanding the physiological importance of TRAIL-induced inflammatory signalling. However, it is clear that there are still many avenues to be explored. Further examination of solid tumour associated ER stress and drug induced inflammation is likely to prove fruitful.

References

ADACHI, Y., YAMAMOTO, K., OKADA, T., YOSHIDA, H., HARADA, A. & MORI, K. 2008. ATF6 is a transcription factor specializing in the regulation of quality control proteins in the endoplasmic reticulum. *Cell Struct Funct,* 33**,** 75-89.

ADAMS, J., CUTHBERT-HEAVENS, D., BASS, S. & KNOWLES, M. A. 2005. Infrequent mutation of TRAIL receptor 2 (TRAIL-R2/DR5) in transitional cell carcinoma of the bladder with 8p21 loss of heterozygosity. *Cancer Lett,* 220**,** 137-44.

AFFARA, N. I., RUFFELL, B., MEDLER, T. R., GUNDERSON, A. J., JOHANSSON, M., BORNSTEIN, S., BERGSLAND, E., STEINHOFF, M., LI, Y., GONG, Q., MA, Y., WIESEN, J. F., WONG, M. H., KULESZ-MARTIN, M., IRVING, B. & COUSSENS, L. M. 2014. B cells regulate macrophage phenotype and response to chemotherapy in squamous carcinomas. *Cancer Cell,* 25**,** 809-21.

AGGARWAL, B. B. 2003. Signalling pathways of the TNF superfamily: a double-edged sword. *Nat Rev Immunol,* 3**,** 745-756.

ANDERS, C., NIEWOEHNER, O., DUERST, A. & JINEK, M. 2014. Structural basis of PAM-dependent target DNA recognition by the Cas9 endonuclease. *Nature,* 513**,** 569-73.

ANDO, M., KAWAZU, M., UENO, T., FUKUMURA, K., YAMATO, A., SODA, M., YAMASHITA, Y., CHOI, Y. L., YAMASOBA, T. & MANO, H. 2013. Cancer-associated missense mutations of caspase-8 activate nuclear factor-kappaB signaling. *Cancer Sci,* 104**,** 1002-8.

ARAKI, K. & NAGATA, K. 2011. Protein folding and quality control in the ER. *Cold Spring Harb Perspect Biol,* 3**,** a007526.

ARENDS, M. J. & WYLLIE, A. H. 1991. Apoptosis: mechanisms and roles in pathology. *Int Rev Exp Pathol,* 32**,** 223-54.

ARTS, H., DE JONG, S., HOLLEMA, H., TEN HOOR, K., VAN DER ZEE, A. & DE VRIES, E. 2004. Chemotherapy induces death receptor 5 in epithelial ovarian carcinoma. *Gynecologic oncology,* 92**,** 794-800.

ASHKENAZI, A., PAI, R. C., FONG, S., LEUNG, S., LAWRENCE, D. A., MARSTERS, S. A., BLACKIE, C., CHANG, L., MCMURTREY, A. E., HEBERT, A., DEFORGE, L., KOUMENIS, I. L., LEWIS, D., HARRIS, L., BUSSIERE, J., KOEPPEN, H., SHAHROKH, Z. & SCHWALL, R. H. 1999. Safety and antitumor activity of recombinant soluble Apo2 ligand. *J Clin Invest,* 104**,** 155-62.

AUF, G., JABOUILLE, A., GUERIT, S., PINEAU, R., DELUGIN, M., BOUCHECAREILH, M., MAGNIN, N., FAVEREAUX, A., MAITRE, M., GAISER, T., VON DEIMLING, A., CZABANKA, M., VAJKOCZY, P., CHEVET, E., BIKFALVI, A. & MOENNER, M. 2010. Inositol-requiring enzyme 1alpha is a key regulator of angiogenesis and invasion in malignant glioma. *Proc Natl Acad Sci U S A,* 107**,** 15553-8.

AZIJLI, K., YUVARAJ, S., PEPPELENBOSCH, M. P., WURDINGER, T., DEKKER, H., JOORE, J., VAN DIJK, E., QUAX, W. J., PETERS, G. J., DE JONG, S. & KRUYT, F. A. 2012. Kinome profiling of non-canonical TRAIL signaling reveals RIP1-Src-STAT3-dependent invasion in resistant non-small cell lung cancer cells. *J Cell Sci,* 125**,** 4651-61.

B'CHIR, W., MAURIN, A. C., CARRARO, V., AVEROUS, J., JOUSSE, C., MURANISHI, Y., PARRY, L., STEPIEN, G., FAFOURNOUX, P. & BRUHAT, A. 2013. The eIF2alpha/ATF4 pathway is essential for stress-induced autophagy gene expression. *Nucleic Acids Res,* 41**,** 7683-99.

BAADER, E., TOLOCZKO, A., FUCHS, U., SCHMID, I., BELTINGER, C., EHRHARDT, H., DEBATIN, K. M. & JEREMIAS, I. 2005. Tumor necrosis factor-related apoptosis-inducing ligand-mediated proliferation of tumor cells with receptor-proximal apoptosis defects. *Cancer Res,* 65**,** 7888-95.

BARRANGOU, R., FREMAUX, C., DEVEAU, H., RICHARDS, M., BOYAVAL, P., MOINEAU, S., ROMERO, D. A. & HORVATH, P. 2007a. CRISPR provides acquired resistance against viruses in prokaryotes. *Science,* 315.

BARRANGOU, R., FREMAUX, C., DEVEAU, H., RICHARDS, M., BOYAVAL, P., MOINEAU, S., ROMERO, D. A. & HORVATH, P. 2007b. CRISPR Provides Acquired Resistance Against Viruses in Prokaryotes. *Science,* 315**,** 1709-1712.

BERG, D., STUHMER, T., SIEGMUND, D., MULLER, N., GINER, T., DITTRICH-BREIHOLZ, O., KRACHT, M., BARGOU, R. & WAJANT, H. 2009. Oligomerized tumor necrosis factor-related apoptosis inducing ligand strongly induces cell death in myeloma cells, but also activates proinflammatory signaling pathways. *Febs j,* 276**,** 6912-27.

BERTOLOTTI, A., ZHANG, Y., HENDERSHOT, L. M., HARDING, H. P. & RON, D. 2000a. Dynamic interaction of BiP and ER stress transducers in the unfolded-protein response. *Nat Cell Biol,* 2**,** 326-332.

BERTOLOTTI, A., ZHANG, Y., HENDERSHOT, L. M., HARDING, H. P. & RON, D. 2000b. Dynamic interaction of BiP and ER stress transducers in the unfolded-protein response. *Nat Cell Biol,* 2**,** 326-32.

BHOJANI, M. S., CHEN, G., ROSS, B. D., BEER, D. G. & REHEMTULLA, A. 2005. Nuclear localized phosphorylated FADD induces cell proliferation and is associated with aggressive lung cancer. *Cell cycle (Georgetown, Tex.),* 4**,** 1478-1481.

BIRNBAUM, M. J., CLEM, R. J. & MILLER, L. K. 1994. An apoptosis-inhibiting gene from a nuclear polyhedrosis virus encoding a polypeptide with Cys/His sequence motifs. *J Virol,* 68**,** 2521-8.

BLAIS, J. D., ADDISON, C. L., EDGE, R., FALLS, T., ZHAO, H., WARY, K., KOUMENIS, C., HARDING, H. P., RON, D., HOLCIK, M. & BELL, J. C. 2006. Perk-dependent translational regulation promotes tumor cell adaptation and angiogenesis in response to hypoxic stress. *Mol Cell Biol,* 26**,** 9517-32.

BOBROVNIKOVA-MARJON, E., GRIGORIADOU, C., PYTEL, D., ZHANG, F., YE, J., KOUMENIS, C., CAVENER, D. & DIEHL, J. A. 2010. PERK promotes cancer cell proliferation and tumor growth by limiting oxidative DNA damage. *Oncogene,* 29**,** 3881-95.

BOLOTIN, A., QUINQUIS, B., SOROKIN, A. & EHRLICH, S. D. 2005. Clustered regularly interspaced short palindrome repeats (CRISPRs) have spacers of extrachromosomal origin. *Microbiology,* 151**,** 2551-61.

BRATTON, S. B., MACFARLANE, M., CAIN, K. & COHEN, G. M. 2000. Protein complexes activate distinct caspase cascades in death receptor and stress-induced apoptosis. *Exp Cell Res,* 256**,** 27-33.

CAIN, K., BROWN, D. G., LANGLAIS, C. & COHEN, G. M. 1999. Caspase Activation Involves the Formation of the Aposome, a Large (∼700 kDa) Caspase-activating Complex. *Journal of Biological Chemistry,* 274**,** 22686-22692.

CANDE, C., COHEN, I., DAUGAS, E., RAVAGNAN, L., LAROCHETTE, N., ZAMZAMI, N. & KROEMER, G. 2002. Apoptosis-inducing factor (AIF): a novel caspase-independent death effector released from mitochondria. *Biochimie,* 84**,** 215-22.

CARRINGTON, P. E., SANDU, C., WEI, Y., HILL, J. M., MORISAWA, G., HUANG, T., GAVATHIOTIS, E., WEI, Y. & WERNER, M. H. 2006. The structure of FADD and its mode of interaction with procaspase-8. *Mol Cell,* 22**,** 599-610.

CARSWELL, E. A., OLD, L. J., KASSEL, R. L., GREEN, S., FIORE, N. & WILLIAMSON, B. 1975. An endotoxin-induced serum factor that causes necrosis of tumors. *Proc Natl Acad Sci U S A,* 72**,** 3666-70.

CHAMULEAU, M. E., OSSENKOPPELE, G. J., VAN RHENEN, A., VAN DREUNEN, L., JIRKA, S. M., ZEVENBERGEN, A., SCHUURHUIS, G. J. & VAN DE LOOSDRECHT, A. A. 2011. High TRAIL-R3 expression on leukemic blasts is associated with poor outcome and induces apoptosis-resistance which can be overcome by targeting TRAIL-R2. *Leuk Res,* 35**,** 741-9.

CHAN, F. K., CHUN, H. J., ZHENG, L., SIEGEL, R. M., BUI, K. L. & LENARDO, M. J. 2000. A domain in TNF receptors that mediates ligand-independent receptor assembly and signaling. *Science,* 288**,** 2351-4.

CHEN, G., BHOJANI, M. S., HEAFORD, A. C., CHANG, D. C., LAXMAN, B., THOMAS, D. G., GRIFFIN, L. B., YU, J., COPPOLA, J. M., GIORDANO, T. J., LIN, L., ADAMS, D., ORRINGER, M. B., ROSS, B. D., BEER, D. G. & REHEMTULLA, A. 2005. Phosphorylated FADD induces NF-kappaB, perturbs cell cycle, and is associated with poor outcome in lung adenocarcinomas. *Proc Natl Acad Sci U S A,* 102**,** 12507-12.

CHEN, L., FAN, J., CHEN, H., MENG, Z., CHEN, Z., WANG, P. & LIU, L. 2014. The IL-8/CXCR1 axis is associated with cancer stem cell-like properties and correlates with clinical prognosis in human pancreatic cancer cases. *Sci Rep,* 4**,** 5911.

CHEN, Y. & BRANDIZZI, F. 2013. IRE1: ER stress sensor and cell fate executor. *Trends Cell Biol,* 23**,** 547-55.

CHEN, Z. J. 2012. Ubiquitination in signaling to and activation of IKK. *Immunological Reviews,* 246**,** 95-106.

CHINNAIYAN, A. M., PRASAD, U., SHANKAR, S., HAMSTRA, D. A., SHANAIAH, M., CHENEVERT, T. L., ROSS, B. D. & REHEMTULLA, A. 2000. Combined effect of tumor necrosis factor-related apoptosis-inducing ligand and ionizing radiation in breast cancer therapy. *Proc Natl Acad Sci U S A,* 97**,** 1754-9.

CHRISTENSEN, S. B., ANDERSEN, A., KROMANN, H., TREIMAN, M., TOMBAL, B., DENMEADE, S. & ISAACS, J. T. 1999. Thapsigargin analogues for targeting programmed death of androgen-independent prostate cancer cells. *Bioorg Med Chem,* 7**,** 1273-80.

CHRISTENSEN, S. B., ANDERSEN, A. & SMITT, U. W. 1997. Sesquiterpenoids from Thapsia species and medicinal chemistry of the thapsigargins. *Fortschr Chem Org Naturst,* 71**,** 129-67.

CHUNTHARAPAI, A., DODGE, K., GRIMMER, K., SCHROEDER, K., MARSTERS, S. A., KOEPPEN, H., ASHKENAZI, A. & KIM, K. J. 2001. Isotype-dependent inhibition of tumor growth in vivo by monoclonal antibodies to death receptor 4. *J Immunol,* 166**,** 4891-8.

CLARKE, HANNA J., CHAMBERS, JOSEPH E., LINIKER, E. & MARCINIAK, STEFAN J. Endoplasmic Reticulum Stress in Malignancy. *Cancer Cell,* 25**,** 563-573.

COHEN, G. M. 1997. Caspases: the executioners of apoptosis. *Biochem J,* 326 (Pt 1)**,** 1-16.

CONG, L., RAN, F. A., COX, D., LIN, S., BARRETTO, R., HABIB, N., HSU, P. D., WU, X., JIANG, W., MARRAFFINI, L. A. & ZHANG, F. 2013. Multiplex Genome Engineering Using CRISPR/Cas Systems. *Science,* 339**,** 819-823.

CORAZZARI, M., RAPINO, F., CICCOSANTI, F., GIGLIO, P., ANTONIOLI, M., CONTI, B., FIMIA, G. M., LOVAT, P. E. & PIACENTINI, M. 2015. Oncogenic BRAF induces chronic ER stress condition resulting in increased basal autophagy and apoptotic resistance of cutaneous melanoma. *Cell Death Differ,* 22**,** 946-958.

CORY, S. & ADAMS, J. M. 2002. The Bcl2 family: regulators of the cellular life-or-death switch. *Nat Rev Cancer,* 2**,** 647-56.

CRIBB, A. E., PEYROU, M., MURUGANANDAN, S. & SCHNEIDER, L. 2005. The endoplasmic reticulum in xenobiotic toxicity. *Drug Metab Rev,* 37**,** 405-42.

CULLEN, S. P., HENRY, C. M., KEARNEY, C. J., LOGUE, S. E., FEOKTISTOVA, M., TYNAN, G. A., LAVELLE, E. C., LEVERKUS, M. & MARTIN, S. J. 2013. Fas/CD95-induced chemokines can serve as "find-me" signals for apoptotic cells. *Mol Cell,* 49**,** 1034-48.

CULLINAN, S. B., ZHANG, D., HANNINK, M., ARVISAIS, E., KAUFMAN, R. J. & DIEHL, J. A. 2003. Nrf2 is a direct PERK substrate and effector of PERK-dependent cell survival. *Mol Cell Biol,* 23**,** 7198-209.

DE FILIPPO, K., DUDECK, A., HASENBERG, M., NYE, E., VAN ROOIJEN, N., HARTMANN, K., GUNZER, M., ROERS, A. & HOGG, N. 2013. Mast cell and macrophage chemokines CXCL1/CXCL2 control the early stage of neutrophil recruitment during tissue inflammation. *Blood,* 121**,** 4930-7.

DE LAURENTIIS, M., CANCELLO, G., D'AGOSTINO, D., GIULIANO, M., GIORDANO, A., MONTAGNA, E., LAURIA, R., FORESTIERI, V., ESPOSITO, A., SILVESTRO, L., PENNACCHIO, R., CRISCITIELLO, C., MONTANINO, A., LIMITE, G., BIANCO, A. R. & DE PLACIDO, S. 2008. Taxane-based combinations as adjuvant chemotherapy of early breast cancer: a meta-analysis of randomized trials. *J Clin Oncol,* 26**,** 44-53.

DEGLI-ESPOSTI, M. A., DOUGALL, W. C., SMOLAK, P. J., WAUGH, J. Y., SMITH, C. A. & GOODWIN, R. G. 1997. The novel receptor TRAIL-R4 induces NF-kappaB and protects against TRAIL-mediated apoptosis, yet retains an incomplete death domain. *Immunity,* 7**,** 813-20.

DELTCHEVA, E., CHYLINSKI, K., SHARMA, C. M., GONZALES, K., CHAO, Y., PIRZADA, Z. A., ECKERT, M. R., VOGEL, J. & CHARPENTIER, E. 2011. CRISPR RNA maturation by trans-encoded small RNA and host factor RNase III. *Nature,* 471**,** 602-607.

DENARDO, D. G., BRENNAN, D. J., REXHEPAJ, E., RUFFELL, B., SHIAO, S. L., MADDEN, S. F., GALLAGHER, W. M., WADHWANI, N., KEIL, S. D., JUNAID, S. A., RUGO, H. S., HWANG, E. S., JIRSTROM, K., WEST, B. L. & COUSSENS, L. M. 2011. Leukocyte complexity predicts breast cancer survival and functionally regulates response to chemotherapy. *Cancer Discov,* 1**,** 54-67.

DENMEADE, S. R., MHAKA, A. M., ROSEN, D. M., BRENNEN, W. N., DALRYMPLE, S., DACH, I., OLESEN, C., GUREL, B., DEMARZO, A. M., WILDING, G., CARDUCCI, M. A., DIONNE, C. A., MØLLER, J. V., NISSEN, P., CHRISTENSEN, S. B. & ISAACS, J. T. 2012. Engineering a Prostate-Specific Membrane Antigen–Activated Tumor Endothelial Cell Prodrug for Cancer Therapy. *Science Translational Medicine,* 4**,** 140ra86-140ra86.

DEVERAUX, Q. L., TAKAHASHI, R., SALVESEN, G. S. & REED, J. C. 1997. X-linked IAP is a direct inhibitor of cell-death proteases. *Nature,* 388**,** 300-304.

DEY, S., SAYERS, C. M., VERGINADIS, I. I., LEHMAN, S. L., CHENG, Y., CERNIGLIA, G. J., TUTTLE, S. W., FELDMAN, M. D., ZHANG, P. J. L., FUCHS, S. Y., DIEHL, J. A. & KOUMENIS, C. 2015. ATF4-dependent induction of heme oxygenase 1 prevents anoikis and promotes metastasis. *The Journal of Clinical Investigation,* 125**,** 2592-2608.

DHAWAN, P. & RICHMOND, A. 2002. Role of CXCL1 in tumorigenesis of melanoma. *J Leukoc Biol,* 72**,** 9-18.

DIAZ, J. F. & ANDREU, J. M. 1993. Assembly of purified GDP-tubulin into microtubules induced by taxol and taxotere: reversibility, ligand stoichiometry, and competition. *Biochemistry,* 32**,** 2747-55.

DIAZ, J. F., MENENDEZ, M. & ANDREU, J. M. 1993. Thermodynamics of ligand-induced assembly of tubulin. *Biochemistry,* 32**,** 10067-10077.

DOENCH, J. G. & FUSI, N. 2016. Optimized sgRNA design to maximize activity and minimize off-target effects of CRISPR-Cas9. 34**,** 184-91.

DOENCH, J. G., HARTENIAN, E., GRAHAM, D. B., TOTHOVA, Z., HEGDE, M., SMITH, I., SULLENDER, M., EBERT, B. L., XAVIER, R. J. & ROOT, D. E. 2014. Rational design of highly active sgRNAs for CRISPR-Cas9-mediated gene inactivation. *Nat Biotechnol,* 32**,** 1262-7.

DORSEY, J. F., MINTZ, A., TIAN, X., DOWLING, M. L., PLASTARAS, J. P., DICKER, D. T., KAO, G. D. & EL-DEIRY, W. S. 2009. Tumor necrosis factor-related apoptosis-inducing ligand (TRAIL) and paclitaxel have cooperative in vivo effects against glioblastoma multiforme cells. *Mol Cancer Ther,* 8**,** 3285-95.

DU, C., FANG, M., LI, Y., LI, L. & WANG, X. 2000. Smac, a mitochondrial protein that promotes cytochrome c-dependent caspase activation by eliminating IAP inhibition. *Cell,* 102**,** 33-42.

DUEBER, E. C., SCHOEFFLER, A. J., LINGEL, A., ELLIOTT, J. M., FEDOROVA, A. V., GIANNETTI, A. M., ZOBEL, K., MAURER, B., VARFOLOMEEV, E., WU, P., WALLWEBER, H. J. A., HYMOWITZ, S. G., DESHAYES, K., VUCIC, D. & FAIRBROTHER, W. J. 2011. Antagonists Induce a Conformational Change in cIAP1 That Promotes Autoubiquitination. *Science,* 334**,** 376-380.

EL-DEIRY, W. S. 2001. Insights into cancer therapeutic design based on p53 and TRAIL receptor signaling. *Cell Death Differ,* 8**,** 1066-75.

ELLIS, P., BARRETT-LEE, P., JOHNSON, L., CAMERON, D., WARDLEY, A., O'REILLY, S., VERRILL, M., SMITH, I., YARNOLD, J., COLEMAN, R., EARL, H., CANNEY, P., TWELVES, C., POOLE, C., BLOOMFIELD, D., HOPWOOD, P., JOHNSTON, S., DOWSETT, M., BARTLETT, J. M., ELLIS, I., PECKITT, C., HALL, E. & BLISS, J. M. 2009. Sequential docetaxel as adjuvant chemotherapy for early breast cancer (TACT): an open-label, phase III, randomised controlled trial. *Lancet,* 373**,** 1681-92.

EMERY, J. G., MCDONNELL, P., BURKE, M. B., DEEN, K. C., LYN, S., SILVERMAN, C., DUL, E., APPELBAUM, E. R., EICHMAN, C., DIPRINZIO, R., DODDS, R. A., JAMES, I. E., ROSENBERG, M., LEE, J. C. & YOUNG, P. R. 1998. Osteoprotegerin is a receptor for the cytotoxic ligand TRAIL. *J Biol Chem,* 273**,** 14363-7.

ESTORNES, Y., AGUILETA, M. A., DUBUISSON, C., DE KEYSER, J., GOOSSENS, V., KERSSE, K., SAMALI, A., VANDENABEELE, P. & BERTRAND, M. J. 2014. RIPK1 promotes death receptor-independent caspase-8-mediated apoptosis under unresolved ER stress conditions. *Cell Death Dis,* 5**,** e1555.

FAN, M., GOODWIN, M., VU, T., BRANTLEY-FINLEY, C., GAARDE, W. A. & CHAMBERS, T. C. 2000. Vinblastine-induced phosphorylation of Bcl-2 and Bcl-XL is mediated by JNK and occurs in parallel with inactivation of the Raf-1/MEK/ERK cascade. *J Biol Chem,* 275**,** 29980-5.

FAN, S., MULLER, S., CHEN, Z. G., PAN, L., TIGHIOUART, M., SHIN, D. M., KHURI, F. R. & SUN, S. Y. 2013. Prognostic impact of Fas-associated death domain, a key component in death receptor signaling, is dependent on the presence of lymph node metastasis in head and neck squamous cell carcinoma. *Cancer Biol Ther,* 14**,** 365-9.

FELTHAM, R., BETTJEMAN, B., BUDHIDARMO, R., MACE, P. D., SHIRLEY, S., CONDON, S. M., CHUNDURU, S. K., MCKINLAY, M. A., VAUX, D. L., SILKE, J. & DAY, C. L. 2011. Smac Mimetics Activate the E3 Ligase Activity of cIAP1 Protein by Promoting RING Domain Dimerization. *Journal of Biological Chemistry,* 286**,** 17015-17028.

FENG, Y. X., SOKOL, E. S., DEL VECCHIO, C. A., SANDUJA, S., CLAESSEN, J. H., PROIA, T. A., JIN, D. X., REINHARDT, F., PLOEGH, H. L., WANG, Q. & GUPTA, P. B. 2014. Epithelial-to-mesenchymal transition activates PERK-eIF2alpha and sensitizes cells to endoplasmic reticulum stress. *Cancer Discov,* 4**,** 702-15.

FEOKTISTOVA, M., GESERICK, P., KELLERT, B., DIMITROVA, D. P., LANGLAIS, C., HUPE, M., CAIN, K., MACFARLANE, M., HACKER, G. & LEVERKUS, M. 2011. cIAPs block Ripoptosome formation, a RIP1/caspase-8 containing intracellular cell death complex differentially regulated by cFLIP isoforms. *Mol Cell,* 43**,** 449-63.

FISHER, D. T., APPENHEIMER, M. M. & EVANS, S. S. 2014. The two faces of IL-6 in the tumor microenvironment. *Semin Immunol,* 26**,** 38-47.

FRIDMAN, W. H., PAGÈS, F., SAUTÈS-FRIDMAN, C. & GALON, J. 2012. The immune contexture in human tumours: impact on clinical outcome. *Nat Rev Cancer,* 12**,** 298-306.

FULDA, S. 2015. Promises and Challenges of Smac Mimetics as Cancer Therapeutics. *Clin Cancer Res,* 21**,** 5030-6.

FULDA, S. & VUCIC, D. 2012. Targeting IAP proteins for therapeutic intervention in cancer. *Nat Rev Drug Discov,* 11**,** 109-124.

GAJEWSKI, T. F., SCHREIBER, H. & FU, Y.-X. 2013. Innate and adaptive immune cells in the tumor microenvironment. *Nat Immunol,* 14**,** 1014-1022.

GARCIA-MARTINEZ, E., GIL, G. L., BENITO, A. C., GONZALEZ-BILLALABEITIA, E., CONESA, M. A., GARCIA GARCIA, T., GARCIA-GARRE, E., VICENTE, V. & AYALA DE LA PENA, F. 2014. Tumor-infiltrating immune cell profiles and their change after neoadjuvant chemotherapy predict response and prognosis of breast cancer. *Breast Cancer Res,* 16**,** 488.

GARRETT, R. A., SHAH, S. A., ERDMANN, S., LIU, G., MOUSAEI, M., LEON-SOBRINO, C., PENG, W., GUDBERGSDOTTIR, S., DENG, L., VESTERGAARD, G., PENG, X. & SHE, Q. 2015. CRISPR-Cas Adaptive Immune Systems of the Sulfolobales: Unravelling Their Complexity and Diversity. *Life (Basel),* 5**,** 783-817.

GERARD, J. 1974. *The herball or generall historie of plantes*, Norton, John.

GESERICK, P., HUPE, M., MOULIN, M., WONG, W. W., FEOKTISTOVA, M., KELLERT, B., GOLLNICK, H., SILKE, J. & LEVERKUS, M. 2009. Cellular IAPs inhibit a cryptic CD95-induced cell death by limiting RIP1 kinase recruitment. *J Cell Biol,* 187**,** 1037-54.

GIBSON, S. B., OYER, R., SPALDING, A. C., ANDERSON, S. M. & JOHNSON, G. L. 2000. Increased expression of death receptors 4 and 5 synergizes the apoptosis response to combined treatment with etoposide and TRAIL. *Mol Cell Biol,* 20**,** 205-12.

GRADISHAR, W. J., TJULANDIN, S., DAVIDSON, N., SHAW, H., DESAI, N., BHAR, P., HAWKINS, M. & O'SHAUGHNESSY, J. 2005. Phase III Trial of Nanoparticle Albumin-Bound Paclitaxel Compared With Polyethylated Castor Oil–Based Paclitaxel in Women With Breast Cancer. *Journal of Clinical Oncology,* 23**,** 7794-7803.

GREER, R. M., PEYTON, M., LARSEN, J. E., GIRARD, L., XIE, Y., GAZDAR, A. F., HARRAN, P., WANG, L., BREKKEN, R. A., WANG, X. & MINNA, J. D. 2011. SMAC Mimetic (JP1201) Sensitizes Non–Small Cell Lung Cancers to Multiple Chemotherapy Agents in an IAP-Dependent but TNF-α–Independent Manner. *Cancer Research,* 71**,** 7640-7648.

GUNDERSON, A. J. & COUSSENS, L. M. 2013. B cells and their mediators as targets for therapy in solid tumors. *Exp Cell Res,* 319**,** 1644-9.

GYRD-HANSEN, M. & MEIER, P. 2010. IAPs: from caspase inhibitors to modulators of NF-κB, inflammation and cancer. *Nat Rev Cancer,* 10**,** 561-574.

HAN, J., BACK, S. H., HUR, J., LIN, Y. H., GILDERSLEEVE, R., SHAN, J., YUAN, C. L., KROKOWSKI, D., WANG, S., HATZOGLOU, M., KILBERG, M. S., SARTOR, M. A. & KAUFMAN, R. J. 2013. ER-stress-induced transcriptional regulation increases protein synthesis leading to cell death. *Nat Cell Biol,* 15**,** 481-90.

HARDING, H. P., ZHANG, Y. & RON, D. 1999. Protein translation and folding are coupled by an endoplasmic-reticulum-resident kinase. *Nature,* 397**,** 271-274.

HARDING, H. P., ZHANG, Y., ZENG, H., NOVOA, I., LU, P. D., CALFON, M., SADRI, N., YUN, C., POPKO, B., PAULES, R., STOJDL, D. F., BELL, J. C., HETTMANN, T., LEIDEN, J. M. & RON, D. 2003. An integrated stress response regulates amino acid metabolism and resistance to oxidative stress. *Mol Cell,* 11**,** 619-33.

HARPER, N., FARROW, S. N., KAPTEIN, A., COHEN, G. M. & MACFARLANE, M. 2001. Modulation of tumor necrosis factor apoptosis-inducing ligand- induced NF-kappa B activation by inhibition of apical caspases. *J Biol Chem,* 276**,** 34743-52.

HARTWIG, T., MONTINARO, A., VON KARSTEDT, S., SEVKO, A., SURINOVA, S., CHAKRAVARTHY, A., TARABORRELLI, L., DRABER, P., LAFONT, E., ARCE VARGAS, F., EL-BAHRAWY, M. A., QUEZADA, S. A. & WALCZAK, H. 2017. The TRAIL-Induced Cancer Secretome Promotes a Tumor-Supportive Immune Microenvironment via CCR2. *Mol Cell,* 65**,** 730-742.e5.

HAZE, K., YOSHIDA, H., YANAGI, H., YURA, T. & MORI, K. 1999. Mammalian transcription factor ATF6 is synthesized as a transmembrane protein and activated by proteolysis in response to endoplasmic reticulum stress. *Mol Biol Cell,* 10**,** 3787-99.

HELMS, J. B. & ROTHMAN, J. E. 1992. Inhibition by brefeldin A of a Golgi membrane enzyme that catalyses exchange of guanine nucleotide bound to ARF. *Nature,* 360**,** 352-354.

HENRY, C. M., HOLLVILLE, E. & MARTIN, S. J. 2013. Measuring apoptosis by microscopy and flow cytometry. *Methods,* 61**,** 90-97.

HENRY, C. M. & MARTIN, S. J. 2017. Caspase-8 Acts in a Non-enzymatic Role as a Scaffold for Assembly of a Pro-inflammatory "FADDosome" Complex upon TRAIL Stimulation. *Mol Cell,* 65**,** 715-729.e5.

HODGE, J. W., GARNETT, C. T., FARSACI, B., PALENA, C., TSANG, K.-Y., FERRONE, S. & GAMEIRO, S. R. 2013. Chemotherapy-induced immunogenic modulation of tumor cells enhances killing by cytotoxic T lymphocytes and is distinct from immunogenic cell death. *International journal of cancer. Journal international du cancer,* 133**,** 624-636.

HOLLIEN, J., LIN, J. H., LI, H., STEVENS, N., WALTER, P. & WEISSMAN, J. S. 2009. Regulated Ire1-dependent decay of messenger RNAs in mammalian cells. *J Cell Biol,* 186**,** 323-31.

HOLLIEN, J. & WEISSMAN, J. S. 2006. Decay of endoplasmic reticulum-localized mRNAs during the unfolded protein response. *Science,* 313**,** 104-7.

HOLLVILLE, E. & MARTIN, S. J. 2001. Measuring Apoptosis by Microscopy and Flow Cytometry. *Current Protocols in Immunology.* John Wiley & Sons, Inc.

HOOGWATER, F. J., NIJKAMP, M. W., SMAKMAN, N., STELLER, E. J., EMMINK, B. L., WESTENDORP, B. F., RAATS, D. A., SPRICK, M. R., SCHAEFER, U., VAN HOUDT, W. J., DE BRUIJN, M. T., SCHACKMANN, R. C., DERKSEN, P. W., MEDEMA, J. P., WALCZAK, H., BOREL RINKES, I. H. & KRANENBURG, O. 2010. Oncogenic K-Ras turns death receptors into metastasis-promoting receptors in human and mouse colorectal cancer cells. *Gastroenterology,* 138**,** 2357-67.

HYMOWITZ, S. G., CHRISTINGER, H. W., FUH, G., ULTSCH, M., O'CONNELL, M., KELLEY, R. F., ASHKENAZI, A. & DE VOS, A. M. 1999. Triggering cell death: the crystal structure of Apo2L/TRAIL in a complex with death receptor 5. *Mol Cell,* 4**,** 563-71.

ICHIKAWA, K., LIU, W., ZHAO, L., WANG, Z., LIU, D., OHTSUKA, T., ZHANG, H., MOUNTZ, J. D., KOOPMAN, W. J., KIMBERLY, R. P. & ZHOU, T. 2001. Tumoricidal activity of a novel anti-human DR5 monoclonal antibody without hepatocyte cytotoxicity. *Nat Med,* 7**,** 954-60.

IDRISSOVA, L., MALHI, H., WERNEBURG, N. W., LEBRASSEUR, N. K., BRONK, S. F., FINGAS, C., TCHKONIA, T., PIRTSKHALAVA, T., WHITE, T. A., STOUT, M. B., HIRSOVA, P., KRISHNAN, A., LIEDTKE, C., TRAUTWEIN, C., FINNBERG, N., EL-DEIRY, W. S., KIRKLAND, J. L. & GORES, G. J. 2015. TRAIL receptor deletion in mice suppresses the inflammation of nutrient excess. *J Hepatol,* 62**,** 1156-63.

IRMLER, M., THOME, M., HAHNE, M., SCHNEIDER, P., HOFMANN, K., STEINER, V., BODMER, J. L., SCHROTER, M., BURNS, K., MATTMANN, C., RIMOLDI, D., FRENCH, L. E. & TSCHOPP, J. 1997. Inhibition of death receptor signals by cellular FLIP. *Nature,* 388**,** 190-5.

IURLARO, R., PUSCHEL, F., LEON-ANNICCHIARICO, C. L., O'CONNOR, H., MARTIN, S. J., PALOU-GRAMON, D., LUCENDO, E. & MUNOZ-PINEDO, C. 2017. Glucose deprivation induces ATF4-mediated apoptosis through TRAIL death receptors. *Mol Cell Biol*.

JANSEN, R., EMBDEN, J. D. A. V., GAASTRA, W. & SCHOULS, L. M. 2002. Identification of genes that are associated with DNA repeats in prokaryotes. *Molecular Microbiology,* 43**,** 1565-1575.

JAVEED, A., ASHRAF, M., RIAZ, A., GHAFOOR, A., AFZAL, S. & MUKHTAR, M. M. 2009. Paclitaxel and immune system. *Eur J Pharm Sci,* 38**,** 283-90.

JEONG, E.-J., BANG, S., LEE, T. H., PARK, Y. I., SIM, W.-S. & KIM, K.-S. 1999. The Solution Structure of FADD Death Domain: STRUCTURAL BASIS OF DEATH DOMAIN INTERACTIONS OF Fas AND FADD. *Journal of Biological Chemistry,* 274**,** 16337-16342.

JEREMIAS, I., KUPATT, C., BAUMANN, B., HERR, I., WIRTH, T. & DEBATIN, K. M. 1998. Inhibition of Nuclear Factor κB Activation Attenuates Apoptosis Resistance in Lymphoid Cells. *Blood,* 91**,** 4624-4631.

JIANG, Y., CHEN, X., FAN, M., LI, H., ZHU, W., CHEN, X., CAO, C., XU, R., WANG, Y. & MA, Y. 2017. TRAIL facilitates cytokine expression and macrophage migration during hypoxia/reoxygenation via ER stress-dependent NF-κB pathway. *Molecular Immunology,* 82**,** 123-136.

JIN, Z., MCDONALD, E. R., 3RD, DICKER, D. T. & EL-DEIRY, W. S. 2004. Deficient tumor necrosis factor-related apoptosis-inducing ligand (TRAIL) death receptor transport to the cell

surface in human colon cancer cells selected for resistance to TRAIL-induced apoptosis. *J Biol Chem,* 279**,** 35829-39.

JINEK, M., CHYLINSKI, K., FONFARA, I., HAUER, M., DOUDNA, J. A. & CHARPENTIER, E. 2012. A programmable dual-RNA-guided DNA endonuclease in adaptive bacterial immunity. *Science,* 337**,** 816-21.

JINEK, M., JIANG, F., TAYLOR, D. W., STERNBERG, S. H., KAYA, E., MA, E., ANDERS, C., HAUER, M., ZHOU, K., LIN, S., KAPLAN, M., IAVARONE, A. T., CHARPENTIER, E., NOGALES, E. & DOUDNA, J. A. 2014. Structures of Cas9 Endonucleases Reveal RNA-Mediated Conformational Activation. *Science,* 343.

JO, M., KIM, T. H., SEOL, D. W., ESPLEN, J. E., DORKO, K., BILLIAR, T. R. & STROM, S. C. 2000. Apoptosis induced in normal human hepatocytes by tumor necrosis factor-related apoptosis-inducing ligand. *Nat Med,* 6**,** 564-7.

JONES, S. E., ERBAN, J., OVERMOYER, B., BUDD, G. T., HUTCHINS, L., LOWER, E., LAUFMAN, L., SUNDARAM, S., URBA, W. J., PRITCHARD, K. I., MENNEL, R., RICHARDS, D., OLSEN, S., MEYERS, M. L. & RAVDIN, P. M. 2005. Randomized phase III study of docetaxel compared with paclitaxel in metastatic breast cancer. *J Clin Oncol,* 23**,** 5542-51.

KAJIYAMA, H., SHIBATA, K., TERAUCHI, M., YAMASHITA, M., INO, K., NAWA, A. & KIKKAWA, F. 2007. Chemoresistance to paclitaxel induces epithelial-mesenchymal transition and enhances metastatic potential for epithelial ovarian carcinoma cells. *Int J Oncol,* 31**,** 277-83.

KANG, T. B., OH, G. S., SCANDELLA, E., BOLINGER, B., LUDEWIG, B., KOVALENKO, A. & WALLACH, D. 2008. Mutation of a self-processing site in caspase-8 compromises its apoptotic but not its nonapoptotic functions in bacterial artificial chromosome-transgenic mice. *J Immunol,* 181**,** 2522-32.

KEANE, M. M., RUBINSTEIN, Y., CUELLO, M., ETTENBERG, S. A., BANERJEE, P., NAU, M. M. & LIPKOWITZ, S. 2000. Inhibition of NF-kappaB activity enhances TRAIL mediated apoptosis in breast cancer cell lines. *Breast Cancer Res Treat,* 64**,** 211-9.

KEESTRA-GOUNDER, A. M., BYNDLOSS, M. X., SEYFFERT, N., YOUNG, B. M., CHÁVEZ-ARROYO, A., TSAI, A. Y., CEVALLOS, S. A., WINTER, M. G., PHAM, O. H., TIFFANY, C. R., DE JONG, M. F., KERRINNES, T., RAVINDRAN, R., LUCIW, P. A., MCSORLEY, S. J., BÄUMLER, A. J. & TSOLIS, R. M. 2016. NOD1 and NOD2 signalling links ER stress with inflammation. *Nature,* 532**,** 394-397.

KEIR, M. E., BUTTE, M. J., FREEMAN, G. J. & SHARPE, A. H. 2008. PD-1 and its ligands in tolerance and immunity. *Annu Rev Immunol,* 26**,** 677-704.

KELLING, J., SULLIVAN, K., WILSON, L. & JORDAN, M. A. 2003. Suppression of centromere dynamics by Taxol in living osteosarcoma cells. *Cancer Res,* 63**,** 2794-801.

KEPP, O., MENGER, L., VACCHELLI, E., LOCHER, C., ADJEMIAN, S., YAMAZAKI, T., MARTINS, I., SUKKURWALA, A. Q., MICHAUD, M., SENOVILLA, L., GALLUZZI, L., KROEMER, G. & ZITVOGEL, L. 2013. Crosstalk between ER stress and immunogenic cell death. *Cytokine Growth Factor Rev,* 24**,** 311-8.

KERR, J. F., WINTERFORD, C. M. & HARMON, B. V. 1994. Apoptosis. Its significance in cancer and cancer therapy. *Cancer,* 73**,** 2013-26.

KETTELHUT, I. C., FIERS, W. & GOLDBERG, A. L. 1987. The toxic effects of tumor necrosis factor in vivo and their prevention by cyclooxygenase inhibitors. *Proc Natl Acad Sci U S A,* 84**,** 4273-7.

KIM, H., TU, H. C., REN, D., TAKEUCHI, O., JEFFERS, J. R., ZAMBETTI, G. P., HSIEH, J. J. & CHENG, E. H. 2009. Stepwise activation of BAX and BAK by tBID, BIM, and PUMA initiates mitochondrial apoptosis. *Mol Cell,* 36**,** 487-99.

KIM, H. M., DO, C. H. & LEE, D. H. 2012. Combined Effects of Multiple Endoplasmic Reticulum Stresses on Cytokine Secretion in Macrophage. *Biomol Ther (Seoul),* 20**,** 346-51.

KIM, S., JOE, Y., KIM, H. J., KIM, Y. S., JEONG, S. O., PAE, H. O., RYTER, S. W., SURH, Y. J. & CHUNG, H. T. 2015. Endoplasmic reticulum stress-induced IRE1alpha activation mediates cross-talk of GSK-3beta and XBP-1 to regulate inflammatory cytokine production. *J Immunol,* 194**,** 4498-506.

KLAUSNER, R. D., DONALDSON, J. G. & LIPPINCOTT-SCHWARTZ, J. 1992. Brefeldin A: insights into the control of membrane traffic and organelle structure. *J Cell Biol,* 116**,** 1071-80.

KODUMUDI, K. N., WOAN, K., GILVARY, D. L., SAHAKIAN, E., WEI, S. & DJEU, J. Y. 2010. A novel chemoimmunomodulating property of docetaxel: suppression of myeloid-derived suppressor cells in tumor bearers. *Clin Cancer Res,* 16**,** 4583-94.

KUNIN, V., SOREK, R. & HUGENHOLTZ, P. 2007. Evolutionary conservation of sequence and secondary structures in CRISPR repeats. *Genome Biology,* 8**,** R61.

KUTOMI, G., TAMURA, Y., TANAKA, T., KAJIWARA, T., KUKITA, K., OHMURA, T., SHIMA, H., TAKAMARU, T., SATOMI, F., SUZUKI, Y., TORIGOE, T., SATO, N. & HIRATA, K. 2013. Human endoplasmic reticulum oxidoreductin 1-alpha is a novel predictor for poor prognosis of breast cancer. *Cancer Sci,* 104**,** 1091-6.

LACASSE, E. C., MAHONEY, D. J., CHEUNG, H. H., PLENCHETTE, S., BAIRD, S. & KORNELUK, R. G. 0000. IAP-targeted therapies for cancer. *Oncogene,* 27**,** 6252-6275.

LEE, B. R., CHANG, S. Y., HONG, E. H., KWON, B. E., KIM, H. M., KIM, Y. J., LEE, J., CHO, H. J., CHEON, J. H. & KO, H. J. 2014. Elevated endoplasmic reticulum stress reinforced immunosuppression in the tumor microenvironment via myeloid-derived suppressor cells. *Oncotarget,* 5**,** 12331-45.

LEE, L. F., HASKILL, J. S., MUKAIDA, N., MATSUSHIMA, K. & TING, J. P. 1997. Identification of tumor-specific paclitaxel (Taxol)-responsive regulatory elements in the interleukin-8 promoter. *Mol Cell Biol,* 17**,** 5097-105.

LEE, S. H., SHIN, M. S., KIM, H. S., LEE, H. K., PARK, W. S., KIM, S. Y., LEE, J. H., HAN, S. Y., PARK, J. Y., OH, R. R., KANG, C. S., KIM, K. M., JANG, J. J., NAM, S. W., LEE, J. Y. & YOO, N. J. 2001. Somatic mutations of TRAIL-receptor 1 and TRAIL-receptor 2 genes in non-Hodgkin's lymphoma. *Oncogene,* 20**,** 399-403.

LERNER, A. G., UPTON, J. P., PRAVEEN, P. V., GHOSH, R., NAKAGAWA, Y., IGBARIA, A., SHEN, S., NGUYEN, V., BACKES, B. J., HEIMAN, M., HEINTZ, N., GREENGARD, P., HUI, S., TANG, Q., TRUSINA, A., OAKES, S. A. & PAPA, F. R. 2012. IRE1alpha induces thioredoxin-interacting protein to activate the NLRP3 inflammasome and promote programmed cell death under irremediable ER stress. *Cell Metab,* 16**,** 250-64.

LEVERKUS, M., NEUMANN, M., MENGLING, T., RAUCH, C. T., BROCKER, E. B., KRAMMER, P. H. & WALCZAK, H. 2000. Regulation of tumor necrosis factor-related apoptosis-inducing ligand sensitivity in primary and transformed human keratinocytes. *Cancer Res,* 60**,** 553-9.

LI, C., EGLOFF, A. M., SEN, M., GRANDIS, J. R. & JOHNSON, D. E. 2014. Caspase-8 mutations in head and neck cancer confer resistance to death receptor-mediated apoptosis and enhance migration, invasion, and tumor growth. *Mol Oncol,* 8**,** 1220-30.

LI, L., THOMAS, R. M., SUZUKI, H., DE BRABANDER, J. K., WANG, X. & HARRAN, P. G. 2004. A small molecule Smac mimic potentiates TRAIL-and TNFα-mediated cell death. *Science,* 305**,** 1471-1474.

LI, Q., MA, Z., LIU, Y., KAN, X., WANG, C., SU, B., LI, Y., ZHANG, Y., WANG, P., LUO, Y., NA, D., WANG, L., ZHANG, G., ZHU, X. & WANG, L. 2016. Low doses of paclitaxel enhance liver metastasis of breast cancer cells in the mouse model. *Febs j,* 283**,** 2836-52.

LIAO, P.-C., TAN, S.-K., LIEU, C.-H. & JUNG, H.-K. 2008. Involvement of endoplasmic reticulum in paclitaxel-induced apoptosis. *Journal of Cellular Biochemistry,* 104**,** 1509-1523.

LIAO, Q., FRIESS, H., KLEEFF, J. & BUCHLER, M. W. 2001. Differential expression of TRAIL-R3 and TRAIL-R4 in human pancreatic cancer. *Anticancer Res,* 21**,** 3153-9.

LIU, B., PENG, D., LU, Y., JIN, W. & FAN, Z. 2002. A novel single amino acid deletion caspase-8 mutant in cancer cells that lost proapoptotic activity. *J Biol Chem,* 277**,** 30159-64.

LIU, G., CHEN, Y., QI, F., JIA, L., LU, X. A., HE, T., FU, Y., LI, L. & LUO, Y. 2015. Specific chemotherapeutic agents induce metastatic behaviour through stromal- and tumour-derived cytokine and angiogenic factor signalling. *J Pathol,* 237**,** 190-202.

LONGLEY, D. B., WILSON, T. R., MCEWAN, M., ALLEN, W. L., MCDERMOTT, U., GALLIGAN, L. & JOHNSTON, P. G. 2006. c-FLIP inhibits chemotherapy-induced colorectal cancer cell death. *Oncogene,* 25**,** 838-48.

LOPEZ, J., JOHN, SIDONIE W., TENEV, T., RAUTUREAU, GILLES J. P., HINDS, MARK G., FRANCALANCI, F., WILSON, R., BROEMER, M., SANTORO, MASSIMO M., DAY, CATHERINE L. & MEIER, P. CARD-Mediated Autoinhibition of cIAP1's E3 Ligase Activity Suppresses Cell Proliferation and Migration. *Molecular Cell,* 42**,** 569-583.

LU, J., ZHU, Y., WANG, J., WANG, L., CHEN, Y., CAI, W., YUAN, J. & WANG, X. 2017. Immunogenic chemotherapy sensitizes non-small cell lung cancer to immune checkpoint blockade therapy in preclinical models. *Biomedical Research,* 28.

LU, M., LAWRENCE, D. A., MARSTERS, S., ACOSTA-ALVEAR, D., KIMMIG, P., MENDEZ, A. S., PATON, A. W., PATON, J. C., WALTER, P. & ASHKENAZI, A. 2014a. Opposing unfolded-protein-response signals converge on death receptor 5 to control apoptosis. *Science,* 345**,** 98-101.

LU, Y., LIANG, F. X. & WANG, X. 2014b. A synthetic biology approach identifies the mammalian UPR RNA ligase RtcB. *Mol Cell,* 55**,** 758-70.

MA, Y. & HENDERSHOT, L. M. 2003. The stressful road to antibody secretion. *Nat Immunol,* 4**,** 310-1.

MABUCHI, S., OHMICHI, M., NISHIO, Y., HAYASAKA, T., KIMURA, A., OHTA, T., SAITO, M., KAWAGOE, J., TAKAHASHI, K., YADA-HASHIMOTO, N., SAKATA, M., MOTOYAMA, T., KURACHI, H., TASAKA, K. & MURATA, Y. 2004. Inhibition of NFkappaB increases the efficacy of cisplatin in in vitro and in vivo ovarian cancer models. *J Biol Chem,* 279**,** 23477-85.

MACFARLANE, M., HARPER, N., SNOWDEN, R. T., DYER, M. J., BARNETT, G. A., PRINGLE, J. H. & COHEN, G. M. 2002. Mechanisms of resistance to TRAIL-induced apoptosis in primary B cell chronic lymphocytic leukaemia. *Oncogene,* 21**,** 6809-18.

MAHADEVAN, N. R., FERNANDEZ, A., RODVOLD, J. J., ALMANZA, G. & ZANETTI, M. 2010. Prostate cancer cells undergoing ER stress in vitro and in vivo activate transcription of pro-inflammatory cytokines. *J Inflamm Res,* 3**,** 99-103.

MAKAROVA, K. S., HAFT, D. H., BARRANGOU, R., BROUNS, S. J. J., CHARPENTIER, E., HORVATH, P., MOINEAU, S., MOJICA, F. J. M., WOLF, Y. I., YAKUNIN, A. F., VAN DER OOST, J. & KOONIN, E. V. 2011. Evolution and classification of the CRISPR–Cas systems. *Nat Rev Micro,* 9**,** 467-477.

MAKKER, V., HENSLEY, M. L., ZHOU, Q., IASONOS, A. & AGHAJANIAN, C. A. 2013. Treatment of advanced or recurrent endometrial carcinoma with doxorubicin in patients progressing after paclitaxel/carboplatin: Memorial Sloan-Kettering Cancer Center experience from 1995 to 2009. *Int J Gynecol Cancer,* 23**,** 929-34.

MALI, P., YANG, L., ESVELT, K. M., AACH, J., GUELL, M., DICARLO, J. E., NORVILLE, J. E. & CHURCH, G. M. 2013. RNA-guided human genome engineering via Cas9. *Science,* 339**,** 823-6.

MARCHETTI, P., URIEN, S., CAPPELLINI, G. A., RONZINO, G. & FICORELLA, C. 2002. Weekly administration of paclitaxel: theoretical and clinical basis. *Crit Rev Oncol Hematol,* 44 Suppl**,** S3-13.

MARCINIAK, S. J., YUN, C. Y., OYADOMARI, S., NOVOA, I., ZHANG, Y., JUNGREIS, R., NAGATA, K., HARDING, H. P. & RON, D. 2004. CHOP induces death by promoting protein synthesis and oxidation in the stressed endoplasmic reticulum. *Genes Dev,* 18**,** 3066-77.

MARINI, P., JENDROSSEK, V., DURAND, E., GRUBER, C., BUDACH, W. & BELKA, C. 2003. Molecular requirements for the combined effects of TRAIL and ionising radiation. *Radiother Oncol,* 68**,** 189-98.

MARJON, P. L., BOBROVNIKOVA-MARJON, E. V. & ABCOUWER, S. F. 2004. Expression of the pro-angiogenic factors vascular endothelial growth factor and interleukin-8/CXCL8 by human breast carcinomas is responsive to nutrient deprivation and endoplasmic reticulum stress. *Mol Cancer,* 3**,** 4.

MARKMAN, M. & BOOKMAN, M. A. 2000. Second-Line Treatment of Ovarian Cancer. *The Oncologist,* 5**,** 26-35.

MARSTERS, S. A., SHERIDAN, J. P., PITTI, R. M., HUANG, A., SKUBATCH, M., BALDWIN, D., YUAN, J., GURNEY, A., GODDARD, A. D., GODOWSKI, P. & ASHKENAZI, A. 1997. A novel receptor for Apo2L/TRAIL contains a truncated death domain. *Curr Biol,* 7**,** 1003-6.

MARTIN-PEREZ, R., NIWA, M. & LOPEZ-RIVAS, A. 2012. ER stress sensitizes cells to TRAIL through down-regulation of FLIP and Mcl-1 and PERK-dependent up-regulation of TRAIL-R2. *Apoptosis,* 17**,** 349-63.

MARTIN, S. J. & COTTER, T. G. 1990. Disruption of microtubules induces an endogenous suicide pathway in human leukaemia HL-60 cells. *Cell Proliferation,* 23**,** 545-559.

MASUD, A., MOHAPATRA, A., LAKHANI, S. A., FERRANDINO, A., HAKEM, R. & FLAVELL, R. A. 2007. Endoplasmic reticulum stress-induced death of mouse embryonic fibroblasts requires the intrinsic pathway of apoptosis. *J Biol Chem,* 282**,** 14132-9.

MCARTHUR, H. L. & PAGE, D. B. 2016. Immunotherapy for the treatment of breast cancer: checkpoint blockade, cancer vaccines, and future directions in combination immunotherapy. *Clin Adv Hematol Oncol,* 14**,** 922-933.

MCCULLOUGH, K. D., MARTINDALE, J. L., KLOTZ, L. O., AW, T. Y. & HOLBROOK, N. J. 2001. Gadd153 sensitizes cells to endoplasmic reticulum stress by down-regulating Bcl2 and perturbing the cellular redox state. *Mol Cell Biol,* 21**,** 1249-59.

MENG, R. D. & EL-DEIRY, W. S. 2001a. p53-independent upregulation of KILLER/DR5 TRAIL receptor expression by glucocorticoids and interferon-gamma. *Exp Cell Res,* 262**,** 154-69.

MENG, R. D. & EL-DEIRY, W. S. 2001b. p53-independent upregulation of KILLER/DR5 TRAIL receptor expression by glucocorticoids and interferon-γ. *Experimental cell research,* 262**,** 154-169.

MIN, S. Y., BYEON, H. J., LEE, C., SEO, J., LEE, E. S., SHIN, B. S., CHOI, H. G., LEE, K. C. & YOUN, Y. S. 2015. Facile one-pot formulation of TRAIL-embedded paclitaxel-bound albumin nanoparticles for the treatment of pancreatic cancer. *Int J Pharm,* 494**,** 506-15.

MOJICA, F. J., DIEZ-VILLASENOR, C., GARCIA-MARTINEZ, J. & ALMENDROS, C. 2009. Short motif sequences determine the targets of the prokaryotic CRISPR defence system. *Microbiology,* 155**,** 733-40.

MOJICA, F. J., DIEZ-VILLASENOR, C., GARCIA-MARTINEZ, J. & SORIA, E. 2005. Intervening sequences of regularly spaced prokaryotic repeats derive from foreign genetic elements. *J Mol Evol,* 60**,** 174-82.

MONGKOLSAPAYA, J., GRIMES, J. M., CHEN, N., XU, X. N., STUART, D. I., JONES, E. Y. & SCREATON, G. R. 1999. Structure of the TRAIL-DR5 complex reveals mechanisms conferring specificity in apoptotic initiation. *Nat Struct Biol,* 6**,** 1048-53.

MONLEON, I., MARTINEZ-LORENZO, M. J., MONTEAGUDO, L., LASIERRA, P., TAULES, M., ITURRALDE, M., PINEIRO, A., LARRAD, L., ALAVA, M. A., NAVAL, J. & ANEL, A. 2001. Differential secretion of Fas ligand- or APO2 ligand/TNF-related apoptosis-inducing ligand-carrying microvesicles during activation-induced death of human T cells. *J Immunol,* 167**,** 6736-44.

MOORE, K. & HOLLIEN, J. 2015. Ire1-mediated decay in mammalian cells relies on mRNA sequence, structure, and translational status. *Mol Biol Cell,* 26**,** 2873-84.

MORANGE, M. 2015. What history tells us XXXVII. CRISPR-Cas: The discovery of an immune system in prokaryotes. *J Biosci,* 40**,** 221-3.

MUSACCHIO, A. & SALMON, E. D. 2007. The spindle-assembly checkpoint in space and time. *Nat Rev Mol Cell Biol,* 8**,** 379-393.

MUZIO, M., STOCKWELL, B. R., STENNICKE, H. R., SALVESEN, G. S. & DIXIT, V. M. 1998. An Induced Proximity Model for Caspase-8 Activation. *Journal of Biological Chemistry,* 273**,** 2926-2930.

NABHOLTZ, J. M., SENN, H. J., BEZWODA, W. R., MELNYCHUK, D., DESCHENES, L., DOUMA, J., VANDENBERG, T. A., RAPOPORT, B., ROSSO, R., TRILLET-LENOIR, V., DRBAL, J., MOLINO, A., NORTIER, J. W., RICHEL, D. J., NAGYKALNAI, T., SIEDLECKI, P., WILKING, N., GENOT, J. Y., HUPPERETS, P. S., PANNUTI, F., SKARLOS, D., TOMIAK, E. M., MURAWSKY, M., ALAKL, M., AAPRO, M. & ET AL. 1999. Prospective randomized trial of docetaxel versus mitomycin plus vinblastine in patients with metastatic breast cancer progressing despite previous anthracycline-containing chemotherapy. 304 Study Group. *J Clin Oncol,* 17**,** 1413-24.

NAGANE, M., PAN, G., WEDDLE, J. J., DIXIT, V. M., CAVENEE, W. K. & HUANG, H. J. 2000. Increased death receptor 5 expression by chemotherapeutic agents in human gliomas causes synergistic cytotoxicity with tumor necrosis factor-related apoptosis-inducing ligand in vitro and in vivo. *Cancer Res,* 60**,** 847-53.

NI, R., TOMITA, Y., MATSUDA, K., ICHIHARA, A., ISHIMURA, K., OGASAWARA, J. & NAGATA, S. 1994. Fas-mediated apoptosis in primary cultured mouse hepatocytes. *Exp Cell Res,* 215**,** 332-7.

NICHOLSON, D. W. 1999. Caspase structure, proteolytic substrates, and function during apoptotic cell death. *Cell Death Differ,* 6**,** 1028-42.

NIETO, M. A., HUANG, RUBY Y.-J., JACKSON, REBECCA A. & THIERY, JEAN P. EMT: 2016. *Cell,* 166**,** 21-45.

NIMMANAPALLI, R., PERKINS, C. L., ORLANDO, M., O'BRYAN, E., NGUYEN, D. & BHALLA, K. N. 2001. Pretreatment with paclitaxel enhances apo-2 ligand/tumor necrosis factor-related apoptosis-inducing ligand-induced apoptosis of prostate cancer cells by inducing death receptors 4 and 5 protein levels. *Cancer Res,* 61**,** 759-63.

NISHIMASU, H., RAN, F. A., HSU, P. D., KONERMANN, S., SHEHATA, S. I., DOHMAE, N., ISHITANI, R., ZHANG, F. & NUREKI, O. 2014. Crystal structure of Cas9 in complex with guide RNA and target DNA. *Cell,* 156**,** 935-49.

NISHIMURA, Y., HIRABAYASHI, Y., MATSUZAKI, Y., MUSETTE, P., ISHII, A., NAKAUCHI, H., INOUE, T. & YONEHARA, S. 1997. In vivo analysis of Fas antigen-mediated apoptosis: effects of agonistic anti-mouse Fas mAb on thymus, spleen and liver. *Int Immunol,* 9**,** 307-16.

NORBURY, C. J. & HICKSON, I. D. 2001. Cellular responses to DNA damage. *Annu Rev Pharmacol Toxicol,* 41**,** 367-401.

NOTTE, A., REBUCCI, M., FRANSOLET, M., ROEGIERS, E., GENIN, M., TELLIER, C., WATILLON, K., FATTACCIOLI, A., ARNOULD, T. & MICHIELS, C. 2015. Taxol-induced unfolded protein response activation in breast cancer cells exposed to hypoxia: ATF4 activation regulates autophagy and inhibits apoptosis. *Int J Biochem Cell Biol,* 62**,** 1-14.

O/' REILLY, L. A., TAI, L., LEE, L., KRUSE, E. A., GRABOW, S., FAIRLIE, W. D., HAYNES, N. M., TARLINTON, D. M., ZHANG, J.-G., BELZ, G. T., SMYTH, M. J., BOUILLET, P., ROBB, L. & STRASSER, A. 2009. Membrane-bound Fas ligand only is essential for Fas-induced apoptosis. *Nature,* 461**,** 659-663.

OBENG, E. A., CARLSON, L. M., GUTMAN, D. M., HARRINGTON, W. J., JR., LEE, K. P. & BOISE, L. H. 2006. Proteasome inhibitors induce a terminal unfolded protein response in multiple myeloma cells. *Blood,* 107**,** 4907-16.

OGASAWARA, J., WATANABE-FUKUNAGA, R., ADACHI, M., MATSUZAWA, A., KASUGAI, T., KITAMURA, Y., ITOH, N., SUDA, T. & NAGATA, S. 1993. Lethal effect of the anti-Fas antibody in mice. *Nature,* 364**,** 806-9.

OHTA, T., OHMICHI, M., HAYASAKA, T., MABUCHI, S., SAITOH, M., KAWAGOE, J., TAKAHASHI, K., IGARASHI, H., DU, B., DOSHIDA, M., MIREI, I. G., MOTOYAMA, T., TASAKA, K. & KURACHI, H. 2006. Inhibition of phosphatidylinositol 3-kinase increases efficacy of cisplatin in in vivo ovarian cancer models. *Endocrinology,* 147**,** 1761-9.

OIKONOMOU, E., KOSMIDOU, V., KATSELI, A., KOTHONIDIS, K., MOURTZOUKOU, D., KONTOGEORGOS, G., ANDERA, L., ZOGRAFOS, G. & PINTZAS, A. 2009. TRAIL receptor upregulation and the implication of KRAS/BRAF mutations in human colon cancer tumors. *Int J Cancer,* 125**,** 2127-35.

OLDEN, K., PRATT, R. M., JAWORSKI, C. & YAMADA, K. M. 1979. Evidence for role of glycoprotein carbohydrates in membrane transport: specific inhibition by tunicamycin. *Proc Natl Acad Sci U S A,* 76**,** 791-5.

OZOREN, N., FISHER, M. J., KIM, K., LIU, C. X., GENIN, A., SHIFMAN, Y., DICKER, D. T., SPINNER, N. B., LISITSYN, N. A. & EL-DEIRY, W. S. 2000. Homozygous deletion of the death receptor DR4 gene in a nasopharyngeal cancer cell line is associated with TRAIL resistance. *Int J Oncol,* 16**,** 917-25.

PAI, S. I., WU, G. S., OZOREN, N., WU, L., JEN, J., SIDRANSKY, D. & EL-DEIRY, W. S. 1998. Rare loss-of-function mutation of a death receptor gene in head and neck cancer. *Cancer Res,* 58**,** 3513-8.

PAL, S., SHANKAR, B. S. & SAINIS, K. B. 2013. Cytokines from the tumor microenvironment modulate sirtinol cytotoxicity in A549 lung carcinoma cells. *Cytokine,* 64**,** 196-207.

PAN, G., O'ROURKE, K., CHINNAIYAN, A. M., GENTZ, R., EBNER, R., NI, J. & DIXIT, V. M. 1997. The receptor for the cytotoxic ligand TRAIL. *Science,* 276**,** 111-3.

PANAYOTOPOULOU, E. G., MULLER, A. K., BORRIES, M., BUSCH, H., HU, G. & LEV, S. 2017. Targeting of apoptotic pathways by SMAC or BH3 mimetics distinctly sensitizes paclitaxel-resistant triple negative breast cancer cells. *Oncotarget*.

PARK, S., KANG, S., CHEN, X., KIM, E. J., KIM, J., KIM, N., KIM, J. & JIN, M. M. 2013. Tumor suppression via paclitaxel-loaded drug carriers that target inflammation marker upregulated in tumor vasculature and macrophages. *Biomaterials,* 34**,** 598-605.

PELHAM, H. R. 1991. Multiple targets for brefeldin A. *Cell,* 67**,** 449-51.

PENSON, R. T., KRONISH, K., DUAN, Z., FELLER, A. J., STARK, P., COOK, S. E., DUSKA, L. R., FULLER, A. F., GOODMAN, A. K., NIKRUI, N., MACNEILL, K. M., MATULONIS, U. A., PREFFER, F. I. & SEIDEN, M. V. 2000. Cytokines IL-1β, IL-2, IL-6, IL-8, MCP-1, GM-CSF and TNFα in patients with epithelial ovarian cancer and their relationship to treatment with paclitaxel. *International Journal of Gynecological Cancer,* 10**,** 33-41.

PFIRSCHKE, C., ENGBLOM, C., RICKELT, S., CORTEZ-RETAMOZO, V., GARRIS, C., PUCCI, F., YAMAZAKI, T., POIRIER-COLAME, V., NEWTON, A., REDOUANE, Y., LIN, Y.-J., WOJTKIEWICZ, G., IWAMOTO, Y., MINO-KENUDSON, M., HUYNH, T. G., HYNES, R. O., FREEMAN, G. J., KROEMER, G., ZITVOGEL, L., WEISSLEDER, R. & PITTET, M. J. Immunogenic Chemotherapy Sensitizes Tumors to Checkpoint Blockade Therapy. *Immunity,* 44**,** 343-354.

PITTI, R. M., MARSTERS, S. A., RUPPERT, S., DONAHUE, C. J., MOORE, A. & ASHKENAZI, A. 1996. Induction of apoptosis by Apo-2 ligand, a new member of the tumor necrosis factor cytokine family. *J Biol Chem,* 271**,** 12687-90.

POURCEL, C., SALVIGNOL, G. & VERGNAUD, G. 2005. CRISPR elements in Yersinia pestis acquire new repeats by preferential uptake of bacteriophage DNA, and provide additional tools for evolutionary studies. *Microbiology,* 151**,** 653-63.

PROBST, B. L., LIU, L., RAMESH, V., LI, L., SUN, H., MINNA, J. D. & WANG, L. 2010. Smac mimetics increase cancer cell response to chemotherapeutics in a TNF-alpha-dependent manner. *Cell Death Differ,* 17**,** 1645-54.

PUSZTAI, L., MENDOZA, T. R., REUBEN, J. M., MARTINEZ, M. M., WILLEY, J. S., LARA, J., SYED, A., FRITSCHE, H. A., BRUERA, E., BOOSER, D., VALERO, V., ARUN, B., IBRAHIM, N., RIVERA, E., ROYCE, M., CLEELAND, C. S. & HORTOBAGYI, G. N. 2004. Changes in plasma levels of inflammatory cytokines in response to paclitaxel chemotherapy. *Cytokine,* 25**,** 94-102.

RAMIREZ-PEINADO, S., ALCAZAR-LIMONES, F., LAGARES-TENA, L., EL MJIYAD, N., CARO-MALDONADO, A., TIRADO, O. M. & MUNOZ-PINEDO, C. 2011. 2-deoxyglucose induces Noxa-dependent apoptosis in alveolar rhabdomyosarcoma. *Cancer Res,* 71**,** 6796-806.

RASMUSSEN, U., BROOGGER CHRISTENSEN, S. & SANDBERG, F. 1978. Thapsigargine and thapsigargicine, two new histamine liberators from Thapsia garganica L. *Acta Pharm Suec,* 15**,** 133-40.

RECK, M., KRZAKOWSKI, M., CHMIELOWSKA, E., SEBASTIAN, M., HADLER, D., FOX, T., WANG, Q., GREENBERG, J., BECKMAN, R. A. & VON PAWEL, J. 2013. A randomized, double-blind, placebo-controlled phase 2 study of tigatuzumab (CS-1008) in combination with carboplatin/paclitaxel in patients with chemotherapy-naive metastatic/unresectable non-small cell lung cancer. *Lung Cancer,* 82**,** 441-8.

REIMERTZ, C., KOGEL, D., RAMI, A., CHITTENDEN, T. & PREHN, J. H. 2003. Gene expression during ER stress-induced apoptosis in neurons: induction of the BH3-only protein Bbc3/PUMA and activation of the mitochondrial apoptosis pathway. *J Cell Biol,* 162**,** 587-97.

ROBERTS, N. J., ZHOU, S., DIAZ, L. A., JR. & HOLDHOFF, M. 2011. Systemic use of tumor necrosis factor alpha as an anticancer agent. *Oncotarget,* 2**,** 739-51.

RON, D. & WALTER, P. 2007. Signal integration in the endoplasmic reticulum unfolded protein response. *Nat Rev Mol Cell Biol,* 8**,** 519-29.

ROUSCHOP, K. M., DUBOIS, L. J., KEULERS, T. G., VAN DEN BEUCKEN, T., LAMBIN, P., BUSSINK, J., VAN DER KOGEL, A. J., KORITZINSKY, M. & WOUTERS, B. G. 2013. PERK/eIF2α signaling protects therapy resistant hypoxic cells through induction of glutathione synthesis and protection against ROS. *Proceedings of the National Academy of Sciences,* 110**,** 4622-4627.

SAGARA, Y. & INESI, G. 1991. Inhibition of the sarcoplasmic reticulum Ca2+ transport ATPase by thapsigargin at subnanomolar concentrations. *J Biol Chem,* 266**,** 13503-6.

SAMUEL, T., WELSH, K., LOBER, T., TOGO, S. H., ZAPATA, J. M. & REED, J. C. 2006. Distinct BIR Domains of cIAP1 Mediate Binding to and Ubiquitination of Tumor Necrosis Factor Receptor-associated Factor 2 and Second Mitochondrial Activator of Caspases. *Journal of Biological Chemistry,* 281**,** 1080-1090.

SAVELJEVA, S., MC LAUGHLIN, S. L., VANDENABEELE, P. & SAMALI, A. 2015. Endoplasmic reticulum stress induces ligand-independent TNFR1-mediated necroptosis in L929 cells. 6**,** e1587.

SCAIEWICZ, V., NAHMIAS, A., CHUNG, R. T., MUELLER, T., TIROSH, B. & SHIBOLET, O. 2013. CCAAT/enhancer-binding protein homologous (CHOP) protein promotes carcinogenesis in the DEN-induced hepatocellular carcinoma model. *PLoS One,* 8**,** e81065.

SCHIFF, P. B., FANT, J. & HORWITZ, S. B. 1979. Promotion of microtubule assembly in vitro by taxol. *Nature,* 277**,** 665-667.

SCHIFF, P. B. & HORWITZ, S. B. 1980. Taxol stabilizes microtubules in mouse fibroblast cells. *Proc Natl Acad Sci U S A,* 77**,** 1561-5.

SCHMUKLE, A. C. & WALCZAK, H. 2012. No one can whistle a symphony alone - how different ubiquitin linkages cooperate to orchestrate NF-kappaB activity. *J Cell Sci,* 125**,** 549-59.

SCHREIBER, R. D., OLD, L. J. & SMYTH, M. J. 2011. Cancer immunoediting: integrating immunity's roles in cancer suppression and promotion. *Science,* 331**,** 1565-70.

SCHWARZ, D. S. & BLOWER, M. D. 2016. The endoplasmic reticulum: structure, function and response to cellular signaling. *Cellular and Molecular Life Sciences,* 73**,** 79-94.

SEVKO, A., MICHELS, T., VROHLINGS, M., UMANSKY, L., BECKHOVE, P., KATO, M., SHURIN, G. V., SHURIN, M. R. & UMANSKY, V. 2013. Antitumor Effect of Paclitaxel Is Mediated by Inhibition of Myeloid-Derived Suppressor Cells and Chronic Inflammation in the Spontaneous Melanoma Model. *The Journal of Immunology,* 190**,** 2464-2471.

SHAO, R. G., SHIMIZU, T. & POMMIER, Y. 1996. Brefeldin A is a potent inducer of apoptosis in human cancer cells independently of p53. *Exp Cell Res,* 227**,** 190-6.

SHEIKH, M. S., HUANG, Y., FERNANDEZ-SALAS, E. A., EL-DEIRY, W. S., FRIESS, H., AMUNDSON, S., YIN, J., MELTZER, S. J., HOLBROOK, N. J. & FORNACE, A. J., JR. 1999. The antiapoptotic decoy receptor TRID/TRAIL-R3 is a p53-regulated DNA damage-inducible gene that is overexpressed in primary tumors of the gastrointestinal tract. *Oncogene,* 18**,** 4153-9.

SHEN, J., CHEN, X., HENDERSHOT, L. & PRYWES, R. 2002. ER stress regulation of ATF6 localization by dissociation of BiP/GRP78 binding and unmasking of Golgi localization signals. *Dev Cell,* 3**,** 99-111.

SHERIDAN, J. P., MARSTERS, S. A., PITTI, R. M., GURNEY, A., SKUBATCH, M., BALDWIN, D., RAMAKRISHNAN, L., GRAY, C. L., BAKER, K., WOOD, W. I., GODDARD, A. D., GODOWSKI, P. & ASHKENAZI, A. 1997. Control of TRAIL-induced apoptosis by a family of signaling and decoy receptors. *Science,* 277**,** 818-21.

SHOULDERS, M. D., RYNO, L. M., GENEREUX, J. C., MORESCO, J. J., TU, P. G., WU, C., YATES, J. R., 3RD, SU, A. I., KELLY, J. W. & WISEMAN, R. L. 2013. Stress-independent activation of XBP1s and/or ATF6 reveals three functionally diverse ER proteostasis environments. *Cell Rep,* 3**,** 1279-92.

SHREE, T., OLSON, O. C., ELIE, B. T., KESTER, J. C., GARFALL, A. L., SIMPSON, K., BELL-MCGUINN, K. M., ZABOR, E. C., BROGI, E. & JOYCE, J. A. 2011. Macrophages and cathepsin proteases blunt chemotherapeutic response in breast cancer. *Genes Dev,* 25**,** 2465-79.

SHRIVASTAV, M., DE HARO, L. P. & NICKOLOFF, J. A. 2008. Regulation of DNA double-strand break repair pathway choice. *Cell Res,* 18**,** 134-147.

SHTIL, A. A., MANDLEKAR, S., YU, R., WALTER, R. J., HAGEN, K., TAN, T. H., RONINSON, I. B. & KONG, A. N. 1999. Differential regulation of mitogen-activated protein kinases by microtubule-binding agents in human breast cancer cells. *Oncogene,* 18**,** 377-84.

SHURIN, G. V., TOURKOVA, I. L., KANENO, R. & SHURIN, M. R. 2009. Chemotherapeutic agents in noncytotoxic concentrations increase antigen presentation by dendritic cells via an IL-12-dependent mechanism. *J Immunol,* 183**,** 137-44.

SIEGMUND, D., LANG, I. & WAJANT, H. 2016. Cell death-independent activities of the death receptors CD95, TRAILR1, and TRAILR2. *Febs j*.

SILKE, J. 2011. The regulation of TNF signalling: what a tangled web we weave. *Curr Opin Immunol,* 23**,** 620-6.

SINGH, S., NANNURU, K. C., SADANANDAM, A., VARNEY, M. L. & SINGH, R. K. 2009. CXCR1 and CXCR2 enhances human melanoma tumourigenesis, growth and invasion. *Br J Cancer,* 100**,** 1638-46.

SLEE, E. A., ADRAIN, C. & MARTIN, S. J. 1999. Serial killers: ordering caspase activation events in apoptosis. *Cell Death Differ,* 6**,** 1067-74.

SMITH, M. H., PLOEGH, H. L. & WEISSMAN, J. S. 2011. Road to ruin: targeting proteins for degradation in the endoplasmic reticulum. *Science,* 334**,** 1086-90.

SOLIMAN, H. H. 2017. nab-Paclitaxel as a potential partner with checkpoint inhibitors in solid tumors. *Onco Targets Ther,* 10**,** 101-112.

SORIA, J. C., MARK, Z., ZATLOUKAL, P., SZIMA, B., ALBERT, I., JUHASZ, E., PUJOL, J. L., KOZIELSKI, J., BAKER, N., SMETHURST, D., HEI, Y. J., ASHKENAZI, A., STERN, H., AMLER, L., PAN, Y. & BLACKHALL, F. 2011. Randomized phase II study of dulanermin in combination with

paclitaxel, carboplatin, and bevacizumab in advanced non-small-cell lung cancer. *J Clin Oncol,* 29**,** 4442-51.

SOUNG, Y. H., LEE, J. W., KIM, S. Y., JANG, J., PARK, Y. G., PARK, W. S., NAM, S. W., LEE, J. Y., YOO, N. J. & LEE, S. H. 2005. CASPASE-8 gene is inactivated by somatic mutations in gastric carcinomas. *Cancer Res,* 65**,** 815-21.

SOUNG, Y. H., LEE, J. W., KIM, S. Y., SUNG, Y. J., PARK, W. S., NAM, S. W., KIM, S. H., LEE, J. Y., YOO, N. J. & LEE, S. H. 2004. Caspase-8 gene is frequently inactivated by the frameshift somatic mutation 1225[lowbar]1226delTG in hepatocellular carcinomas. *Oncogene,* 24**,** 141-147.

STERNBERG, S. H., REDDING, S., JINEK, M., GREENE, E. C. & DOUDNA, J. A. 2014. DNA interrogation by the CRISPR RNA-guided endonuclease Cas9. *Nature,* 507**,** 62-67.

SUN, H., NIKOLOVSKA-COLESKA, Z., YANG, C. Y., QIAN, D., LU, J., QIU, S., BAI, L., PENG, Y., CAI, Q. & WANG, S. 2008. Design of small-molecule peptidic and nonpeptidic Smac mimetics. *Acc Chem Res,* 41**,** 1264-77.

SWART, M., VERBRUGGE, I. & BELTMAN, J. B. 2016. Combination Approaches with Immune-Checkpoint Blockade in Cancer Therapy. *Front Oncol,* 6**,** 233.

TAKATSUKI, A., KOHNO, K. & TAMURA, G. 1975. Inhibition of Biosynthesis of Polyisoprenol Sugars in Chick Embryo Microsomes by Tunicamycin. *Agricultural and Biological Chemistry,* 39**,** 2089-2091.

TAKATSUKI, A. & TAMURA, G. 1971. Tunicamycin, a new antibiotic. II. Some biological properties of the antiviral activity of tunicamycin. *J Antibiot (Tokyo),* 24**,** 224-31.

TAKEDA, K., STAGG, J., YAGITA, H., OKUMURA, K. & SMYTH, M. J. 0000. Targeting death-inducing receptors in cancer therapy. *Oncogene,* 26**,** 3745-3757.

TAMURA, G., ANDO, K., SUZUKI, S., TAKATSUKI, A. & ARIMA, K. 1968. Antiviral activity of brefeldin A and verrugarin A. *The Journal of antibiotics,* 21**,** 160-161.

TAYLOR, R. C., CULLEN, S. P. & MARTIN, S. J. 2008. Apoptosis: controlled demolition at the cellular level. *Nat Rev Mol Cell Biol,* 9**,** 231-241.

TENEV, T., BIANCHI, K., DARDING, M., BROEMER, M., LANGLAIS, C., WALLBERG, F., ZACHARIOU, A., LOPEZ, J., MACFARLANE, M., CAIN, K. & MEIER, P. 2011. The Ripoptosome, a signaling platform that assembles in response to genotoxic stress and loss of IAPs. *Mol Cell,* 43**,** 432-48.

TERLIZZI, M., DI CRESCENZO, V. G., PERILLO, G., GALDERISI, A., PINTO, A. & SORRENTINO, R. 2015. Pharmacological inhibition of caspase-8 limits lung tumour outgrowth. *Br J Pharmacol,* 172**,** 3917-28.

THASTRUP, O., CULLEN, P. J., DROBAK, B. K., HANLEY, M. R. & DAWSON, A. P. 1990. Thapsigargin, a tumor promoter, discharges intracellular Ca2+ stores by specific inhibition of the endoplasmic reticulum Ca2(+)-ATPase. *Proc Natl Acad Sci U S A,* 87**,** 2466-70.

THORNBERRY, N. A. & LAZEBNIK, Y. 1998. Caspases: enemies within. *Science,* 281**,** 1312-6.

TIAN, A., WILSON, G. S., LIE, S., WU, G., HU, Z., HEBBARD, L., DUAN, W., GEORGE, J. & QIAO, L. 2014. Synergistic effects of IAP inhibitor LCL161 and paclitaxel on hepatocellular carcinoma cells. *Cancer Lett,* 351**,** 232-41.

TKACZ, J. S. & LAMPEN, J. O. 1975. Tunicamycin inhibition of polyisoprenyl N-acetylglucosaminyl pyrophosphate formation in calf-liver microsomes. *Biochemical and biophysical research communications,* 65**,** 248-257.

TOMAR, D., PRAJAPATI, P., SRIPADA, L., SINGH, K., SINGH, R., SINGH, A. K. & SINGH, R. 2013. TRIM13 regulates caspase-8 ubiquitination, translocation to autophagosomes and activation during ER stress induced cell death. *Biochim Biophys Acta,* 1833**,** 3134-44.

TOPALIAN, S. L., HODI, F. S., BRAHMER, J. R., GETTINGER, S. N., SMITH, D. C., MCDERMOTT, D. F., POWDERLY, J. D., CARVAJAL, R. D., SOSMAN, J. A., ATKINS, M. B., LEMING, P. D., SPIGEL, D. R., ANTONIA, S. J., HORN, L., DRAKE, C. G., PARDOLL, D. M., CHEN, L., SHARFMAN, W. H., ANDERS, R. A., TAUBE, J. M., MCMILLER, T. L., XU, H., KORMAN, A.

J., JURE-KUNKEL, M., AGRAWAL, S., MCDONALD, D., KOLLIA, G. D., GUPTA, A., WIGGINTON, J. M. & SZNOL, M. 2012. Safety, Activity, and Immune Correlates of Anti–PD-1 Antibody in Cancer. *New England Journal of Medicine,* 366**,** 2443-2454.

TOSTE, P. A., NGUYEN, A. H., KADERA, B. E., DUONG, M., WU, N., GAWLAS, I., TRAN, L. M., BIKHCHANDANI, M., LI, L., PATEL, S. G., DAWSON, D. W. & DONAHUE, T. R. 2016. Chemotherapy-Induced Inflammatory Gene Signature and Protumorigenic Phenotype in Pancreatic CAFs via Stress-Associated MAPK. *Mol Cancer Res,* 14**,** 437-47.

TRACEY, K. J., LOWRY, S. F. & CERAMI, A. 1988. Cachetin/TNF-alpha in septic shock and septic adult respiratory distress syndrome. *Am Rev Respir Dis,* 138**,** 1377-9.

TRACEY, K. J., LOWRY, S. F., FAHEY, T. J., 3RD, ALBERT, J. D., FONG, Y., HESSE, D., BEUTLER, B., MANOGUE, K. R., CALVANO, S., WEI, H. & ET AL. 1987. Cachectin/tumor necrosis factor induces lethal shock and stress hormone responses in the dog. *Surg Gynecol Obstet,* 164**,** 415-22.

TRAUTH, B. C., KLAS, C., PETERS, A. M., MATZKU, S., MOLLER, P., FALK, W., DEBATIN, K. M. & KRAMMER, P. H. 1989. Monoclonal antibody-mediated tumor regression by induction of apoptosis. *Science,* 245**,** 301-5.

URANO, F., WANG, X., BERTOLOTTI, A., ZHANG, Y., CHUNG, P., HARDING, H. P. & RON, D. 2000. Coupling of stress in the ER to activation of JNK protein kinases by transmembrane protein kinase IRE1. *Science,* 287**,** 664-6.

VAN DER OOST, J., JORE, M. M., WESTRA, E. R., LUNDGREN, M. & BROUNS, S. J. J. CRISPR-based adaptive and heritable immunity in prokaryotes. *Trends in Biochemical Sciences,* 34**,** 401-407.

VARFOLOMEEV, E., MAECKER, H., SHARP, D., LAWRENCE, D., RENZ, M., VUCIC, D. & ASHKENAZI, A. 2005. Molecular Determinants of Kinase Pathway Activation by Apo2 Ligand/Tumor Necrosis Factor-related Apoptosis-inducing Ligand. *Journal of Biological Chemistry,* 280**,** 40599-40608.

VARFOLOMEEV, E., WAYSON, S. M., DIXIT, V. M., FAIRBROTHER, W. J. & VUCIC, D. 2006. The Inhibitor of Apoptosis Protein Fusion c-IAP2·MALT1 Stimulates NF-κB Activation Independently of TRAF1 AND TRAF2. *Journal of Biological Chemistry,* 281**,** 29022-29029.

VERFAILLIE, T., VAN VLIET, A., GARG, A. D., DEWAELE, M., RUBIO, N., GUPTA, S., DE WITTE, P., SAMALI, A. & AGOSTINIS, P. 2013. Pro-apoptotic signaling induced by photo-oxidative ER stress is amplified by Noxa, not Bim. *Biochem Biophys Res Commun,* 438**,** 500-6.

VERHAGEN, A. M., EKERT, P. G., PAKUSCH, M., SILKE, J., CONNOLLY, L. M., REID, G. E., MORITZ, R. L., SIMPSON, R. J. & VAUX, D. L. 2000. Identification of DIABLO, a mammalian protein that promotes apoptosis by binding to and antagonizing IAP proteins. *Cell,* 102**,** 43-53.

VERHAGEN, A. M., KRATINA, T. K., HAWKINS, C. J., SILKE, J., EKERT, P. G. & VAUX, D. L. 2006. Identification of mammalian mitochondrial proteins that interact with IAPs via N-terminal IAP binding motifs. *Cell Death Differ,* 14**,** 348-357.

VOLK, L. D., FLISTER, M. J., BIVENS, C. M., STUTZMAN, A., DESAI, N., TRIEU, V. & RAN, S. 2008. Nab-paclitaxel Efficacy in the Orthotopic Model of Human Breast Cancer Is Significantly Enhanced By Concurrent Anti-Vascular Endothelial Growth Factor A Therapy. *Neoplasia,* 10**,** 613-23.

VOLMER, R., VAN DER PLOEG, K. & RON, D. 2013. Membrane lipid saturation activates endoplasmic reticulum unfolded protein response transducers through their transmembrane domains. *Proc Natl Acad Sci U S A,* 110**,** 4628-33.

VON PAWEL, J., HARVEY, J. H., SPIGEL, D. R., DEDIU, M., RECK, M., CEBOTARU, C. L., HUMPHREYS, R. C., GRIBBIN, M. J., FOX, N. L. & CAMIDGE, D. R. 2014. Phase II trial of mapatumumab, a fully human agonist monoclonal antibody to tumor necrosis factor-related apoptosis-inducing ligand receptor 1 (TRAIL-R1), in combination with paclitaxel and carboplatin in patients with advanced non-small-cell lung cancer. *Clin Lung Cancer,* 15**,** 188-196.e2.

VON KARSTEDT, S., CONTI, A., NOBIS, M., MONTINARO, A., HARTWIG, T., LEMKE, J., LEGLER, K., ANNEWANTER, F., CAMPBELL, ANDREW D., TARABORRELLI, L., GROSSE-WILDE, A., COY, JOHANNES F., EL-BAHRAWY, MONA A., BERGMANN, F., KOSCHNY, R., WERNER, J., GANTEN, TOM M., SCHWEIGER, T., HOETZENECKER, K., KENESSEY, I., HEGEDÜS, B., BERGMANN, M., HAUSER, C., EGBERTS, J.-H., BECKER, T., RÖCKEN, C., KALTHOFF, H., TRAUZOLD, A., ANDERSON, KURT I., SANSOM, OWEN J. & WALCZAK, H. Cancer Cell-Autonomous TRAIL-R Signaling Promotes KRAS-Driven Cancer Progression, Invasion, and Metastasis. *Cancer Cell,* 27**,** 561-573.

VYAS, D., LAPUT, G. & VYAS, A. K. 2014. Chemotherapy-enhanced inflammation may lead to the failure of therapy and metastasis. *Onco Targets Ther,* 7**,** 1015-23.

WAGNER, K. W., PUNNOOSE, E. A., JANUARIO, T., LAWRENCE, D. A., PITTI, R. M., LANCASTER, K., LEE, D., VON GOETZ, M., YEE, S. F., TOTPAL, K., HUW, L., KATTA, V., CAVET, G., HYMOWITZ, S. G., AMLER, L. & ASHKENAZI, A. 2007. Death-receptor O-glycosylation controls tumor-cell sensitivity to the proapoptotic ligand Apo2L/TRAIL. *Nat Med,* 13**,** 1070-7.

WALCZAK, H. 2011. TNF and ubiquitin at the crossroads of gene activation, cell death, inflammation, and cancer. *Immunological Reviews,* 244**,** 9-28.

WALCZAK, H., DEGLI-ESPOSTI, M. A., JOHNSON, R. S., SMOLAK, P. J., WAUGH, J. Y., BOIANI, N., TIMOUR, M. S., GERHART, M. J., SCHOOLEY, K. A., SMITH, C. A., GOODWIN, R. G. & RAUCH, C. T. 1997. TRAIL-R2: a novel apoptosis-mediating receptor for TRAIL. *Embo j,* 16**,** 5386-97.

WALCZAK, H., MILLER, R. E., ARIAIL, K., GLINIAK, B., GRIFFITH, T. S., KUBIN, M., CHIN, W., JONES, J., WOODWARD, A., LE, T., SMITH, C., SMOLAK, P., GOODWIN, R. G., RAUCH, C. T., SCHUH, J. C. & LYNCH, D. H. 1999. Tumoricidal activity of tumor necrosis factor-related apoptosis-inducing ligand in vivo. *Nat Med,* 5**,** 157-63.

WALTER, P. & RON, D. 2011. The unfolded protein response: from stress pathway to homeostatic regulation. *Science,* 334**,** 1081-6.

WANG, B., HENDRICKS, D. T., WAMUNYOKOLI, F. & PARKER, M. I. 2006. A growth-related oncogene/CXC chemokine receptor 2 autocrine loop contributes to cellular proliferation in esophageal cancer. *Cancer Res,* 66**,** 3071-7.

WANG, M. & KAUFMAN, R. J. 2014. The impact of the endoplasmic reticulum protein-folding environment on cancer development. *Nat Rev Cancer,* 14**,** 581-97.

WANG, S. & EL-DEIRY, W. S. 2003. Requirement of p53 targets in chemosensitization of colonic carcinoma to death ligand therapy. *Proc Natl Acad Sci U S A,* 100**,** 15095-100.

WANG, T. H., WANG, H. S. & SOONG, Y. K. 2000. Paclitaxel-induced cell death. *Cancer,* 88**,** 2619-2628.

WANG, Y., ALAM, G. N., NING, Y., VISIOLI, F., DONG, Z., NOR, J. E. & POLVERINI, P. J. 2012. The unfolded protein response induces the angiogenic switch in human tumor cells through the PERK/ATF4 pathway. *Cancer Res,* 72**,** 5396-406.

WANI, M. C., TAYLOR, H. L., WALL, M. E., COGGON, P. & MCPHAIL, A. T. 1971. Plant antitumor agents. VI. Isolation and structure of taxol, a novel antileukemic and antitumor agent from Taxus brevifolia. *Journal of the American Chemical Society,* 93**,** 2325-2327.

WEHNER, R., BITTERLICH, A., MEYER, N., KLOSS, A., SCHAKEL, K., BACHMANN, M. & SCHMITZ, M. 2013. Impact of chemotherapeutic agents on the immunostimulatory properties of human 6-sulfo LacNAc+ (slan) dendritic cells. *Int J Cancer,* 132**,** 1351-9.

WERTZ, I. E., KUSAM, S., LAM, C., OKAMOTO, T., SANDOVAL, W., ANDERSON, D. J., HELGASON, E., ERNST, J. A., EBY, M., LIU, J., BELMONT, L. D., KAMINKER, J. S., O'ROURKE, K. M., PUJARA, K., KOHLI, P. B., JOHNSON, A. R., CHIU, M. L., LILL, J. R., JACKSON, P. K., FAIRBROTHER, W. J., SESHAGIRI, S., LUDLAM, M. J., LEONG, K. G., DUEBER, E. C., MAECKER, H., HUANG, D. C. & DIXIT, V. M. 2011. Sensitivity to antitubulin chemotherapeutics is regulated by MCL1 and FBW7. *Nature,* 471**,** 110-4.

WHITE, C. M., MARTIN, B. K., LEE, L. F., HASKILL, J. S. & TING, J. P. 1998. Effects of paclitaxel on cytokine synthesis by unprimed human monocytes, T lymphocytes, and breast cancer cells. *Cancer Immunol Immunother,* 46**,** 104-12.

WILEY, S. R., SCHOOLEY, K., SMOLAK, P. J., DIN, W. S., HUANG, C. P., NICHOLL, J. K., SUTHERLAND, G. R., SMITH, T. D., RAUCH, C., SMITH, C. A. & ET AL. 1995. Identification and characterization of a new member of the TNF family that induces apoptosis. *Immunity,* 3**,** 673-82.

WU, G., CHAI, J., SUBER, T. L., WU, J.-W., DU, C., WANG, X. & SHI, Y. 2000. Structural basis of IAP recognition by Smac/DIABLO. *Nature,* 408**,** 1008-1012.

WU, Y., FABRITIUS, M. & IP, C. 2009. Chemotherapeutic Sensitization by Endoplasmic Reticulum Stress: Increasing the Efficacy of Taxane Against Prostate Cancer. *Cancer Biol Ther,* 8**,** 146-52.

YAMAGUCHI, H. & WANG, H.-G. 2004. CHOP Is Involved in Endoplasmic Reticulum Stress-induced Apoptosis by Enhancing DR5 Expression in Human Carcinoma Cells. *Journal of Biological Chemistry,* 279**,** 45495-45502.

YAREMKO, M. L., KUTZA, C., LYZAK, J., MICK, R., RECANT, W. M. & WESTBROOK, C. A. 1996. Loss of heterozygosity from the short arm of chromosome 8 is associated with invasive behavior in breast cancer. *Genes Chromosomes Cancer,* 16**,** 189-95.

YE, J., RAWSON, R. B., KOMURO, R., CHEN, X., DAVE, U. P., PRYWES, R., BROWN, M. S. & GOLDSTEIN, J. L. 2000. ER stress induces cleavage of membrane-bound ATF6 by the same proteases that process SREBPs. *Mol Cell,* 6**,** 1355-64.

YONEHARA, S., ISHII, A. & YONEHARA, M. 1989. A cell-killing monoclonal antibody (anti-Fas) to a cell surface antigen co-downregulated with the receptor of tumor necrosis factor. *J Exp Med,* 169**,** 1747-56.

YOSHIDA, H., HAZE, K., YANAGI, H., YURA, T. & MORI, K. 1998. Identification of the cis-acting endoplasmic reticulum stress response element responsible for transcriptional induction of mammalian glucose-regulated proteins. Involvement of basic leucine zipper transcription factors. *J Biol Chem,* 273**,** 33741-9.

YOSHIDA, H., MATSUI, T., YAMAMOTO, A., OKADA, T. & MORI, K. 2001. XBP1 mRNA is induced by ATF6 and spliced by IRE1 in response to ER stress to produce a highly active transcription factor. *Cell,* 107**,** 881-91.

ZHANG, K. & KAUFMAN, R. J. 2008. From endoplasmic-reticulum stress to the inflammatory response. *Nature,* 454**,** 455-62.

ZHANG, L., DERMAWAN, K., JIN, M., LIU, R., ZHENG, H., XU, L., ZHANG, Y., CAI, Y., CHU, Y. & XIONG, S. 2008. Differential impairment of regulatory T cells rather than effector T cells by paclitaxel-based chemotherapy. *Clin Immunol,* 129**,** 219-29.

ZHU, Y., LIU, N., XIONG, S. D., ZHENG, Y. J. & CHU, Y. W. 2011. CD4+Foxp3+ regulatory T-cell impairment by paclitaxel is independent of toll-like receptor 4. *Scand J Immunol,* 73**,** 301-8.

ZOBEL, K., WANG, L., VARFOLOMEEV, E., FRANKLIN, M. C., ELLIOTT, L. O., WALLWEBER, H. J., OKAWA, D. C., FLYGARE, J. A., VUCIC, D. & FAIRBROTHER, W. J. 2006. Design, synthesis, and biological activity of a potent Smac mimetic that sensitizes cancer cells to apoptosis by antagonizing IAPs. *ACS chemical biology,* 1**,** 525-533.

ZOU, H., LI, Y., LIU, X. & WANG, X. 1999. An APAF-1.cytochrome c multimeric complex is a functional apoptosome that activates procaspase-9. *J Biol Chem,* 274**,** 11549-56.